




University of
Stavanger

Faculty of Science and Technology

MASTER'S THESIS

Study program/ Specialization: Well Engineering / Master of Science Degree Program	Spring semester, 2014 Open / Restricted access
Writer: Endiandika Tri Putranto	 (Writer's signature)
Faculty supervisor: Professor Aly Anis Hamouda External supervisor(s): -	
Thesis title: Investigation of Gas Composition on Production Performance of J-shaped Gas-lift Well	
Credits (ECTS): 30	
Key words: J-shaped well, Gas-lift, Flow regime, Composition, Pure component, Binary component, Multicomponent, Surface tension, Solubility, Production	Pages: 62 pages + Front part: 9 pages + Appendixes : 9 pages + CD Stavanger, 16 th June 2014

Abstract

The J-shaped gas-lift well showed complex dynamic phenomena. The downward inclination of the J-shaped well introduces periodic waves over time as a result of mixing gas and liquid. This behavior introduces periodic fluctuations of the superficial gas and liquid velocities along tubing. The velocity fluctuation is due to the accumulation of liquid in the heel of the inclined section of J-shaped well and the development of reservoir gas pressure to overcome the accumulated liquid column making the J-shaped gas-lift well to be prone to production under slugging regime.

The investigation here is addressing two aspects with the objective to optimize the gas-lift performance. The first addresses the production behavior and the mechanism that leads to development of slugging regime in the J-shaped well. Secondly it addresses the effect of the gas composition of the gas-lift on the production performance. Different gas-lift gas composition causes the gas and liquid compositions to change with the pressure and temperature profile in the production tubing.

Gas-lift contains C1 as a major component. The work here shows that a fraction of 0.15 nC5 combined with C1 gives highest oil production rates. In the contrary, high content of 0.20 iC4 with C1 give lowest oil rates. This outcome would assist in designing optimum gas-lift injection system.

Acknowledgements

In the name of Allah, the Most Gracious and the Most Merciful

I would like to express my thanks and praise to Allah for His guidance and granting me the capability so that I can complete this work. I hope that my work would be beneficial to science in general. My special appreciations of gratitude to my academic supervisor Professor Aly Anis Hamouda who gave me the opportunity to do this project and were very determined to help me finishing this work until such great extent.

This work was carried out at University of Stavanger in the period of January – June 2014. I would like to acknowledge the support of my colleagues Surya Dharma and Hafiz Adi Kurnia for their contribution to build the model and understand the simulator. I would like to express my sincere thanks to all my Indonesian friends, Lurohman Mamin Masturi, Deannisa Teddy Hilman, Rizky Amanda, Dody Aldilana, Kosdar Gideon Haro, Suryanto Ang, Rifel Landong Pordiman, Dini Adyasari, Wening Lestari Ambarwati, and Raisya Noor Pertiwi, for their kinship during my study period in Stavanger.

I am heartily thankful to my wife, Rosi Maria Adha Pasaribu for her support and encouragement throughout my study. I would also give my deepest gratitude to my parents, Soedirun D.S. and Endang Subekti, and also to Sudarmono S.H. for their huge support so I can pursue my dream to continue study.

I would like to express my thanks to all of my friends of the Department of Petroleum Engineering and all of whom I met during my memorable study period at the University of Stavanger. Also for those who have helped me but not mentioned here, thank you very much.

Endiandika Putranto, June 2014

Table of Contents

Abstract	i
Acknowledgements	ii
Table of Contents	iii
List of Figures.....	v
List of Tables.....	vii
List of Abbreviation	viii
Nomenclature.....	ix
1. Introduction	1
1.1 Background Information.....	1
1.2 Objective.....	2
1.3 Outline	2
2. Theory and Literature Study	4
2.1 Gas-lift Concept	4
2.2 Gas-lift Instability & Optimization	7
2.3 Dynamic Simulator: OLGA	11
2.4 Flow Regime	13
2.5 Hydrocarbon Phase Behavior	14
3. Model Development	17
3.1 J-shaped Well.....	17
3.2 PVT Data of Reservoir Fluid and Gas-lift Injection Gas.....	21
3.3 OLGA model.....	25
3.4 Gas-lift Performance Evaluation.....	27
4. Sensitivity Study Results and Discussion	32
4.1 Base Case	33
4.2 Pure Component.....	46
4.3 Binary Component.....	51
4.4 Multicomponent Mixture	55
5. Conclusion.....	59
6. Bibliography	61
Appendix.....	63

Appendix A1.....	63
Appendix A2.....	64
Appendix B1.....	65
Appendix B2.....	66
Appendix B3.....	67
Appendix B4.....	68
Appendix B5.....	69
Appendix B6.....	70
Appendix C1.....	71

List of Figures

Figure 1-1 Model Building and Evaluation Method	3
Figure 2-1 Pressure and Depth Relationship in Gas-lift Well (Guo, Lyons, & Ghalambor, 2007)	5
Figure 2-2 Gas-lift Unloading Sequences (Guo, Lyons, & Ghalambor, 2007)	6
Figure 2-3 Example of Unstable Oil Productions (Avest & Oudeman, 1995).....	8
Figure 2-4 Gas-lift Optimization Procedure (Xu & Golan, 1989).....	9
Figure 2-5 Two-phase Horizontal Flow Regime Map (Beggs, 1991)	14
Figure 2-6 P-T Phase Diagram for Multicomponent System (Ahmed, 2007).....	15
Figure 3-1 J-Shaped Well Profile	17
Figure 3-2 Liquid Blockage in J-section of J-shaped Well (Dharma, 2012)	18
Figure 3-3 Model Layout	21
Figure 3-4 Mesh Discretization Applied to Flow Path in the Model	26
Figure 3-5 IPR - VLP Curve of the System Without the Aid of Gas-lift	29
Figure 3-6 IPR - VLP Curve of the System With the Aid of Gas-lift.....	29
Figure 3-7 Pressure vs TVD in the J-shaped Well	30
Figure 4-1 Base Case Oil and Gas Production on Wellhead.....	33
Figure 4-2 Pressure and Pressure Drop Profile Along J-section.....	35
Figure 4-3 Liquid Holdup in J-section (Left) and Tubing Section (Right).....	36
Figure 4-4 Pressure and Pressure Drop Profile Along Tubing Section	36
Figure 4-5 Dynamic Unloading Sequence Shown as Liquid Holdup (a)	38
Figure 4-6 Dynamic Unloading Sequence Shown as Liquid Holdup (b)	39
Figure 4-7 Two-phase Vertical Flow Regime Map (Beggs, 1991).....	41
Figure 4-8 Pressure and Temperature Profile at Stable Flow Period	43
Figure 4-9 Liquid Holdup Profile at Stable Flow Period	43
Figure 4-10 Velocity Profile	44
Figure 4-11 Flow Regime	44
Figure 4-12 Gas Composition	45
Figure 4-13 Oil Composition.....	45
Figure 4-14 Oil Production Sensitivities of Pure Gas-lift Gas Injection ($5^{\circ}\text{C } T_{\text{INJ}}$)	46
Figure 4-15 Pressure Profile of Pure Component Case with P_{INJ} 163 bara at Stable Flow Period	47
Figure 4-16 Density at different Points in The Well for Individual Pure Component Cases	48
Figure 4-17 Pressure Profile of C2 Case with Different Casing Pressure at Stable Flow Period	50
Figure 4-18 Compressibility of Fluid Around Injection Point (P_{INJ} 175 bara, C2 Gas-lift Gas) Before and After Gas-lift Injection	51
Figure 4-19 Oil Production on Wellhead for Binary Component Gas-lift Gas Injection Cases	53
Figure 4-20 IFT at Wellhead at Stable Flow Period (Binary Component Cases)	54
Figure 4-21 IFT at Injection Point at Stable Flow Period (Binary Component Case.....	54

Figure 4-22 Oil Production on Wellhead for Multicomponent Mixture Gas-lift Gas Injection Cases.....	56
Figure 4-23 IFT at Wellhead at Stable Flow Period (Multicomponent Cases)	57
Figure 4-24 IFT at Injection Point at Stable Flow Period (Multicomponent Cases).....	57
Figure 4-25 Oil Rate for Binary Cases and Multicomponent Cases	58

List of Tables

Table 3-1 Geometry of Tubing	18
Table 3-2 Geometry of J-section	19
Table 3-3 Geometry of Gas-lift Gas Injection Section (Annulus)	20
Table 3-4 Reservoir Fluid Composition	22
Table 3-5 Gas-lift Gas Injection Composition.....	23
Table 3-6 Composition of Gas-lift Gas Injection with 1% Content Change.....	24
Table 3-7 Composition of Gas-lift Gas Injection with 5% Content Change.....	24
Table 3-8 Composition of Gas-lift Gas Injection with 8% Content Change.....	24
Table 3-9 Composition of Gas-lift Gas Injection with 10% Content Change.....	25
Table 3-10 Operating Point of the J-shaped Gas-lift Well System	28
Table 4-1 Result of Base Case.....	39
Table 4-2 Pressure and Temperature at Different Point in the Wellbore	43
Table 4-3 Recombined Fluid Composition	44
Table 4-4 P_{WF} of Pure Components Case at P_{INJ} 163 bara.....	46
Table 4-5 Pressure and Temperature at Wellbore for Pure Component Cases	49
Table 4-6 P_{WF} of C2 Gas-lift Gas Injection Case at Different P_{INJ}	50

List of Abbreviation

DPR	: Discharge Pressure Relationship
EOS	: Equation of State
GLR	: Gas-Liquid Ratio
GLV	: Gas-lift Valve
GOR	: Gas-oil Ration
GPR	: Gas Performance Relationship
IFT	: Interfacial Tension / Surface Tension
IPR	: Inflow Performance Relationship
LPR	: Lift Performance Relationship
mD	: Measured Depth
PI	: Productivity Index
PVT	: Pressure, Volume, Temperature
SRK	: Soave-Redlich-Kwong
TPR	: Tubing Performance Relationship
TVD	: True Vertical Depth
VLP	: Vertical Lift Performance
VPC TM	: Valve Performance Clearinghouse TM

Nomenclature

ΔP_V	: Delta Pressure due to Gas-lift Valve
D	: Depth
D_V	: Depth of Valve
P_{ID}	: Pressure at Injection Depth
P_{INJ}	: Injection Pressure
P_R, P_{RES}	: Reservoir Pressure
P_{WF}	: Tubing Flowing Pressure
P_{WH}	: Wellhead Pressure
Q_{GAS}	: Gas Rate
Q_{INJ}	: Injection Rate
Q_{OIL}	: Oil Rate
T_{RES}	: Reservoir Temperature

1. Introduction

1.1 Background Information

Gas-lift has been proven as an efficient method to increase oil production rate. It works on a well by injection of compressed gas into selected lower section of production tubing through the annulus and valve(s) installed in the tubing string. There are several gas-lift installations which are used depending on the well conditions (Guo, Lyons, & Ghalambor, 2007). The installations are open, semi-closed, closed, and chamber. Additionally there are cases of gas-lift well in which the gas is not injected through the annulus, for example coiled tubing gas-lift or self-lift by using gas coming from shallower reservoir. Only semi-closed installation is considered in this thesis. It uses a packer that is set between the tubing and casing, but doesn't utilize a standing valve. If there's standing valve installed below the lowermost gas-lift valve, the dynamic of multiphase behavior below gas-lift valve would not be captured and affect the flow above the gas-lift valve. It is interesting to investigate the dynamic of multiphase behavior in a well, especially in a well with complex geometry.

J-shaped well is one example of well with complex geometry that has a risk of terrain slugging (Dharma, 2012). J-shaped well is a well that has lower perforation section inclining downward to the bottom point of the J-shaped tube with an inclined section continues upward vertical section. The perforation section is called toe, and the bottom point is called heel (Figure 3-1). The toe is placed in the reservoir section, so the fluid from reservoir flows through it. Terrain slugging has an inherent transient nature, thus it has to be modelled as a time dependent process (Danielson, Brown, & Bansal, 2000). One way to diagnose this time dependent process is by using a dynamic transient computer aided simulator in this case OLGA multiphase flow software is used. The simulator computes the transient flow of gas and liquid through the production tubing, variable injection of gas, and pressure transient in the annulus. Valve models are used to calculate the passage of gas or fluid through the valves as a function of pressures local to the valves.

The model used in this work has the ability to track the spatial and temporal change in flow rate and composition of the hydrocarbon fluid in every element of gas lift process. Mahmudi and Sadeghi point out that the gas lift process is transient and the model has to deal with the change in the composition of the reservoir fluid and gas injection (Mahmudi & Sadeghi, 2013). They show that the performance of the gas lift system is highly composition dependent and this should also be taken into account explicitly.

OLGA Multiphase flow software used in this work has the ability to simulate slow transients associated with mass transport. The flow regimes are treated as an integral part of the multiphase system (Bendiksen, Maines, Moe, & Nuland, *The Dynamic Two-Fluid Model OLGA: Theory and Application*, 1991). The system also has the ability to perform compositional tracking. These abilities make this software suit favorably to do the investigation of dynamic process in J-shaped gas-lift well.

1.2 Objective

The objectives of this study are:

- to build a J-shaped gas-lift well model
- to validate the model by comparing the model in PROSPER, steady state OLGA, dynamic OLGA
- to simulate the dynamic of J-shaped gas-lift well
- to explain the mechanism of the dynamic accumulation of the fluid and the development of pressure in the J-section and injection point
- to explain the effect of composition to the production performance

1.3 Outline

This study is presented into six chapters. The ongoing chapter has given the motivations and objectives of the study. Next chapter introduces the concepts and the terms used in this thesis such as gas-lift concept, gas-lift instabilities and optimization, OLGA software, multiphase flow and flow regime, and PVT and hydrocarbon phase behavior. The third chapter addresses information about how to build and validate the J-shaped gas-lift well model.

The subsequent chapter presents sensitivity studies of detailed modeling using dynamic simulator OLGA. These sensitivities of gas-lift gas compositions are performed to study the expected behavior of the well over time. This chapter also discusses the results from the sensitivity studies. The closing chapter gives the conclusions of this thesis. The references used in this study are listed in bibliography.

In the following diagram, the methodology of how the model is built and evaluated is presented.

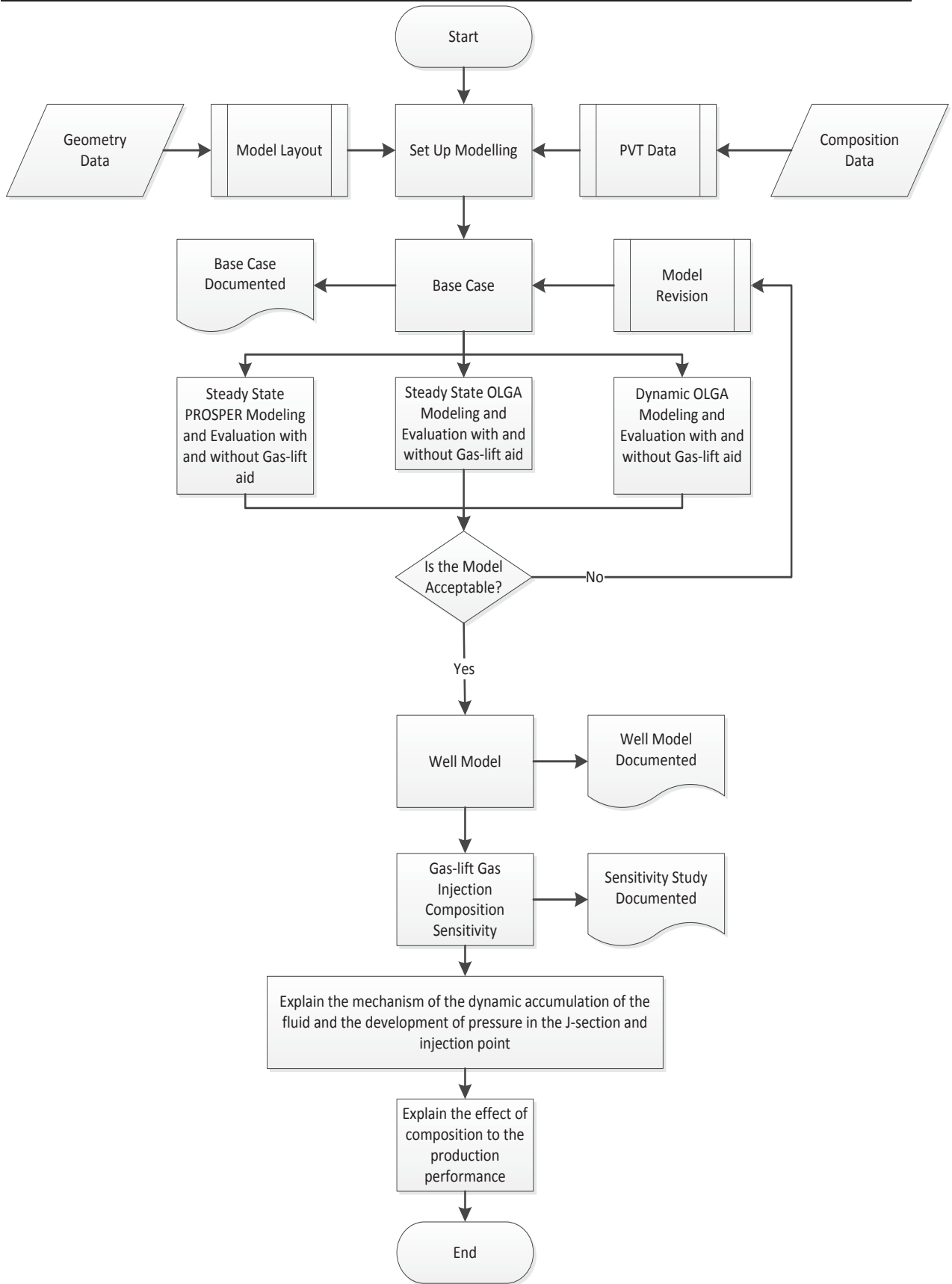


Figure 1-1 Model Building and Evaluation Method

2. Theory and Literature Study

2.1 Gas-lift Concept

Hydrocarbon production declines with time. The decline is caused by the change of inflow condition (IPR) which is the reservoir's deliverability and the change of outflow condition (VLP) which is the well's deliverability. There will be time where the corresponding IPR-VLP curves are not intersecting any longer. Methods are available to modify both the inflow and outflow performance of the well so the curves would intersect once more. The IPR depends on P_{WF} and reservoir pressure. Any methods for generating IPR can be used for naturally flowing or artificial lift wells. The IPR is completely independent of any methods used to obtain the particular P_{WF} . One method to modify VLP is by using gas-lift by which the gas is continuously injected into tubing through gas lift valve installed in side pocket mandrel at a fixed depth. For this study of J-shaped gas-lift well, the system initially is treated as if it is a flowing well, hence IPR-VLP curve is prepared to see if the well is capable of flowing and at what rate. If the well has no capability of flowing, the gas-lift evaluation is performed on the same IPR-VLP curve.

It is shown in this work that the gas affects the fluid flow in two ways as has been indicated by Guo et al. Gas injection first gives expansion energy to push the fluid column above the injection point to the surface, then increases the gas-liquid ratio (GLR) started from the injection point up to surface and decreases the hydrostatic gradient in the production tubing, thus decreases the tubing flowing pressure (Guo, Lyons, & Ghalambor, 2007) as shown by Figure 2-1. With lower hydrostatic gradient in the tubing, the VLP curve can be shifted until it intersects with the corresponding IPR resulting lower P_{WF} . Larger drawdown can be achieved with lower P_{WF} and this drawdown certainly increases the liquid production rate. Production optimization is also done by manipulating this VLP curve and the injected GLR with their corresponding gas injection rate, gas injection pressure, compressor discharge pressure, and gas-lift valve performance relationships.

Techniques to evaluate gas lift potential used in this thesis as explained in section 3.4 are built based on the determination of well performance once it is unloaded and in stabilized operation, and spacing and pressure setting of the upper gas lift valves used in unloading the well (Beggs, 1991). Well performance is characterized by nodal analysis of a given point in the system. The node is chosen to be at the reservoir thus the intersection of the well IPR curve and VLP curves at the node are the operation points. These intersections give the liquid production rates corresponding to each GLR and other parameters that build the VLPs.

The continuous gas-lift operation is used typically in well with high PI and high reservoir pressure. There are no restriction concerning any lower completion compatibility, well profiles, well depth, and onshore/offshore operation. A complete gas lift system consists of a gas compression station, a gas injection manifold with injection chokes and time cycle surface controllers, a tubing string with installations of unloading valves and operating

valves, and an optional down-hole chamber. Complete overview of gas-lift system has been addressed by Hu (Hu, 2004) and Guo et al. (Guo, Lyons, & Ghalambor, 2007). This overview includes design of gas compression station to provide sufficient gas lift gas flow rate at desired pressure, and method and selection to place the gas lift valves. The method to place the injection valve and the unloading valve depends mainly on the gas injection pressure available, the wellhead pressure and the fluid's pressure gradient along the production tubing. Unloading valves are needed to unload prefilled fluid in production tubing and initiate the well.

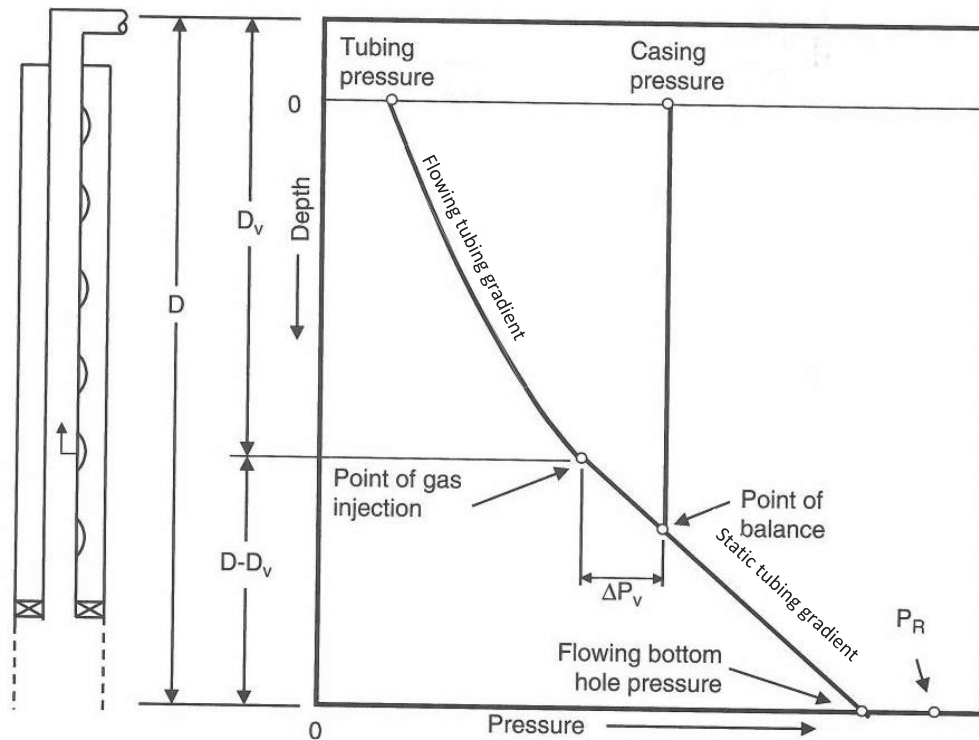


Figure 2-1 Pressure and Depth Relationship in Gas-lift Well (Guo, Lyons, & Ghalambor, 2007)

Figure 2-2 shows the unloading sequences of typical gas-lift well. At (a), all valves are open at initial condition. When the gas enters the first top valve as shown in (b), it creates a slug of liquid-gas mixture of lower density in the tubing above the valve depth. Expansion of the slug pushes the liquid column above it. As the length of the slug grows, the bottom-hole pressure will eventually decrease to below reservoir pressure initiating inflow from reservoir. When the tubing pressure at the depth of the first valve is low enough, the first valve should begin to close and the gas should be forced to the second valve as seen in (c). Gas injection to the second valve will disperse the liquid in the tubing between the first and second valve. This will further reduce bottom-hole pressure and cause more inflow. By the time the slug reaches the depth of the first valve, the first valve should be close, allowing more gas to be injected to the second valve. The same process should occur until the gas enters the main valve as shown in (d). The main valve is usually the lower valve in the tubing. In continuous gas-lift operation, once the well is fully unloaded and a steady-state flow is established, the main valve is the only valve open and in operation as seen in (e).

Even so this thesis only considers the main valve to be applied to the model. The well is unloaded and operated through a single main valve. Though the unloading sequence may not be the same as discussed above, the expansion of the slug and the dispersion of the gas into the liquid may still be applicable to explain the unloading mechanism of J-shaped gas-lift well as further discussed in section 4.1.

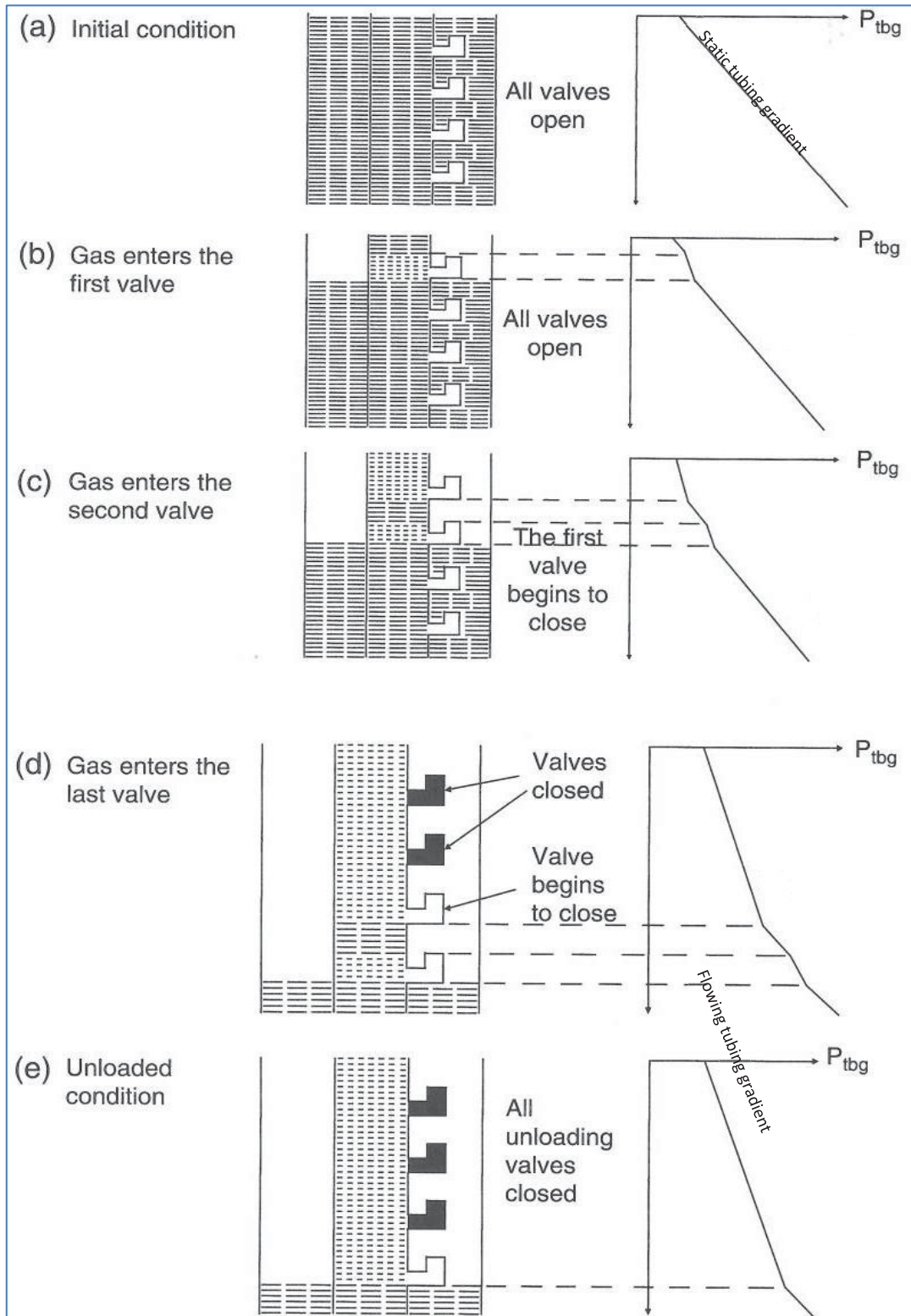


Figure 2-2 Gas-lift Unloading Sequences (Guo, Lyons, & Ghalambor, 2007)

2.2 Gas-lift Instability & Optimization

Gas-lift system optimization can be applied either on individual well or in a field-scale evaluation. This optimization is a complicated issue and often depends on the practical conditions that vary from well to well and field to field as has been addressed by Hu (Hu, 2004). For individual well, optimization mainly focuses on determining and using the optimal gas-lift gas injection rate. Different effects will occur with different gas injection rates. For example if the rate is too small, the gas will go into the liquid as small semi-spherical bubbles. On the other hand if the rate is large, there would be excessive gas injection reducing and might even reach to no liquid flow as a result of the tubing undergoes a friction dominated flow. There are also maximum efficiency gas rates where a minimum gas rate will give relatively high liquid rate and a rate that will give maximum liquid rate.

For a field-scale evaluation, optimization focuses on determining gas allocation for the whole wells. If limited amount of gas is available for the gas-lift, the gas should be distributed to each individual well based on the desired lifting performance. The wells that produce oil at higher rates at a given amount of lift gas are preferably chosen to receive more lift gas. If unlimited amount of lift gas is available, the injection rates to individual wells should be chosen so that it can yield maximum oil rates.

Continuous gas-lift operation faces difficulties to maintain the production rate or the gas injection rate at desired level as defined by gas-lift performance curve. It conventionally focuses on determining and using the optimal gas-lift gas injection rate. Different injection rates gives different operating liquid rates as depicted by gas-lift performance curve. However, choosing injection rate that delivers maximum liquid rate may not be optimum because slightly lower gas injection rate may obtain similar liquid production rate with lower gas consumption. An economic assessment should also be made for justifying gas-lift gas consumption. Selection of injection rate and economic assessment are beyond the discussion of this work as many works have been done on those subjects.

Moreover the production rate is unstable swinging between certain maximum and minimum levels as seen in Figure 2-3. It is obvious that gas lift efficiency is affected by this unstable behavior of wells. This unstable production results in period of reduced production which will create significant oil deferment therefore maintaining the production rate is also a form of optimization. This instability can occur in consideration of casing heading, the performance of the gas-lift valve, and the nature of multiphase flow when the injection gas and reservoir fluid are mixed in the tubing. It might also as a result of the composition change due to the variation of pressure and temperature along the production tubing. However, there has been a little discussion so far about the effect of composition to production performance. This thesis examines the significant effect of composition to production performance as further discussed in chapter 4.

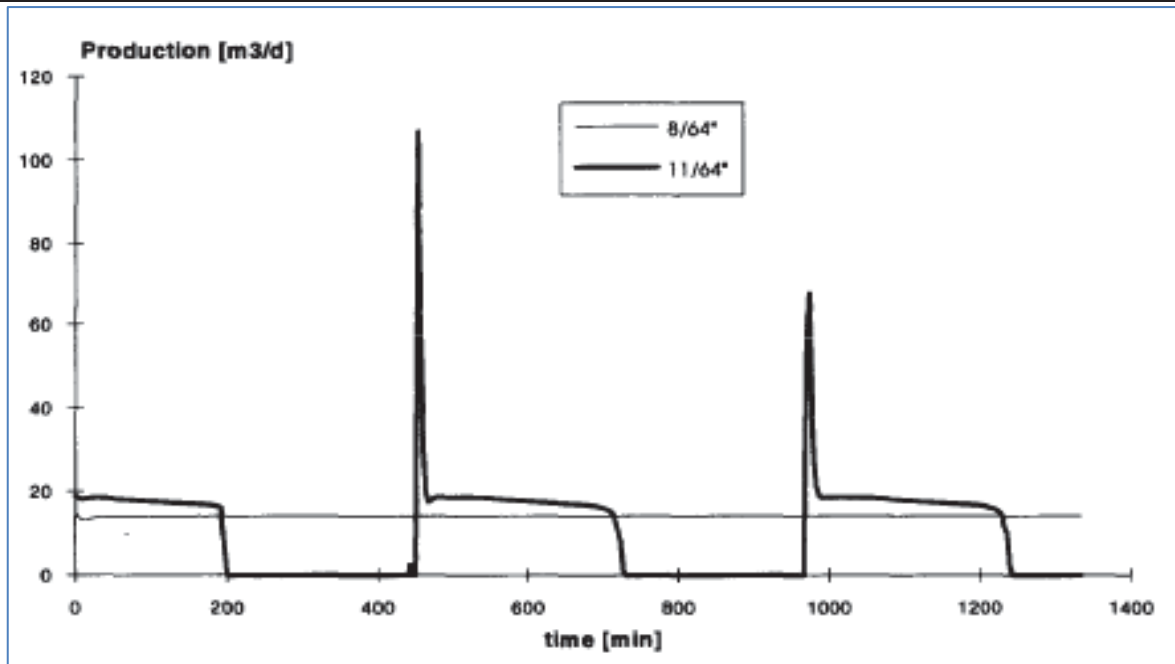


Figure 2-3 Example of Unstable Oil Productions (Avest & Oudeman, 1995)

There are two basic instabilities, steady state and dynamic. Conventionally gas-lift system instability evaluation is investigated by using steady state equilibrium flow condition at some cross section along the flow path of the well as has been reported by Xu and Golan (Xu & Golan, 1989). This steady state instability analysis requires that equilibrium state exists only if the back pressure from separator and manifold equals the upstream pressure from the reservoir. Injection point or reservoir was used as an analysis point where the equilibrium state exists. Such static stability consideration is unsatisfactory because the pressure fluctuation constantly forces the system out of balance which is nature of multiphase flow. So it is important to use dynamic analysis to study the instability.

In the example of gas lift well in Figure 2-4, injection point is used as an arbitrary cross section to determine the equilibrium flow condition. At this point there are three available pressure vs rate relationships. The first one which relates gas injection flow rate with the pressure at injection point calculated from annulus called gas discharge performance relationship (DPR). Secondly the one which relates liquid flow rate with the pressure at injection point calculated from the reservoir called IPR. And the last one which relates liquid flow rate with the pressure at injection point calculated from the wellhead called VLP also called tubing performance relationship (TPR).

The equilibrium condition is at the point when the TPR and IPR are crossed. As seen from Figure 2-4, there are several points where the TPRs crossed the IPR. Those TPRs depend on the gas injection rates. Those equilibrium points are used to build a relationship between gas injection rate and liquid rate called lift performance relationship (LPR). The IPR and TPRs relationship are also used to establish a relationship between pressure at injection point and gas injection rate called gas injection performance relationship (GPR).

As mentioned before two major sources of instability among other are heading and slug flow. The heading is an unstable production because of the string design, the size of injection valve port, the variation of supply pressure, and the valve plugging/leaking. The slug flow on the other hand is a natural flow regime that is difficult to control due to the gas-liquid phase interaction. Heading however is related to controllable parameter.

There are two mechanisms of heading as explained by Avest and Ouderman, one mechanism is based on the change of pressure inside the tubing and one is based on the change of pressure inside the annulus (Avest & Ouderman, 1995). The first mechanism is at high gas injection rate, the pressure drop over the tubing is dominated by friction. If for some reason the GOR rise, the tubing pressure increases which reduces the gas injection rate. Furthermore at low gas injection rate, the hydrostatic pressure drop dominates the tubing pressure. Further increase in GOR causes a lower tubing pressure which leads to a higher injection rate. The second mechanism is if the volume of gas being injected in the annulus was higher than the volume which the installation has been design to handle, the pressure in the annulus rises. However, if the gas injection rate decreases, the casing pressure also decreases. These mechanisms affect the stability of injection rate at the injection valve.

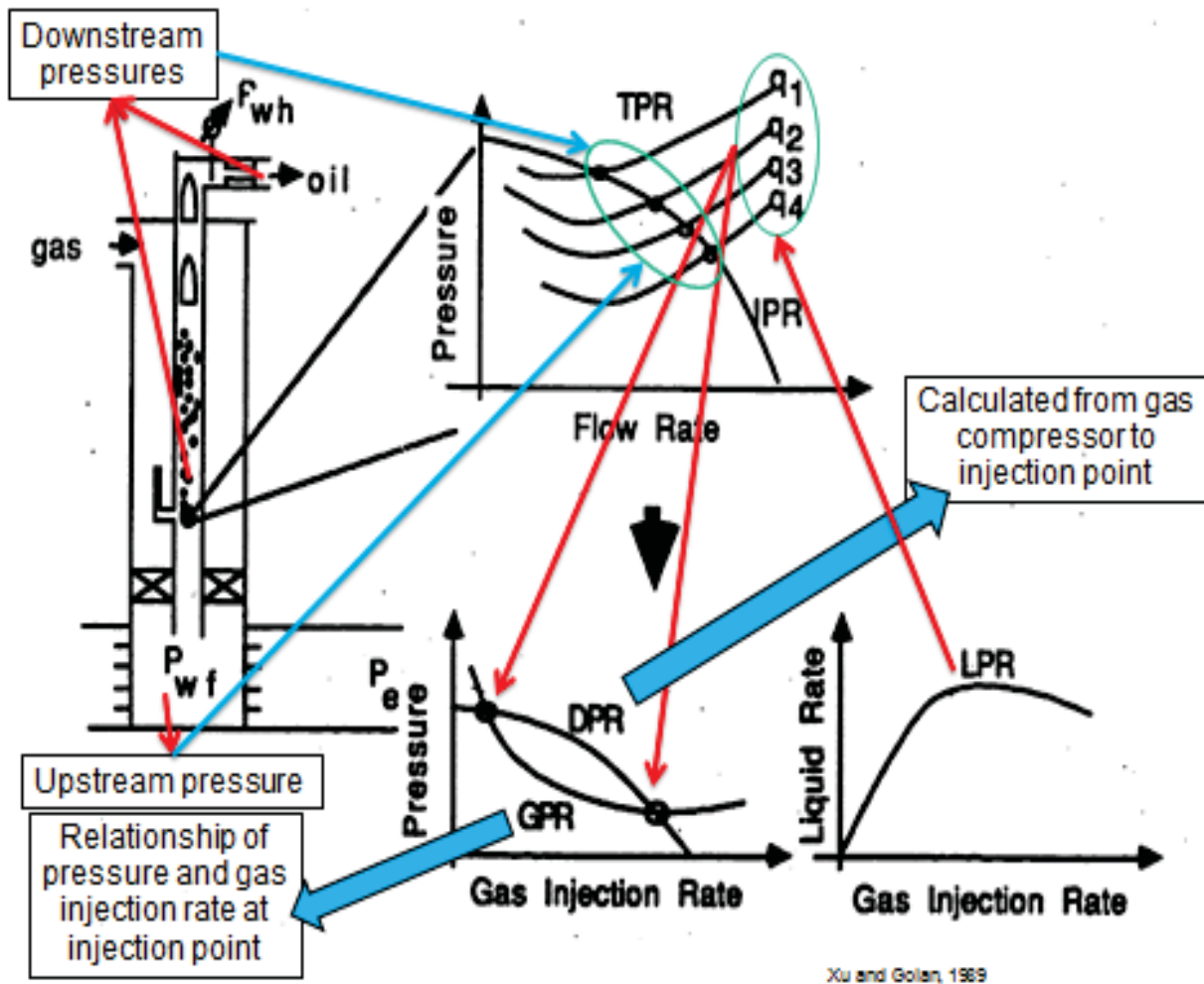


Figure 2-4 Gas-lift Optimization Procedure (Xu & Golan, 1989)

Asheim also reported that if the inflow rate of the heavier reservoir fluids is more sensitive to pressure than the gas lift flow rate, then the average density of the flowing fluid mixture increases in response to the decrease in tubing pressure (Asheim, Criteria for Gas-Lift Stability, 1988). This makes the tubing pressure to increase again which stabilizes the flow. However, if this is not fulfilled, a decrease in tubing pressure causes the gas lift flow rate to increase more than the reservoir fluid flow rate. This results a decreasing tubing pressure and depletes the gas conduit pressure. Furthermore if the gas conduit pressure depletes faster than tubing pressure, the pressure differences between the gas conduit and the tubing decrease and so the gas-lift gas rate.

Maijoni and Hamouda concluded that there is effect of gas-lift gas composition on oil production (Maijoni & Hamouda, 2011). They argued that the heavier gas is easily soluble in oil due to lower interfacial tension between oil and gas. The higher the molecular weight, the better the gas solubility and the lower IFT are. It results a higher mixture fluid velocity inside tubing. The importance of phase behavior was also supported by Mahmudi and Sadeghi (Mahmudi & Sadeghi, 2013). These previous studies have indicated that the model used to perform stability analysis should have the ability to track the spatial and temporal change in flow rate and composition of the hydrocarbon fluid in every element of gas lift process. The model used in this thesis has those abilities. The gas lift process is transient and the model takes the change in the flow rate and composition of the reservoir into account. The performance of the gas lift system is highly composition dependent and this is also taken into consideration in the model. The oil and gas compositions considered as multi-component mixtures change significantly due to inter-phase exchange of components. At each point in the wellbore, the superficial velocity, composition, and thermodynamics properties of the oil and gas phases are computed using phase stability and flash calculation based on an appropriate equation of state. Once the superficial gas and liquid velocity are determined, a two phase flow map and its associated correlation are used to identify the local flow regime and pressure gradient. Having the compositions, fluid properties are obtained from the phase behavior calculations. This also means that the bubble pressure of the oil may change significantly as it rises in the well bore. It should be noted that the inevitable drawback of the compositional treatment is the large increase in computation time as a result of many multi-component phase stability and flash calculations performed.

There are many stability criteria that had been proposed by many studies. The most used one is stability criterion proposed by Asheim (Asheim, Criteria for Gas-Lift Stability, 1988). He proposed two theoretical-stability criteria F1 and F2. Alhanati et al. extended Asheim's model and formulated unified criteria that consider the flow regime at the surface gas injection valve and the gas lift valve (Alhanati, Schmidt, Doty, & Lagerlef, 1993). Xu and Golan classified instability phenomena in gas lift system into two groups, static and dynamic (Xu & Golan, 1989). Poblano et al. proposed the used of stability maps as a method for analyzing flow stability in gas lift systems (Poblano, Camacho, & Fairuzov, 2005). They used Asheim and Alhanati's criteria as basis to build the stability map. These criteria are called

linear analysis. In this type of analysis, Guerrero-Sarabia and Fairuzov reported that the response of the system which is initially at equilibrium, to an infinitesimal perturbation of tubing pressure at the injection point is predicted (Guerrero-Sarabia & Fairuzov, 2013). However, there are certain drawbacks associated with the use of this linear analysis. One drawback is to obtain practical analytical criteria several strong simplifications in the description of the system are made. The other disadvantage of the linear stability analysis is that it only predicts the onset of instability and cannot be used to model the operation of well in the unstable region. It was not possible to investigate the significant effect of composition to production performance with those drawbacks. Thus those linear analyses are not used in this work.

The other approach to study flow instability in gas lift wells is the non-linear analysis as also reported by Guerrero-Sarabia and Fairuzov (Guerrero-Sarabia & Fairuzov, 2013). This approach is usually based on numerical modeling of multiphase flow in the tubing that has been used to develop active control systems to eliminate heading. Moreover this analysis can be used to study the system behavior when the operating parameters of a gas-lift well exceed the stability limits. This non-linear well model also predicts the amplitude and frequency of oscillations of flow parameters such as tubing and casing pressure, liquid and gas flow rates, and liquid holdup.

These aforementioned analytical capabilities are found in a dynamic transient computer aided simulator therefore it can be used to diagnose the gas-lift non-linear instabilities found in this work. The simulator computes the transient flow of gas and liquid through the production tubing, variable injection of gas, and pressure transient in the annulus. Furthermore valve models are used to calculate the passage of gas or fluid through the valves as a function of pressures local to the valves. Unloading could be a potential problem. Pressure will vary as unloading valves open or close and fluid is displaced from the tubing. Valve opening and closing may not be as planned that result in unsuccessful unloading and also could damage the valves. The main disadvantage of this simulator is that it is time-consuming. Moreover it takes a lot of efforts to obtain an agreement between the model predictions and field data for all operations. Despite of having those disadvantages, it was decided that the best method to investigate the effect of composition in production performance is by using the dynamic transient computer aided simulator.

2.3 Dynamic Simulator: OLGA

As reported by Avest and Ouderman (Avest & Oudeman, 1995), the algorithm that is used in OLGA and many dynamic simulator works as follow:

- Calculate the inflow from the reservoir (reservoir model)
- Calculate the local pressure drop along the tubing by multiphase flow correlation
- Calculate the dynamic hold up, based on the mass balance and phase behavior, also include the gas solubility in oil.

- Calculate the amount of gas injected based on the valve model also consider the upstream and downstream pressure local to the valve.
- The gas injected is calculated based upon a constant compressor output pressure and a correlation for pressure drop over the gas line and choke.

Asheim in his study concluded that analytical solutions are restricted by simplifying assumptions therefore simply provide mathematically proper reference cases (Asheim, Verification of Transient, Multi-Phase Flow Simulation for Gas Lift Applications, 1999). However, when being compared to OLGA, it provided steady state prediction similar to the analytical model, but the dynamic properties were completely different. He said that the reason for this can only be speculated about. The software accounts separately for liquid film flow and liquid droplet flow (Bendiksen, Maines, Moe, & Nuland, The Dynamic Two-Fluid Model OLGA: Theory and Application, 1991).

Nevertheless, OLGA is proven to be valuable for commissioning the gas-lift system as the industry renowned transient software package. OLGA were maintained and validated in joint industry project (JIP) by Nossen and Rasmussen 2001 (Salman, Wittfeld, Lee, Yick, & Derkinderen, 2009)(Bendiksen, Maines, Moe, & Nuland, The Dynamic Two-Fluid Model OLGA: Theory and Application, 1991). The software was developed to simulate slow transients associated with mass transport, including terrain slugging, pipeline startup and shut-in, rate variation, and pigging. The slow simulation has time span ranging from hours to weeks.

OLGA uses unified empirical correlations for gas fraction and pressure drop, and integrated flow regime to the multiphase system. OLGA model is built by applying continuity equations/conservation of mass for gas, liquid bulk, and liquid droplet which may be coupled through interphasial mass transfer as addressed by Bendiksen et al. (Bendiksen, Maines, Moe, & Nuland, The Dynamic Two-Fluid Model OLGA: Theory and Application, 1991). A combined equation for gas and liquid droplet and a separate one for liquid film are used for expressing the conservation of momentum. A mixture energy conservation equation is applied. The software performs thermal calculation by computing the overall heat transfer coefficient from flowing fluid, pipe wall, and anything defined outside the wall. The program can also take into account special phenomena by using built-in PVT package to generate the fluid property tables. These tables are based on a Peng-Robinson, Soave-Redlich-Kwong, or another equation of state. The total mixture composition is assumed to be constant in time along pipeline while the gas and liquid compositions change with pressure and temperatures as result of interfacial mass transfer. In real systems, the velocity difference between the oil and gas phases may cause changes in the total composition of the mixture. This can be fully accounted only in a compositional model. OLGA can treat interface mass-transfer for normal condensation or evaporation and retrograde condensation. This simulator does not require separate correlations for liquid holdup. For each pipeline section, a dynamic flow-regime prediction is required resulting the suitable flow regime as a function of average flow

parameters. The things discussed above shows how OLGA is the most suitable tool to perform investigation of J-shaped gas-lift well model.

2.4 Flow Regime

The study of flow regime provides important insights in explaining the dynamic process of gas-lift system in J-shaped well involving oil and gas which is multiphase in nature. These two fluids have their own physical properties. When they are mixed, there is a wide range of possible flow pattern/regime. They may separate due to differences in densities and velocities and form a rough interface between the liquid and gas phases. It can be more complicated with the presence of water, sand, and wax. This flow regime occurs as a competition between gravitational forces including buoyancy, turbulence, interfacial friction, and lift force. Flow regime itself is a large scale variation in the physical distribution of the gas and liquid phases in a flow conduit as addressed by Danielson et al. (Danielson, Brown, & Bansal, 2000). The regime can affect significantly to pressure drop in the production tubing.

The flow regimes may differ for horizontal pipe, inclined pipe, and vertical pipe. The flow regimes that have been identified for horizontal pipe are stratified flow, slug flow, annular flow, and bubble flow. They occur as a flow development of increasing gas rate for a given liquid rate. In stratified flow, a continuous liquid stream flows at the bottom of the pipe with a continuous stream of gas flowing over as reported by Danielson et al. (Danielson, Brown, & Bansal, 2000). In slug flow, the flow has stratified flow characteristic punctuated by slug of highly turbulent liquid. In the other regime, annular flow, a thin liquid film adheres to the pipe wall and a gas streams through the middle of the conduit containing entrained liquid droplets. Whereas in the bubble flow, a continuous liquid flows with entrained gas bubbles distributed in the liquid.

For vertical pipe, the flow regimes are bubble, slug, churn, and annular flow. In bubble flow, gas phase is dispersed in the form of small bubbles in a continuous liquid phase. On the other hand in slug flow, gas bubbles coalesce into larger bubbles that eventually fill the entire pipe cross section. Between the large bubbles, there are slugs of liquid that contain smaller bubbles of entrained gas. In the other regime churn flow, the larger gas bubbles become unstable and collapse resulting in a highly turbulent flow pattern with both phases dispersed. Whereas in annular flow, gas becomes the continuous phase with liquid flowing in an annulus coating the surface of the pipe, however, there are some droplets entrain in the gas phase.

The J-shaped well has all of these types of pipe. It starts with slight downward inclination, follows with the upward-inclined section, and ends with vertical section. Each of these pipe sections would have effect to the flow regime from time to time in the simulation of the J-shaped gas-lift model as further discussed in section 4.1. Moreover the flow regime may be used as the explanation of why the system produces or not.

Choosing the flow regime can be done by using the flow regime map. In most cases the superficial liquid velocity is plotted against the superficial gas velocity for a given pipe diameter, inclination, and fluids. Flow regime map for horizontal pipe had been proposed among other by Mandhane et al. and Taitel & Duckler (Danielson, Brown, & Bansal, 2000) while the map for vertical pipe had been proposed among other by Barnea et al. (Kaya, Sarica, & Brill, 2001). The determination of flow regime border to another is done by a series of curves based on a variety of dimensionless parameter.

Figure 2-5 shows an example of flow regime map of two-phase horizontal flow. It illustrates that in low superficial gas and liquid velocity the flow is stratified. If the superficial gas velocity is increased with low superficial liquid velocity, the flow changes into stratified wavy. If it is increased further the flow becomes annular. If the superficial liquid velocity is increased with low gas velocity, the flow changes into elongated bubble. If it is further increased the flow becomes dispersed bubble. Slug happens when mixture of fluid having relatively low superficial liquid velocity flowing with high superficial gas velocity. The picture also shows the physic of gas and liquid spatial distribution from each flow regime.

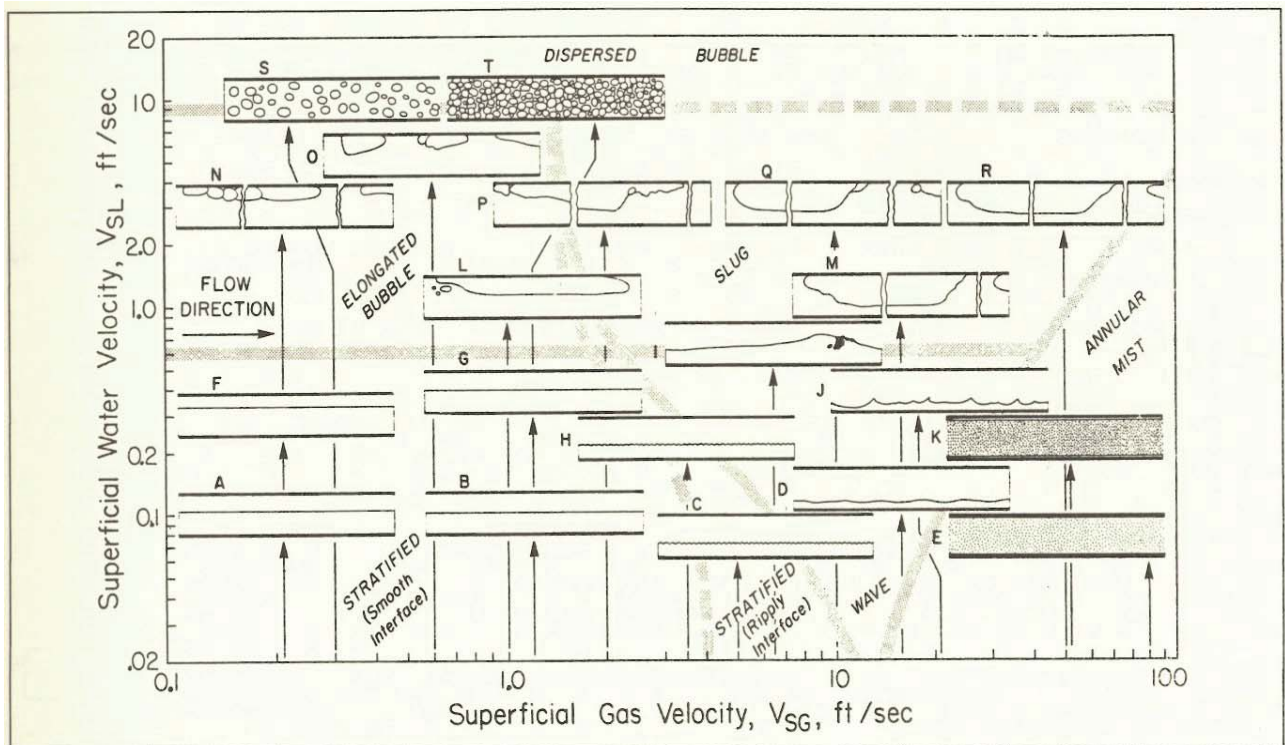


Figure 2-5 Two-phase Horizontal Flow Regime Map (Beggs, 1991)

2.5 Hydrocarbon Phase Behavior

Fluid used in the J-shaped gas-lift model follows hydrocarbon multiphase behavior. Hydrocarbon can be described as single-component, two-component, and multicomponent system. The phase behavior of hydrocarbon may vary with different temperature, pressure, and volume. This relationship is expressed in phase diagrams which are derived from experimental measurements.

Pure component such as methane, ethane, propane, isobutane, n-butane, isopentane, and n-pentane are used in the model as sensitivity studies as further explained in section 3.2. They are done to investigate the effect of those components to the production performance. In a pure/single-component system, at fixed temperature, vapor and liquid can exist in equilibrium at only one pressure which is vapor pressure. Two-component systems are also used in the study. For two-component systems or binary systems, two phases can exist in equilibrium at various pressures at the same temperature. In binary system, the thermodynamic and physical properties of the systems change with the compositions. The phase behavior of multicomponent hydrocarbon systems in the liquid-vapor region is very similar to that of binary system. These systems which are also used in the study as further explained in section 3.2 are more complex with more number of components involved.

Figure 2-6 shows an example of phase diagram for multicomponent system. It is seen from the figure, the gas phase lay above dew point curve and the right side of critical point. Liquid phase lay above the bubble point curve and the left side of critical point. Below bubble point curve and dew point curve lay the two phase region. At point 1, the fluid is in liquid phase. As the pressure decrease to point 2, the fluid is still at liquid phase while at the bubble point meaning that if the pressure is further decreased gas phase start to occur in the fluid solution. Decreasing the pressure further to point 3 makes the gas occur more than 50% of fluid's volume.

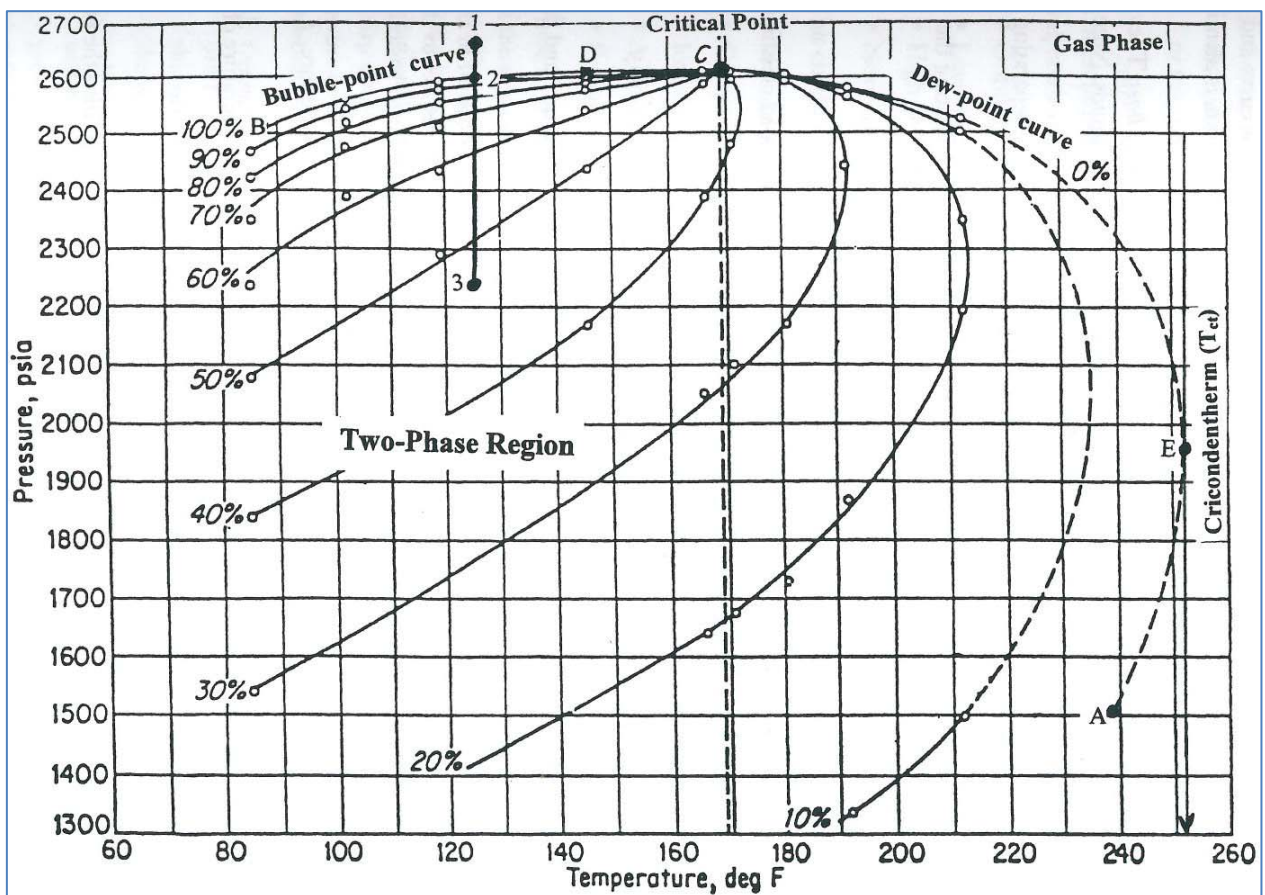


Figure 2-6 P-T Phase Diagram for Multicomponent System (Ahmed, 2007)

Hydrocarbon in liquid and gas phase can coexist in the state of equilibrium when pressure, temperature, and composition of the system remain constant. One concept, among other, to describe the calculation of equilibrium state is to perform volumetric and compositional calculation on a hydrocarbon system as explained by Ahmed (Ahmed, 2007) which is called flash calculation. The flash calculation concept is done to identify the amounts of mole of liquid and gas coexisting in a system at a given pressure and temperature. These amounts of mole are the composition of the existing hydrocarbon phase. With the use of compositional tracking on the J-shaped gas-lift model, every single fluid component is accounted throughout the calculation. However, the gas phase and liquid phase in hydrocarbon fluid mixture can move at different velocities so there is no sufficient time to reach the equilibrium. Therefore, the model also considers the effect of slip velocities. Pourafshary et al. discussed that to consider this effect at each block in the wellbore the gas phase was assumed in equilibrium with only a portion of the liquid phase (Pourafshary, Varavei, Sepehmoori, & Podio, 2008).

3. Model Development

3.1 J-shaped Well

Complex well geometry causes slugging as indicated by Dharma (Dharma, 2012). It is complex because of the pipeline terrain or the designed well profile as can be seen in Figure 3-1. J-shaped well in Figure 3-1 is an example of a well with complex geometry and used in this work. The well consists of a vertical section followed by a build-up section, an inclined section, one more build-up section, and one last inclined section with different inclination to the first one. It also comprises of the toe where the perforation is located and the heel where the bottom point is located. J-section in J-shaped well can develop liquid blockage as depicted in Figure 3-2. This liquid blockage initiates slugging. The liquid coming from reservoir accumulates in the heel section creating high gravity dominated pressure drop. It blocks the fluid flow from toe. The gas which is also coming from toe builds up the pressure downstream of the liquid blockage until it has sufficient pressure to displace the accumulated liquid. The repetition of these would happen when the reservoir pressure is not sufficient against the liquid accumulating effect (Dharma, 2012).

Gas-lift operation is proposed to solve this slugging problem. The well is modeled in OLGA to analyze the mechanism of how gas lift can initiate the well and gas-lift gas composition can affect the liquid production. The well geometry in the model is constructed as close as possible to the real well geometry. Perforation is placed at the toe and a gas-lift valve is placed at a fixed point considered as the end of the J-section. Cased hole is used as a completion technique. Table 3-1, Table 3-2, and Table 3-3 show complete geometry of the well.

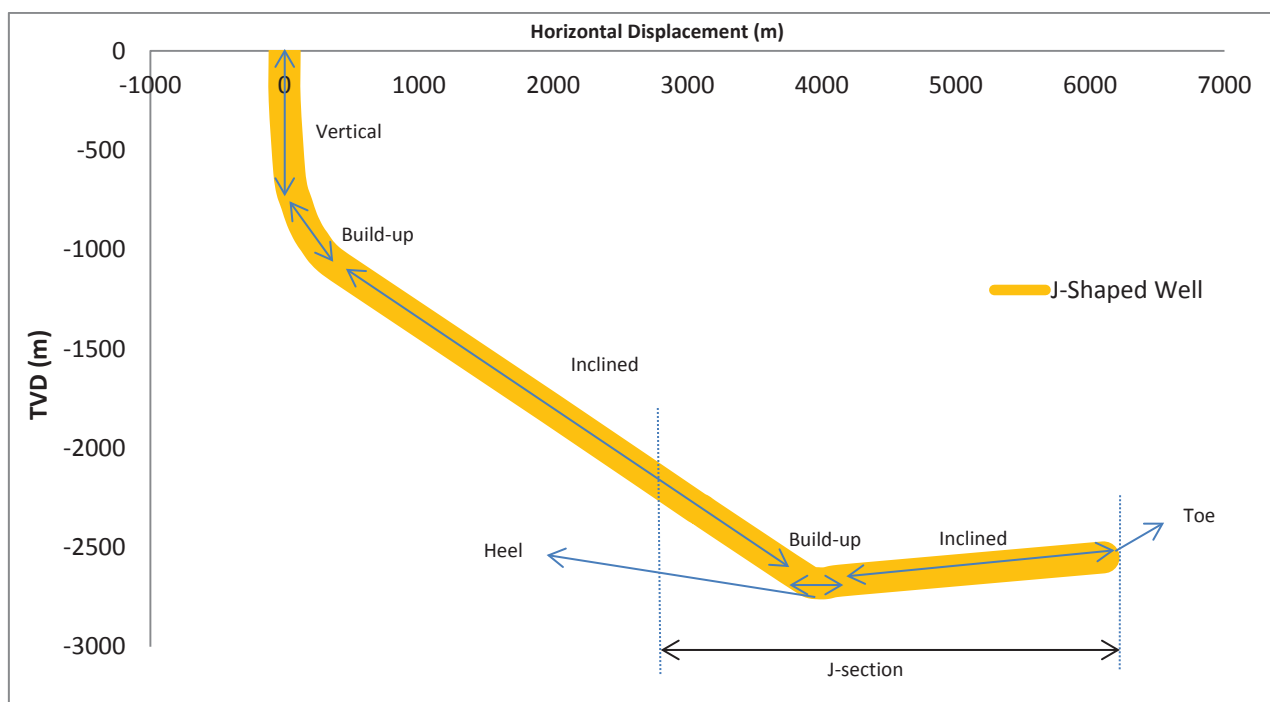


Figure 3-1 J-Shaped Well Profile

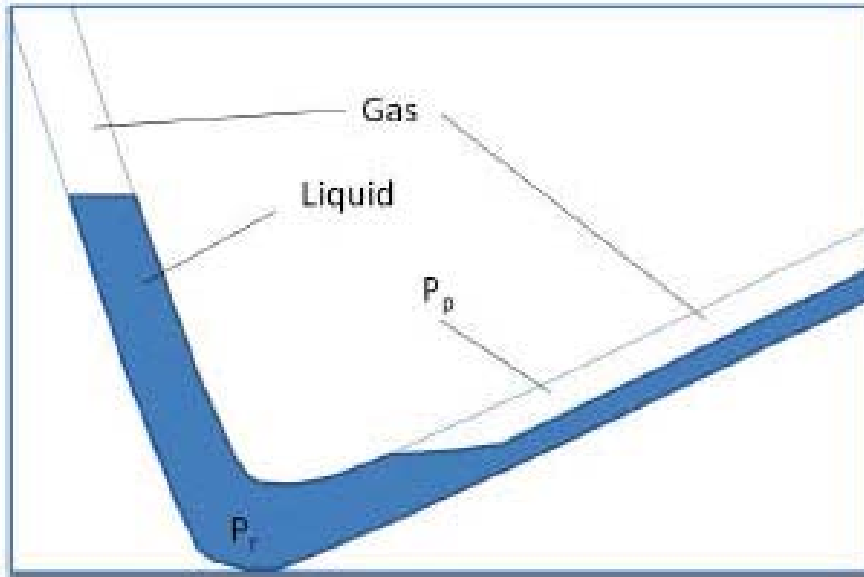


Figure 3-2 Liquid Blockage in J-section of J-shaped Well (Dharma, 2012)

Table 3-1 Geometry of Tubing

Pipe	x [m]	y [m]	Length [m]	Elevation [m]	# Section	Length of sections (list [m])	Diameter [m]	Roughness [m]
Start Point	3070	-2300						
Lower Inclined	1980	-1800	1199.21	500	3	3:399.736	0.100533	1.52E-05
Upper Inclined	410	-1090	1723.08	710	3	3:574.36	0.100533	1.52E-05
Lower Build Up	330	-1050	89.4427	40	2	2:44.7214	0.100533	1.52E-05
Build up 1	285	-1020	54.0833	30	1	54.0833	0.100533	1.52E-05
Build up 2	260	-1000	32.0156	20	1	32.0156	0.100533	1.52E-05
Build up 3	220	-960	56.5685	40	1	56.5685	0.100533	1.52E-05
Build up 4	180	-920	56.5685	40	1	56.5685	0.100533	1.52E-05
Build up 5	130	-850	86.0233	70	1	86.0233	0.100533	1.52E-05
Build up 6	90	-770	89.4427	80	1	89.4427	0.100533	1.52E-05
Build up 7	55	-700	78.2624	70	1	78.2624	0.100533	1.52E-05
Upper Build Up	35	-610	92.1954	90	1	92.1954	0.100533	1.52E-05
Lower Vertical	0.5	-250	361.649	360	4	4:90.4123	0.100533	1.52E-05
Upper Vertical	0	0	250	250	5	5:50.0001	0.100533	1.52E-05

The well is divided into 3 geometry sections. One section represents the J-section geometry of the well as detailed in Table 3-2. Table 3-1 shows the rest of production tubing geometry from injection point to the wellhead. The last section is gas-lift gas injection conduit from the compressor to the well head and goes through the annulus all the way to injection point as described by Table 3-3. Each of these geometry sections is further divided into several pipe-parts and subsections to give better definition to pipe-bent geometry, to allow easier simulation, and to perform accurate calculation. Appropriate dimensions, such as length, position, inclination, diameter, and pipe surface roughness, are assigned to each of these pipe sections.

To accommodate these three sections, four nodes are incorporated in the model. These nodes represent perforation, injection point in the tubing, injection point of gas-lift gas injection on the surface, and wellhead. Starting from the perforation node, the J-section is attached to it and J-section is ended at injection point in the tubing node. The tubing section starts from injection point in the tubing node and ends at wellhead node whereas the gas-lift gas injection section starts from injection point of gas-lift gas injection on the surface node and ends at injection point in the tubing node. The injection point in the tubing node plays an important role as a mixing point of liquid and gas coming from reservoir and gas-lift gas injection from annulus. There are critical multiphase flow phenomena occurring around this point which has not been fully understood, that governing the unloading mechanism of gas-lift operation.

In the model layout, the bottomhole node and injection point of gas-lift gas injection on the surface node are modeled by using closed boundary node. The closed node represents a closed boundary with no flow through it. This node can be combined with a source or a well definition in the flow path to state flow source. The injection point node is modeled by internal node which represents branch where the flow is merging or splitting. Wellhead node is modeled by pressure node which represents pressure boundary of the model.

Table 3-2 Geometry of J-section

Pipe	x [m]	y [m]	Length [m]	Elevation [m]	# Section	Length of sections (list [m])	Diameter [m]	Roughness [m]
Start Point	6100	-2550						
Toe	4250	-2660	1853.27	-110	5	5:370.653	0.154788	1.52E-05
Start of heel	4100	-2670	150.333	-10	3	3:50.111	0.154788	1.52E-05
Middle of heel	4030	-2680	70.7107	-10	3	3:23.5702	0.154788	1.52E-05
Bottom point	3970	-2680	60	0	0		0.154788	1.52E-05
End of heel	3900	-2670	70.7107	10	3	3:23.5702	0.154788	1.52E-05
Start of inclined	3140	-2330	832.586	340	5	5:166.517	0.154788	1.52E-05
Gauge depth	3100	-2310	44.7214	20	2	2:22.3607	0.154788	1.52E-05
Injection depth	3070	-2300	31.6228	10	2	2:15.8114	0.154788	1.52E-05

For modeling purpose, it is also important to utilize instrumentation to the well. Gas-lift gas injection source needs to be installed at the start of gas-lift gas injection section. It is done to set the mass or volumetric flow rate or volume fraction of the feed which is entering the gas-lift pipeline system. A gas-lift valve is installed at the end of this section to make it possible to introduce gas injection into production tubing to lift the fluid to the surface. As an addition a check valve is installed just before it. The gas-lift valve (GLV) performance relationship on the specific pressure and temperature condition used in the model uses GLV

response from correlation taken from the Valve Performance Clearinghouse™ (VPC™) database from SPT Group. A check valve prevents the total flow from flowing in the wrong direction. Well/Perforation is set at the start of J-section. A well Module is available for well flow applications where the reservoir properties and the inflow relationships play an important role in the modeling. Surface choke/valve is installed at the end of tubing section. The valve models the pressure drop for flow through chokes and/or valves. Figure 3-3 shows the layout of the model.

Table 3-3 Geometry of Gas-lift Gas Injection Section (Annulus)

Pipe	x [m]	y [m]	Length [m]	Elevation [m]	# Section	Length of sections (list [m])	Diameter [m]	Roughness [m]
Start Point	3070	-2300						
Lower inclined + GLM	1980	-1800	1199.21	500	3	3:399.736	0.254	1.00E-05
Upper inclined	410	-1090	1723.08	710	3	3:574.36	0.254	1.00E-05
Lower build up	330	-1050	89.4427	40	2	2:44.7214	0.254	1.00E-05
Build up 1	285	-1020	54.0833	30	1	54.0833	0.254	1.00E-05
Build up 2	260	-1000	32.0156	20	1	32.0156	0.254	1.00E-05
Build up 3	220	-960	56.5685	40	1	56.5685	0.254	1.00E-05
Build up 4	180	-920	56.5685	40	1	56.5685	0.254	1.00E-05
Build up 5	130	-850	86.0233	70	1	86.0233	0.254	1.00E-05
Build up 6	90	-770	89.4427	80	1	89.4427	0.254	1.00E-05
Build up 7	55	-700	78.2624	70	1	78.2624	0.254	1.00E-05
Upper build up	35	-610	92.1954	90	1	92.1954	0.254	1.00E-05
Lower vertical	0.5	-250	361.649	360	4	4:90.4123	0.254	1.00E-05
Upper vertical	0	0	250	250	5	5:50.0001	0.254	1.00E-05
Surface line	-12	0	12	0	2	02:06	0.254	1.00E-05

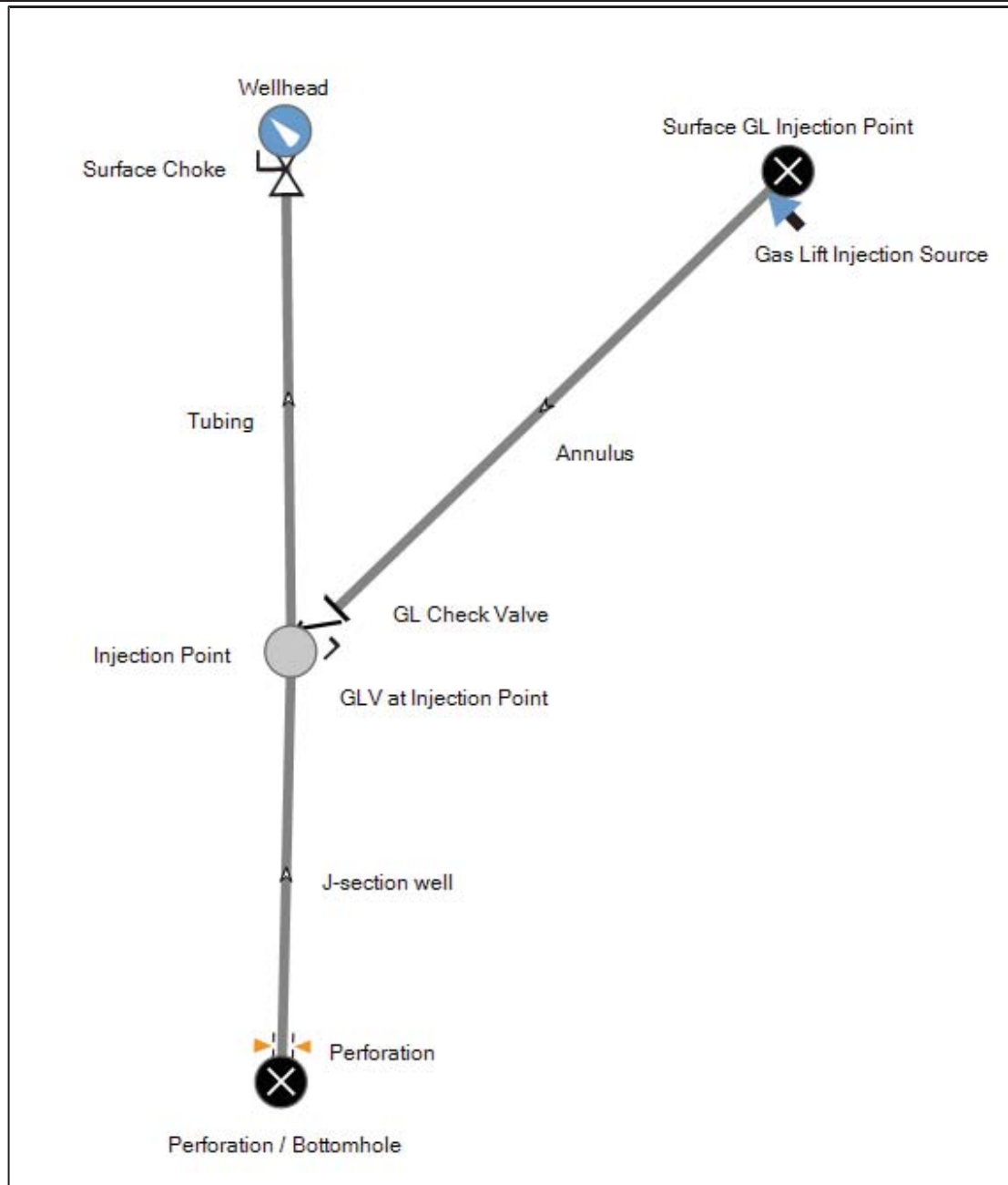


Figure 3-3 Model Layout

3.2 PVT Data of Reservoir Fluid and Gas-lift Injection Gas

To be able to track the spatial and temporal change in flow rate and composition of the hydrocarbon fluid in every element of gas lift process, the model utilizes the compositional tracking model. It combines the multiphase simulation with customized calculation for fluid properties and mass transfer. In this model, every single fluid component in each phase is accounted throughout the calculation. The model needs PVT feed file generated by PVTsim-Calsep. This PVT feed file contains information about the main fluid composition used in a perforation/well and boundary or initial conditions used in the simulation, and the composition of the feed's components. It's also necessary to define additional feeds containing the fluid composition used in gas-lift gas injection source.

PVT data contains the composition of reservoir fluid and gas-lift injection gas which need to be defined. This data is stated in the model explicitly and used in the simulation. This data definition is important because the compositional effect of particularly gas-lift injection gas to the production performance needs to be investigated. The fluid properties along the pipelines will be calculated continuously during the simulation based upon the current pressure, temperature, and composition. These calculations are part of a built-in PVT package in OLGA delivered by Calsep with very similar functions to PVTsim. Table 3-4 shows the reservoir fluid composition.

Table 3-4 Reservoir Fluid Composition

Component	Mol %	Mol weight (g/mol)	Liquid Density (g/cm ³)
N ₂	0.224	28.014	
CO ₂	0.224	44.01	
C1	49.883	16.043	
C2	5.642	30.07	
C3	3.418	44.097	
iC4	0.953	58.124	
nC4	3.585	58.124	
iC5	1.232	72.151	
nC5	1.681	72.151	
C6	3.137	86.178	0.664
C7	2.063	96	0.7672
C8	1.956	107	0.7762
C9	1.855	121	0.7841
C10-C19	9.284	195.264	0.8166
C20-C27	5.773	322.745	0.8487
C28-C34	3.634	428.459	0.8674
C40+	5.457	519.876	0.8803

Furthermore the molar fractions and their derivatives with respect to the current conditions at phase equilibrium, and physical limit for the temperature and pressure used in the PVT calculations, are also delivered by this package. The temperature range is from -200 to 500 C and the pressure range is from 0.05 to 1000 bara. If the temperature or pressure goes out of range, they are reset to the upper or lower limits. These reset values are only used in the PVT calculations and not fed back to the overall calculations of temperature and pressure. The phase equilibrium / flash calculation in the model in this work is based on the Soave-Redlich-Kwong (SRK) equation of state (EOS). The fluid data in the feed file are based on this equation and the same EOS will be adopted in the PVT package in OLGA simulation.

The algorithm used in flash calculation in OLGA is a two-phase flash-type. This flash-type is chosen because no aqueous components are included as a part of the feed. It treats water and hydrate inhibitors as an inert components. A two-phase flash is carried out for the hydrocarbon components. There will neither be any aqueous components in the

hydrocarbon phases nor hydrocarbon components in the water phase. Classical mixing rule is used for all component pairs for the two-phase flash calculation.

Table 3-5 Gas-lift Gas Injection Composition

Component	Mol %	Mol weight (g/mol)
N ₂	0.3	28.014
CO ₂	0.4	44.01
C1	85	16.043
C2	8	30.07
C3	4	44.097
iC4	0.6	58.124
nC4	0.8	58.124
iC5	0.5	72.151
nC5	0.4	72.151

Table 3-5 shows the composition of gas-lift gas injection. This composition is a base composition case used to validate the model as further reviewed in section 4.1. Both gas-lift gas injection and reservoir fluid are multicomponent hydrocarbon system. To investigate the gas-lift gas injection compositions effect to production performance, sensitivity studies of their compositions need to be performed. To study this effect, precise selection of gas-lift gas injection composition's sensitivities are prepared. Individual pure and binary components of gas-lift gas are selected to investigate what effect each component gives to the production performance as will be discussed in section 4.2 and section 4.3. Component boundary to the system's composition is drawn from the study to conclude the effect. The cases are prepared with the following combinations:

- Pure systems: C1, C2, C3, iC4, nC4, iC5, and nC5
- Binary systems (in mol% of each component):
 - C1/C2 : 95/05, 90/10, 85/15, 80/20, 75/25, 70/30, 65/45, 60/40, 55/45, & 50/50
 - C1/C3 : 95/05, 90/10, 85/15, 80/20, 75/25, 70/30, 65/45, 60/40, 55/45, & 50/50
 - C1/iC4 : 95/05, 90/10, 85/15, 80/20, 75/25, 70/30, 65/45, 60/40, 55/45, & 50/50
 - C1/nC4 : 95/05, 90/10, 85/15, 80/20, 75/25, 70/30, 65/45, 60/40, 55/45, & 50/50
 - C1/iC5 : 95/05, 90/10, 85/15, 80/20, 75/25, 70/30, 65/45, 60/40, 55/45, & 50/50
 - C1/nC5 : 95/05, 90/10, 85/15, 80/20, 75/25, 70/30, 65/45, 60/40, 55/45, & 50/50

In addition to the pure single and binary components, the sensitivity study was extended to include industrial multicomponent gas-lift system as further discussed in section 4.4. As mentioned before, Table 3-5 comprises the base composition of gas-lift gas injection. This was done by reducing the content of each individual component and compensating by addition to other component to reach a composition of 100% mole. For example, to observe the effect of increasing C1 fraction the rest of the components i.e. C2, C3, iC4, nC4, iC5, and nC5 fraction are reduced for balancing the composition. The investigated variation was 1%, 5%, 8%, and 10%. In this analysis, C1 was kept to be highest fraction to be realistic in the

investigation. The same approach was followed for the other components. The detailed composition for each variation is presented in Table 3-6, Table 3-7, Table 3-8, and Table 3-9.

Table 3-6 Composition of Gas-lift Gas Injection with 1% Content Change

Component	Increased Component (mol %)						
	C1	C2	C3	iC4	nC4	iC5	nC5
N ₂	0.297	0.297	0.297	0.297	0.297	0.297	0.297
CO ₂	0.396	0.396	0.396	0.396	0.396	0.396	0.396
C1	85.15	84.15	84.15	84.15	84.15	84.15	84.15
C2	7.92	8.92	7.92	7.92	7.92	7.92	7.92
C3	3.96	3.96	4.96	3.96	3.96	3.96	3.96
iC4	0.594	0.594	0.594	1.594	0.594	0.594	0.594
nC4	0.792	0.792	0.792	0.792	1.792	0.792	0.792
iC5	0.495	0.495	0.495	0.495	0.495	1.495	0.495
nC5	0.396	0.396	0.396	0.396	0.396	0.396	1.396

Table 3-7 Composition of Gas-lift Gas Injection with 5% Content Change

Component	Increased Component (mol %)						
	C1	C2	C3	iC4	nC4	iC5	nC5
N ₂	0.285	0.285	0.285	0.285	0.285	0.285	0.285
CO ₂	0.38	0.38	0.38	0.38	0.38	0.38	0.38
C1	85.75	80.75	80.75	80.75	80.75	80.75	80.75
C2	7.6	12.6	7.6	7.6	7.6	7.6	7.6
C3	3.8	3.8	8.8	3.8	3.8	3.8	3.8
iC4	0.57	0.57	0.57	5.57	0.57	0.57	0.57
nC4	0.76	0.76	0.76	0.76	5.76	0.76	0.76
iC5	0.475	0.475	0.475	0.475	0.475	5.475	0.475
nC5	0.38	0.38	0.38	0.38	0.38	0.38	5.38

Table 3-8 Composition of Gas-lift Gas Injection with 8% Content Change

Component	Increased Component (mol %)						
	C1	C2	C3	iC4	nC4	iC5	nC5
N ₂	0.276	0.276	0.276	0.276	0.276	0.276	0.276
CO ₂	0.368	0.368	0.368	0.368	0.368	0.368	0.368
C1	86.2	78.2	78.2	78.2	78.2	78.2	78.2
C2	7.36	15.36	7.36	7.36	7.36	7.36	7.36
C3	3.68	3.68	11.68	3.68	3.68	3.68	3.68
iC4	0.552	0.552	0.552	8.552	0.552	0.552	0.552
nC4	0.736	0.736	0.736	0.736	8.736	0.736	0.736
iC5	0.46	0.46	0.46	0.46	0.46	8.46	0.46
nC5	0.368	0.368	0.368	0.368	0.368	0.368	8.368

Table 3-9 Composition of Gas-lift Gas Injection with 10% Content Change

Component	Increased Component (mol %)						
	C1	C2	C3	iC4	nC4	iC5	nC5
N ₂	0.27	0.27	0.27	0.27	0.27	0.27	0.27
CO ₂	0.36	0.36	0.36	0.36	0.36	0.36	0.36
C1	86.5	76.5	76.5	76.5	76.5	76.5	76.5
C2	7.2	17.2	7.2	7.2	7.2	7.2	7.2
C3	3.6	3.6	13.6	3.6	3.6	3.6	3.6
iC4	0.54	0.54	0.54	10.54	0.54	0.54	0.54
nC4	0.72	0.72	0.72	0.72	10.72	0.72	0.72
iC5	0.45	0.45	0.45	0.45	0.45	10.45	0.45
nC5	0.36	0.36	0.36	0.36	0.36	0.36	10.36

3.3 OLGA model

OLGA simulation is organized by defining a simulation, information, and administration object. Simulation object is defined by creating flow path geometry & component network, boundary and initial condition, process equipment, thermal component, and well model. These objects are combined later to form a simulation network. To give value and reference to the simulation object, information object is used. After that, various parts of simulation need to be controlled by administration objects. The controlled parts are general information about the model, feed file used, simulation time, activation of steady state pre-processor, activation of compositional tracking, type of flash calculation used, calculated parameter(s), and presentation of the result(s).

As mentioned before, Table 3-1, Table 3-2, Table 3-3, and Figure 3-3 show the flow path geometries and component network respectively used in the model. Each flow path is made up of a sequence of pipes and each pipe is divided into sections representing a controlled volume. Each path must start and end at a node. These sections division creates spatial mesh discretization in the numerical model. Boundary and initial condition are applied to this mesh. The variable can be flow and/or volume variable. Flow variables, such as velocity and mass flow, are applied to section boundary while volume variables, such as pressure and temperature, are applied as average values to the section volumes.

Another simulation object that needs to be defined in the model is the process equipment. Process equipment is used to regulate or control the varying flow conditions in a multi-phase flow line. The process equipment simulated in OLGA includes critical and sub-critical chokes with fixed or controlled openings, check-valves, compressors with speed and anti-surge controllers, separators, heat exchangers, pumps and mass sources and sinks. Only valve with choke function, gas-lift valve and check valve are used in the J-shaped gas-lift well model. A surface choke valve is installed at the end of tubing section representing the wellhead. It models the pressure drop and controls the flow to critical flow. Hydrovalve valve model is

chosen from available data sheet because it is used for choke with liquid/gas characteristic. A discharge coefficient, C_D , and maximum choke diameter must be defined for the choke. The model uses the default value as discharge coefficient that is 0.84. The valve diameter is 0.100533 m. The relative opening of the valve can be set as a function of time; however, the valve in this model opens from the start of simulation with 10 seconds stroke time.

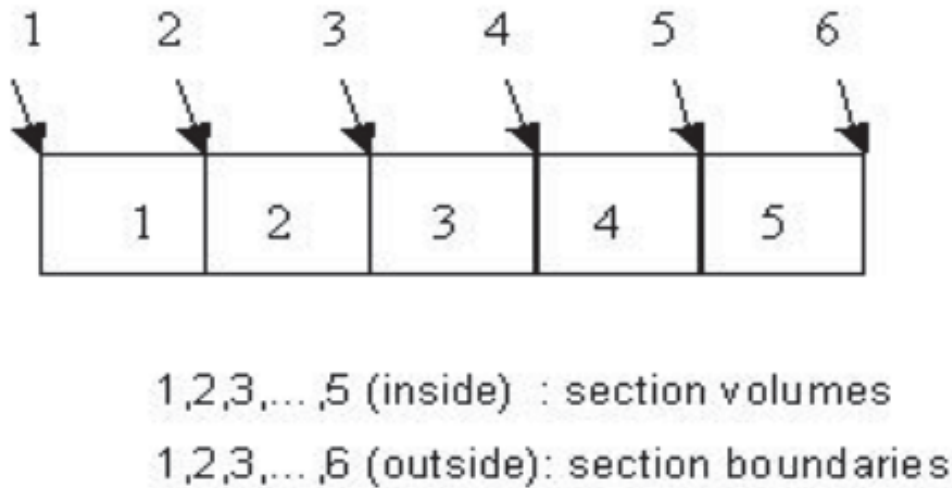


Figure 3-4 Mesh Discretization Applied to Flow Path in the Model

A check valve is installed at the end of annulus section just before the gas-lift valve, to prevent the flow going back into the annulus. This valve closes if the total volume flow across the valve is in the wrong direction. It remains closed until the pressure difference across it is sufficiently large to give flow in the desired direction. A gas-lift valve is installed at the end of annulus section and its response is computed by using data from a demo database of Valve Performance Clearinghouse™ (VPC™) provided within the OLGA. The port size is 12/64 inches. The relative opening of the valve can be set as a function of time. The gas-lift valve in the model opens from 8.01 hours of simulation time with no stroke time, to simulate when the gas-lift gas is injected.

A source of gas-lift gas injection is installed at the start of annulus section to model the inflow of gas-lift gas. In this model, the source type is set to be a pressure driven. It means that the mass flow rate is to be calculated based on the opening of the choke/valve/orifice through which a mass source is introduced into the pipe section. The choke opening is regulated by a specified stroke time which is 0 second with 2 inches diameter of valve. The upstream or downstream pressure and temperature of the source can be specified to consider the expansion. The source pressure chosen for this model is 163 bara, and the source temperature is 5°C. Mole fraction of gas mass flow relative to the equilibrium fluid composition at the source temperature and pressure are specified. Fluid composition used as gas-lift gas injection is referred to Table 3-5 and it is defined as the feed file for the gas-lift gas injection source. The complete list of OLGA information and administration objects are presented in Appendix B1, Appendix B2, Appendix B3, Appendix B4, Appendix B5, and Appendix B6.

3.4 Gas-lift Performance Evaluation

Evaluation of the well performance is required to justify whether the well needs gas-lift or not. Furthermore evaluation of gas-lifted well is also necessary to check the validity of the model. To completely building the model, a well/source is placed at the bottom of the J-section. The well statement in OLGA is used to define required data for calculating the flow performance of wells which can be defined by specifying the coefficients used in the inflow correlations directly, or specifying well/reservoir variables. This model uses linear formula for the production of typical oil reservoir. Linear model uses productivity index (PI) as a mathematical means of expressing the ability of reservoir to deliver fluids to the wellbore. The PI unit is stated as the volumetric rate per pressure of drawdown at the sandface (bbl/d/psi).

In this model, the base PI used is 11 bbl/d/psi. This PI is also used in OLGA modeling based on the P_{RES} of 185 bara and T_{RES} of 93 °C. The water fraction and gas fraction in the model are taken from the equilibrium PVT table. The isothermal option in the model assumes that the reservoir fluid enters the well at the reservoir temperature and reservoir fluid enthalpy is calculated on the basis of reservoir temperature and well pressure.

Nodal analysis is performed to this model to evaluate the system's performance. The intersection between the IPR and VLP of the model defines the operating flow rate and pressure at bottom node. Figure 3-5 shows the IPR-VLP curve of the model without the aid of gas-lift. The curves are not intersecting, meaning that there's no flow rate can be produced out of the model naturally. Later on gas-lift is employed to the model and installed at 4168.5 m mD with injected gas rate Q_{INJ} 2.1 MMSCF/d and gas injection density at standard condition. The reservoir oil density is 836.2 kg/m³ and the reservoir gas specific gravity is 0.81712 at standard condition. The gas-lift gas specific density is 0.6537 at standard condition. Those densities are calculated by PVTsim from the composition given in Table 3-4 and Table 3-5.

Figure 3-6 shows the intersecting IPR-VLP curve of the system when gas-lift is installed. These IPR-VLP curves are generated by using IPM PROSPER software as steady state analytical software to analyze the system in steady state. It uses petroleum experts 2 as the vertical lift correlation with tope node pressure P_{WH} 30 bara. The operating point of the system with gas-lift is at Q_{OIL} 5648.5 STB/d and P_{WF} 149.24 bara with Q_{GAS} 3.1 MMSCF/d.

In dynamic OLGA modeling, the system is first simulated without the aid of gas lift. There is no production on the wellhead and as can be seen from Figure 3-7, the pressure at injection depth P_{ID} is 177.36 bara. Therefore, the injection pressure from annulus should be greater than this pressure. The topside gas-lift gas injection pressure P_{INJ} is set to be at 163 bara for the system and the whole sensitivity study.

For this system to work with gas-lift injection, the injection pressure at injection point from the annulus is 200 bara. The gas injection used is the one that has composition presented in Table 3-5. For this case the P_{WF} is 147.21 bara as seen from Figure 3-7 which is comparable to steady state PROSPER simulation. Figure 3-7 shows that with the aid of gas-lift, the pressure gradient becomes lower thus lowering the P_{WF} .

One more comparison is done to validate the model. With steady state pre-processor activated, OLGA modeling computes a steady state solution for the system. Steady state pressures, temperatures, mass flows, liquid hold-ups, and flow regimes are calculated along the pipelines. The steady state pre-processor calculation is needed to get a consistent initial state as a basis for dynamic simulations. The solution calculated by the steady state pre-processor and the solution obtained by the dynamic solver until a steady state is achieved may not be equal. For slugging, the steady state pre-processor may find a solution that varies from the average value in the transient solution as there is no truly steady-state condition.

Operating point achieved by the steady state pre-processor OLGA simulation is at Q_{OIL} 5655 STB/d and P_{WF} 149.78 bara. The Q_{GAS} is 5 MMSCF/d. On the other hand, operating point achieved by dynamic OLGA simulation is at Q_{OIL} 6043.82 STB/d and P_{WF} 147.21 bara. The Q_{GAS} is 6.97 MMSCF/d. Overall comparison value of each operating point by different simulator is shown in Table 3-10. By comparing these points, IPR-VLP relationships of the J-shaped gas-lift well system from different simulator are evaluated.

Q_{OIL} from PROSPER is in a good agreement with the one from steady state OLGA due to similar productivity index linear formula used in the model to model the reservoir's deliverability in a steady state simulation. However, dynamic OLGA gives different result. It shows higher oil production. This is happening because in fully compositional modeling, the gas and liquid compositions change with pressure, temperatures, and velocity difference between those phases as the result of interfacial mass transfer. In dynamic modelling, the slugging is accounted in the simulation. Slugging happens when gas-lift gas is injected to the tubing until the flow in the tubing is fully stable. This rate of fluctuation is caused by multiphase behavior during that period and would certainly affect the rate when flow stability is achieved.

Table 3-10 Operating Point of the J-shaped Gas-lift Well System

	PROSPER	STEADY STATE OLGA	DYNAMIC OLGA
Q_{OIL} (STB/d)	5648.5	5655	6043.82
Q_{GAS} (MMSCF/d)	3.1	5	6.97
P_{WF} (bara)	149.24	149.78	147.21

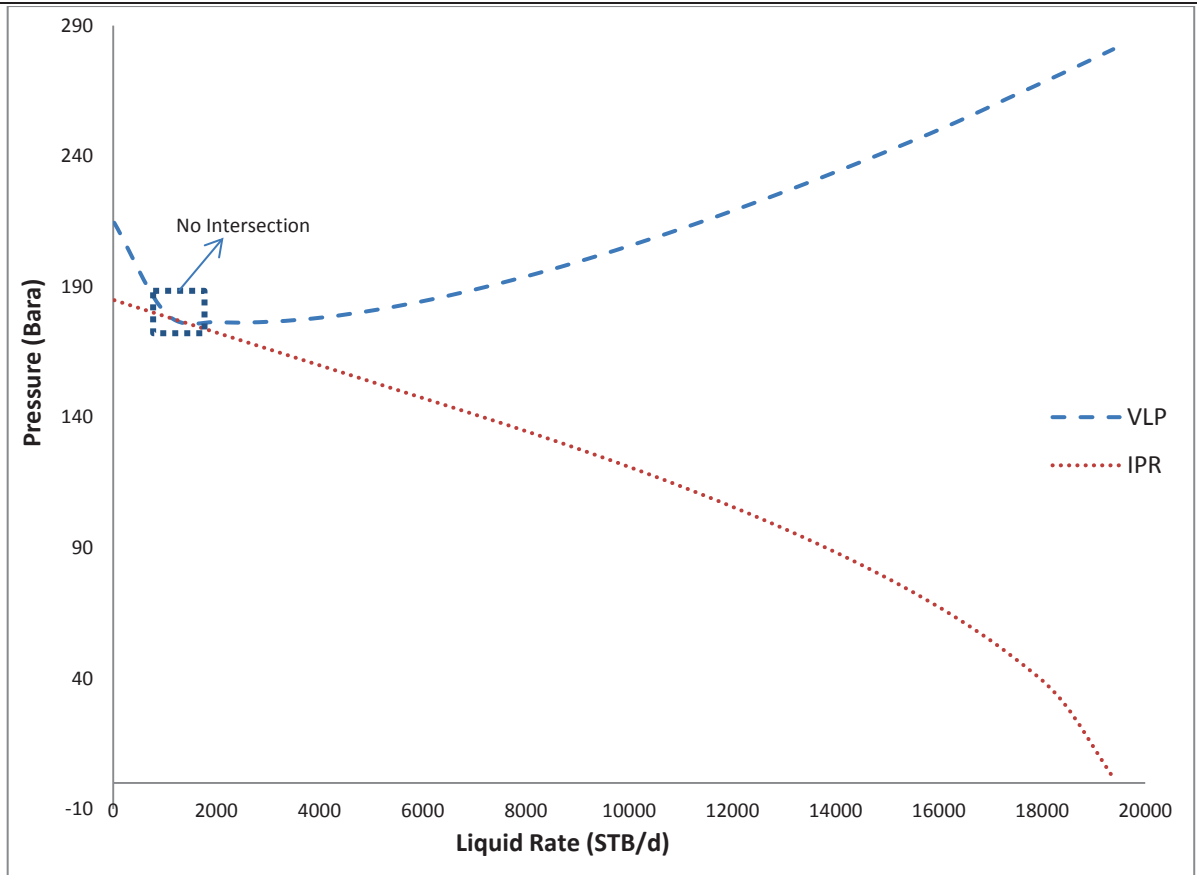


Figure 3-5 IPR - VLP Curve of the System Without the Aid of Gas-lift

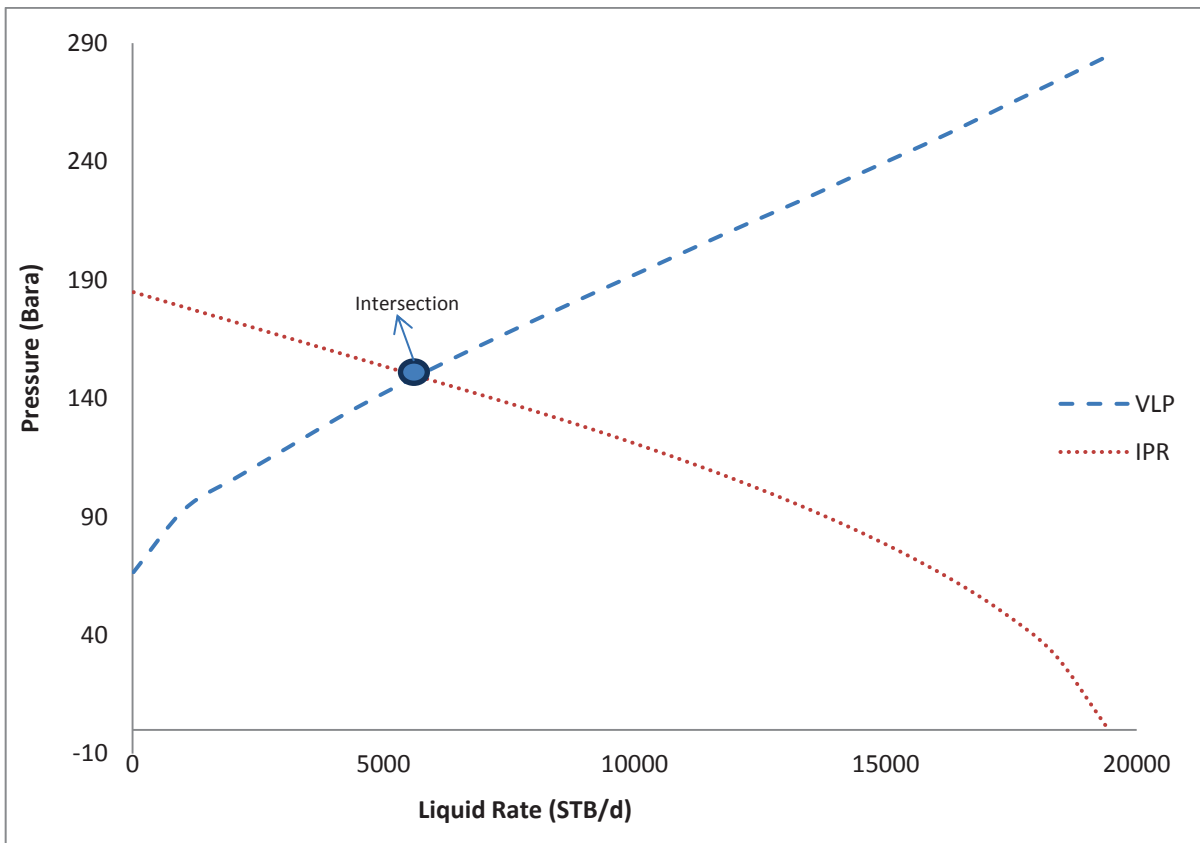


Figure 3-6 IPR - VLP Curve of the System With the Aid of Gas-lift

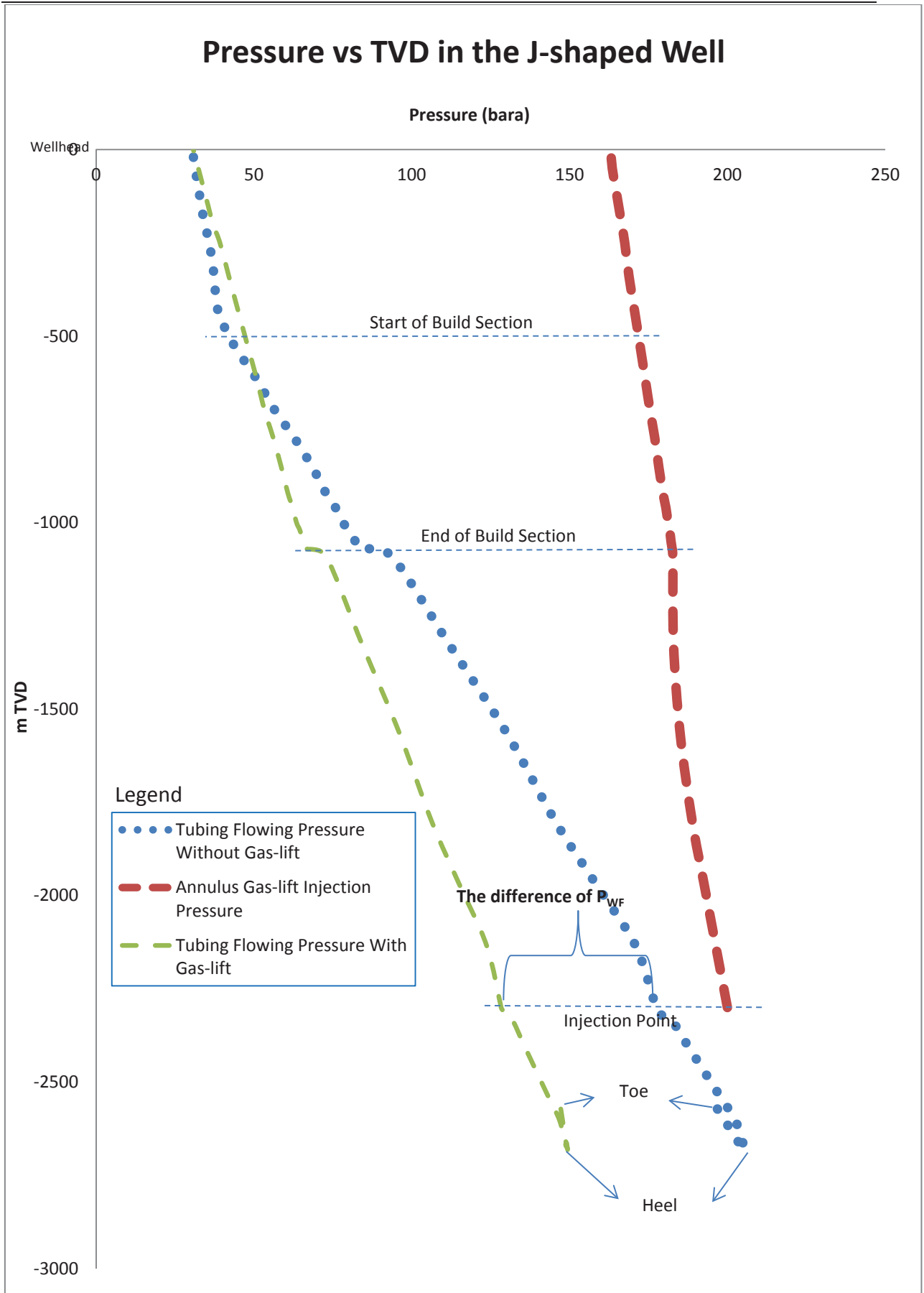


Figure 3-7 Pressure vs TVD in the J-shaped Well

Different value of Q_{GAS} occur because different approach is used in PROSPER and OLGA. In PROSPER Q_{GAS} is calculated only based on GOR using the selected black oil PVT correlation. Otherwise in OLGA, the gas volume fraction is dynamically calculated using selected EOS in equilibrium based on current pressure, temperature, and composition in each pipe sections which certainly would affect the Q_{GAS} . The P_{WF} are in a good agreement because similar liquid holdup and pressure gradient are predicted from the multiphase correlation used in PROSPER and the flow model used in OLGA.

4. Sensitivity Study Results and Discussion

Sensitivity study is most suitable to design application where a number of hypothetical cases must be run. The specific combinations of hypothetical cases are applied to the model. They are run to see and give more clear understanding of what effect each combination has on the simulation result. Optimum result criterion is defined by finding the corresponding input combination. The sensitivity is approached by changing one variable at a time while keeping others at their baseline values to see what effects the variable yields on the simulation output. The process is repeated with different value on the same or different variable. The sensitivity is measured by monitoring changes in the output. This seems a logical approach as any change observed in the output is due to the one variable changed. Moreover all effects are computed with reference to the same base case.

The objectives of this sensitivity study are to explain comprehensively the mechanism of dynamic accumulation of the fluid and development of pressure in the J-section and injection point, and to investigate the effect of gas-lift gas composition to the production performance. In the chapter 3, the J-shaped model has been described and evaluated. This model is used as a base case to the sensitivity study performed. As mentioned before, sensitivity study is needed to see and understand specific combinations of hypothetical cases. Case of pure and binary system of gas-lift gas injection are selected to determine what effect each component gives to the production performance.

As preliminary result, it is identified which cases are producing oil at wellhead and which cases aren't. Then, the results obtained from this preliminary analysis are sorted based on the amount of production such as maximum, minimum, and no production. The results are also composed to see whether any trend could be drawn. Afterwards those preliminary results are compared to each other to understand the dynamic mechanism taking place in the system. Furthermore component boundary to the system's composition is drawn from the study representing the most affecting component to the system. These boundaries are implemented to the industrial multicomponent system to see the effect in a realistic system which would conclude the effect of gas-lift gas composition to the production performance.

The complete variable combination used in the study has been presented in section 3.2, with total of 72 cases combination including the base case. These cases combination are appointed as an input in a form of gas-lift gas injection feed object to the OLGAs model. These cases are run and evaluated one by one to see the effect of each case has to the production performance. Afterwards oil rates at stable flow period are extracted, as well as the time oil to produce at wellhead after the injection and time to stable after producing are noted. Operating conditions used in the model are the same with the base case for all cases unless mentioned otherwise.

4.1 Base Case

The base case models the well when it uses the base composition of gas-lift gas injection according to Table 3-5. The objective of this case is to understand the dynamic of J-shaped gas-lift well. Figure 4-1 shows the base case oil and gas production of the J-shaped gas-lift well throughout the simulation period. The simulation runs for 60 hours. Figure 4-1 explains that during the beginning of simulation, the well is opened without gas-lift injection to see how it behaves without gas-lift. At 8.01 hours (28836 s), the gas-lift gas is injected through the annulus and gas-lift valve. Thus, it undergoes unloading period and after some time, it reaches stable flow period.

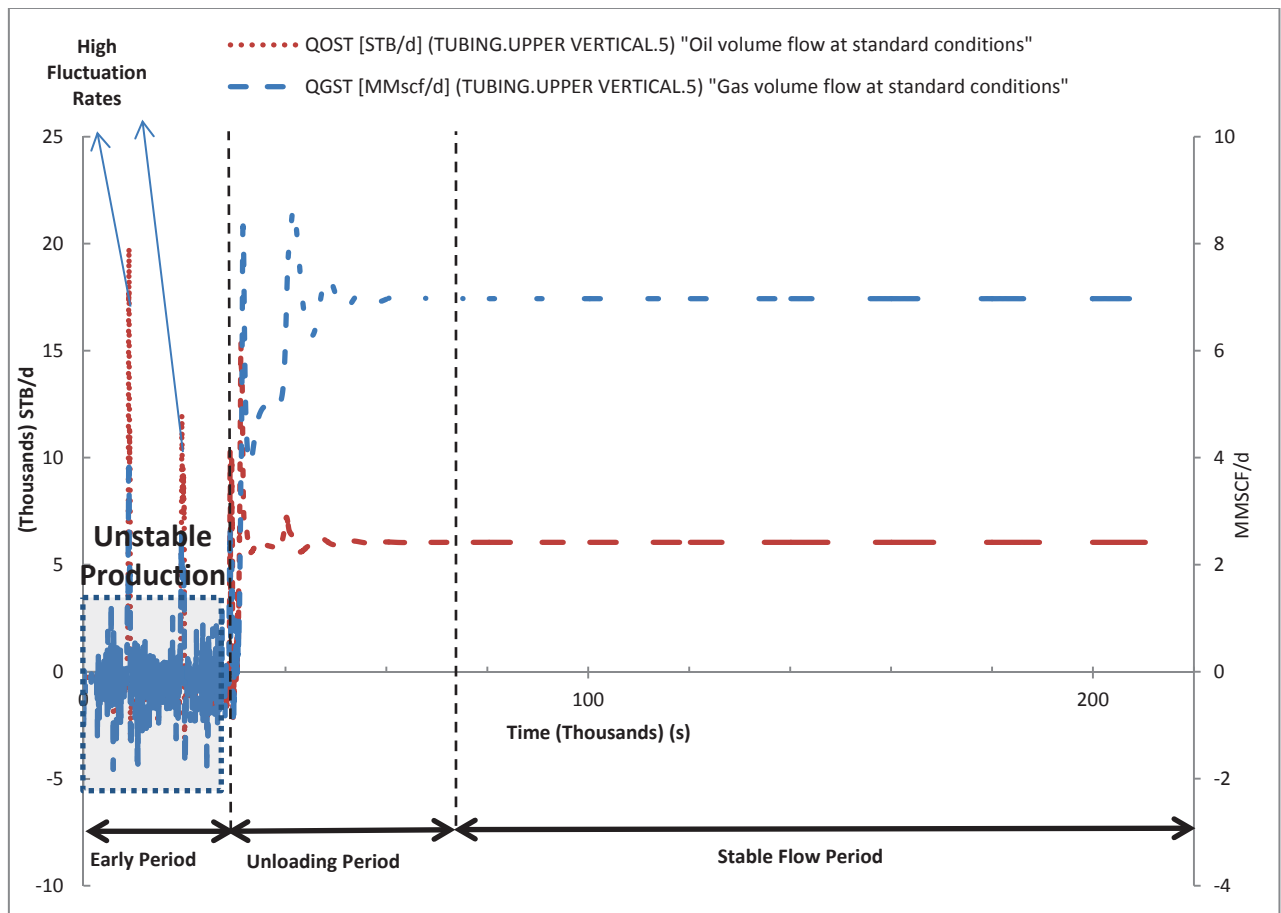


Figure 4-1 Base Case Oil and Gas Production on Wellhead

The only flow source is coming from reservoir. At early period, the wellhead is opened for 8 hours and during this period, the production is highly unstable. It can be seen from Figure 4-1 during the early period, the oil rate is fluctuated around zero. It means that the oil is unable to produce. Gas rate experiences similar behavior with oil rate, except there are times when the gas and oil rate are very high in a very short period. Those show that the gas escapes from reservoir through the liquid column filling the tubing to the well head carrying some oil with it. Even though the gas can escape to the wellhead, the liquid occupies most volume of the well then creates high gravity dominated pressure drop. Therefore it makes P_{WF} high, even higher than P_{RES} .

Figure 4-1 also shows unloading period and stable flow period. At unloading period, the well starts to produce. However, there is a rate fluctuation as the gas-lift is injected and initiates the unloading process. As the gas-lift gas is introduced in the liquid filled tubing through injection valve, it expands and creates slug. Small bubble also splits from the slug and disperses into the liquid. After 13 hours since injection, Figure 4-1 shows that the production stabilizes. At this stable flow period, the oil and gas production are constant at 6043.7 STB/d and 6.97 MMSCF/d respectively until the end of simulation. The flow shows no more slugs as it reaches bubble flow regime in which the gas bubble disperse into the liquid and lifts the liquid to the wellhead.

Figure 4-2 shows pressure and pressure drops profile along the J-section of the well for the early period post the startup period that occurs immediately after opening the well until a period immediately before gas-lift injection. It can be seen that at perforation, the P_{WF} (194 bara) is higher than P_{RES} (185 bara) causing no inflow from reservoir into the well. The frictional pressure drop, as shown by Figure 4-2, is zero from toe to injection point as there is no inflow from reservoir. This indicates that there is no flow throughout the section making it a gravity dominated pressure drop throughout the whole J-section. The gravitational pressure drop is negative from toe to heel as shown by Figure 4-2. This is due to the low downward inclination that makes the pressure at the bottom point of the J-section increases to 202 bara which is higher than P_{WF} .

Figure 4-2 shows that at the start of toe section boundary, the gravitational pressure drop is zero as it is the section boundary where the liquid column starts. At the end of this section boundary, the gravitational pressure drop starts to have almost constant value. The pressure drops are first calculated at the beginning and the end of each pipe section boundaries and the values between these boundaries are extrapolated from the values at the same boundaries. The gravitational pressure drop goes from -397.7 Pa/m to -422.3 Pa/m from toe to heel. The change of gravitational pressure drop at this section is very small as shown by Figure 4-2 because the small downward inclination.

At heel section, as shown by Figure 4-2, the gravitational pressure drop changes drastically from -422.3 Pa/m at the start of the section to -977.3 Pa/m at the bottom point and 2600 Pa/m at the end of the section. The negative values of this pressure drop are caused by the downward inclination at the start of the heel section. The value of this pressure drop changes to positive as a result of it builds up to a large upward inclination at the end of the section as can be seen from Figure 4-2. Elevation increase causes the pressure drop to increase as well. Gravitational pressure drop is a function of density and elevation, so this pressure drop increases with elevation. From the end of heel section, the gravitational pressure drop has positive values 2811 Pa/m and keeps increasing to 2905.4 Pa/m at injection point which is the end of J-section. This indicates that this end of J-section has high upward inclination which is the same as the end of heel. With these pressure drops, the pressure changes from 202 bara at the bottom point to 176 bara at injection point.

As previously discussed, fluid comes from reservoir and fills the well starting from perforation and quickly accumulates throughout the tubing. The liquid occupies most volume of the well, creating high gravity dominated pressure drop and making the P_{WF} in the well quickly becomes higher than P_{RES} . The P_{WF} that is higher than P_{RES} causes no inflow from reservoir just like mentioned before. The liquid occupying the J-section is shown in Figure 4-3 (left side). Nevertheless, from the figure, it can be seen that there is a gas void at the perforation section, showing that there is gas flux coming from reservoir.

Furthermore, this gas dissolves into the liquid throughout the rest of the J-section and tubing section up to the wellhead. As seen from Figure 4-3 (right side), the liquid column ends at some level in the vertical section. The dissolved gas which comes from reservoir migrates all the way upward until the end of liquid column where the gas comes out of liquid solutions and escapes through the liquid column carrying some oil with it. The gas is soluble in the bottomhole where the tubing pressure is high. Moreover when there are sufficient gas dissolved into the liquid migrating upward and the lower pressure at vertical section, it comes out of the solution (O'bryan, Bourgoyne Jr, Monger, & Kopsco, 1988)(Thomas, Lea Jr., & Turek, 1984). This gas breakthrough carrying oil appears as the gas and oil rate that are very high in a very short period which depicted in Figure 4-1.

Figure 4-4 shows pressure and pressure drops profile along the tubing section for the early period post the startup period that occurs immediately after opening the well until a period immediately before gas-lift injection. This section starts from the injection point and ends at the wellhead. The pressure profile continues from the profile of previous J-section. The pressure at injection point is 170 bara as can be seen from Figure 4-4.

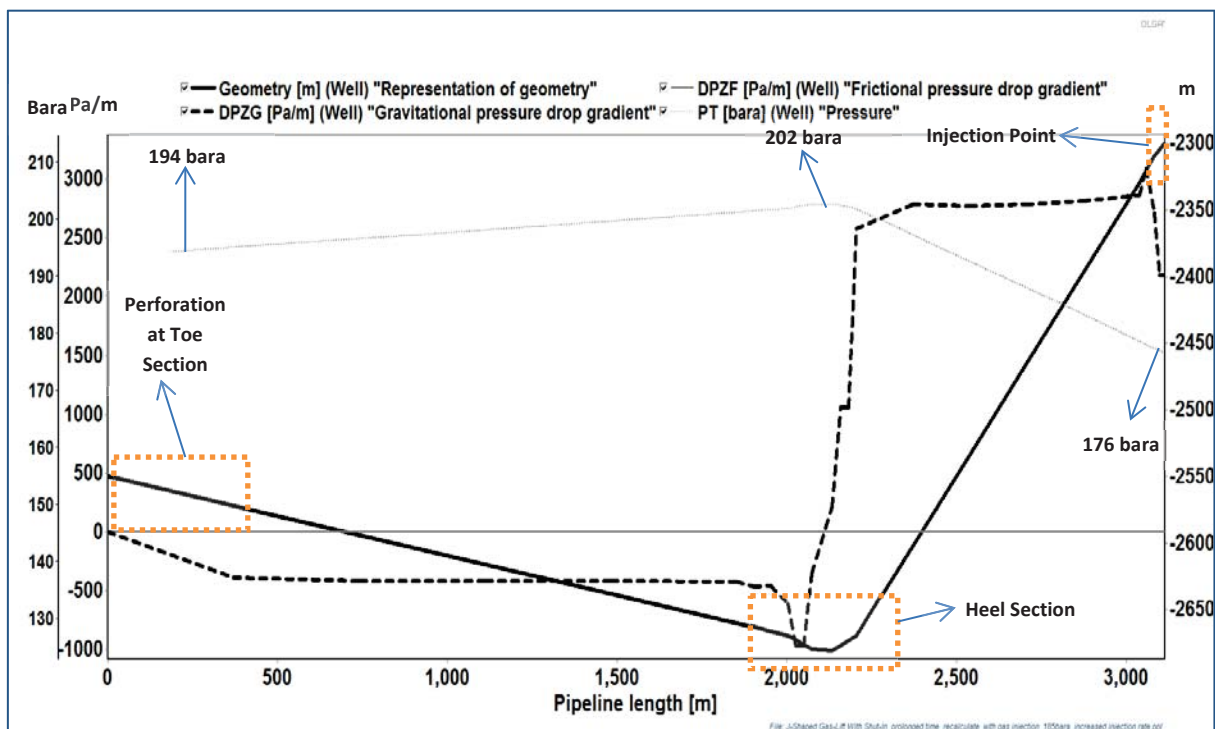


Figure 4-2 Pressure and Pressure Drop Profile Along J-section

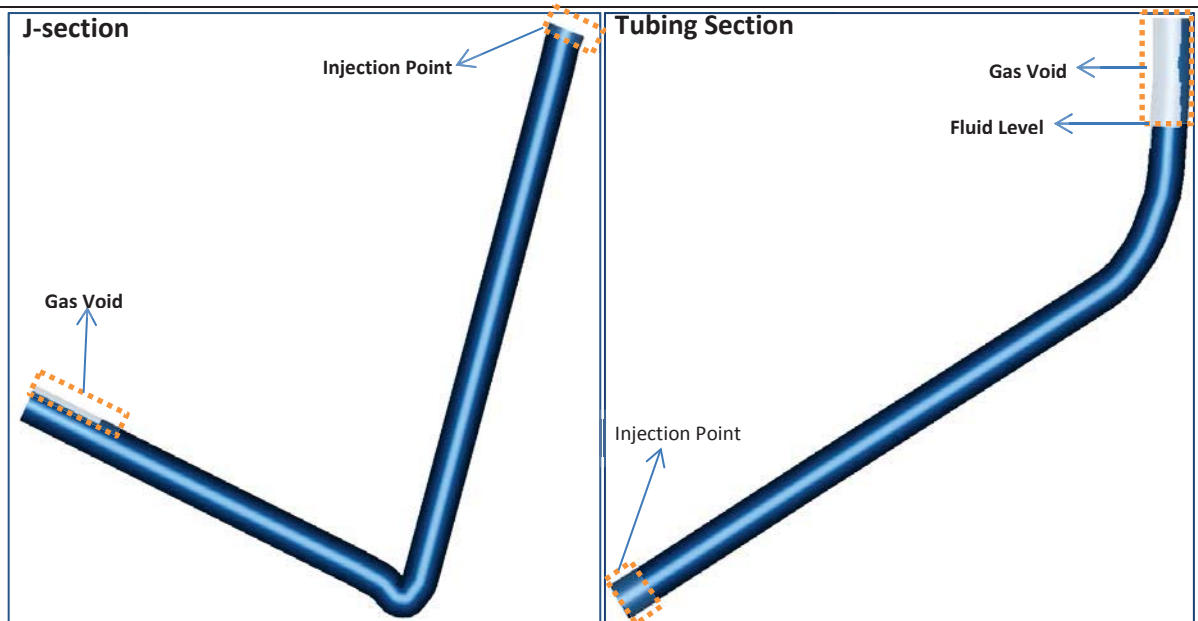


Figure 4-3 Liquid Holdup in J-section (Left) and Tubing Section (Right)

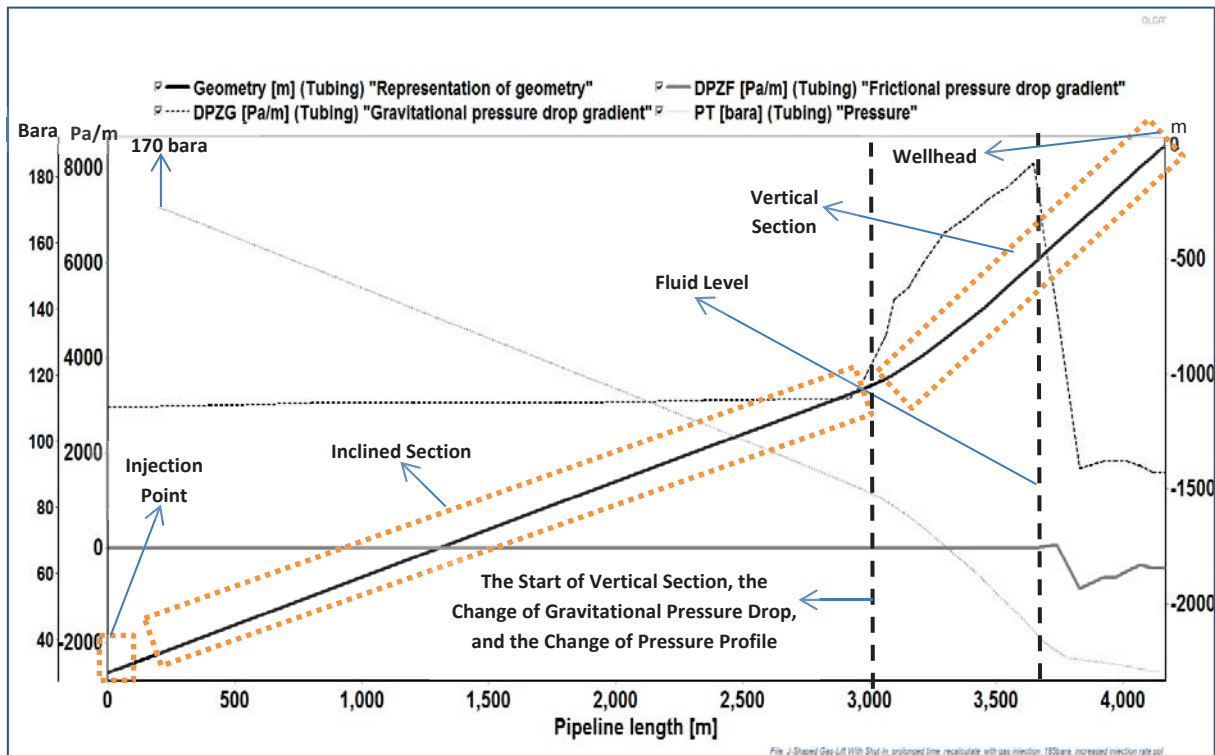


Figure 4-4 Pressure and Pressure Drop Profile Along Tubing Section

The gravitational pressure drop is 3008.2 Pa/m at injection point and 3170.9 Pa/m at the end of inclined section. It increases in a very small slope due to the well inclination. This pressure drop is a function of density and elevation, so it increases with elevation. The frictional pressure drop is almost zero throughout the most of tubing section. It is clear that the flow is gravity dominated pressure drop as the liquid occupies most volume of the well. This is caused by the absence of inflow from reservoir because P_{WF} in the well is higher than P_{RES} as previously discussed.

From the start of vertical section, the gravitational pressure drop changes. It has a very steep increase as can be seen from Figure 4-4 due to the changes of the profile of the well from inclining upward, now it builds-up to vertical continuing to wellhead. As previously mentioned, this pressure drop increases with the elevation increases. In Figure 4-4, the pressure profile also changes correspond to the elevation increase. The pressure decrease is now larger than the decrease of the inclined section. Until some level, the pressure profile changes again coinciding with the change of gravitational pressure drop.

This pressure drop reaches its peak at 7998.1 Pa/m and drops into its lowest point on 1173.5 Pa/m which indicates that the fluid level ends at this level as shown in Figure 4-3 (right side). It is shown from Figure 4-4 that the pressure experiences slow changes from 170 bara at injection point to 85 bara at the end of inclined section. Next it changes rapidly to 41.7 bara at fluid level then it experiences slow changes again to 30.6 bara at the wellhead. Those pressure changes correspond to the gravitational pressure drop changes.

Unloading period starts when the gas-lift gas is injected. After the gas-lift gas enters the tubing, the gas occupies and displaces the liquid column from injection point upward. The presence of gas pushes the liquid thus it creates slug as shown in Figure 4-5 and Figure 4-6. The figures show only the liquid holdup demonstration. In OLGA, liquid holdup and flow regime are presented separately. Since Figure 4-5 and Figure 4-6 show liquid holdup, it's not necessary demonstrating the flow regime. However, it is pointed out in the figures at which section the slugs has developed according to flow regime calculation from OLGA.

From Figure 4-5, at t_1 , the gas-lift gas just enters the tubing. The gas continues to push the liquid upward building up in form of slug as shown at t_2 . At t_3 , on the other hand, there are bubbles splitting up from the slug. These bubbles disperse into the liquid column lowering the hydrostatic pressure of the liquid column above the slug. The slug loses its energy to push the liquid as some of the gas is dispersed into the above liquid column. Thus, the liquid column falls back again as shown in t_4 .

From Figure 4-5, at t_5 , the liquid starts to accumulate again. It combines the already present liquid column with additional liquid coming from reservoir. This additional liquid has passed the injection point, thus the gas-lift gas has already dispersed partially into the liquid, lowering the mixture density. The remaining gas that is not dispersed into the liquid starts to develop slug to push the liquid column upward as can be seen in t_6 .

From Figure 4-6, at t_7 , the gas continues to develop and the slug continues to push the liquid. The liquid column above the slug now has lower hydrostatic pressure as the bubble is dispersed into it. At t_8 , the slug further pushes the liquid and up to some point it reaches sufficient energy then it displaces the whole liquid column as shown at t_9 . The flow undergoes unstable period as it balances the kinetic energy and the gravitational effect. When the balance has been reached, the flow undergoes stable production as shown at t_{10} . The dynamic mechanism in form of gas pressure development, slug growth, bubble

dispersion, and liquid accumulation discussed here are the phenomena which are appeared as production fluctuation shown in Figure 4-1 in unloading period.

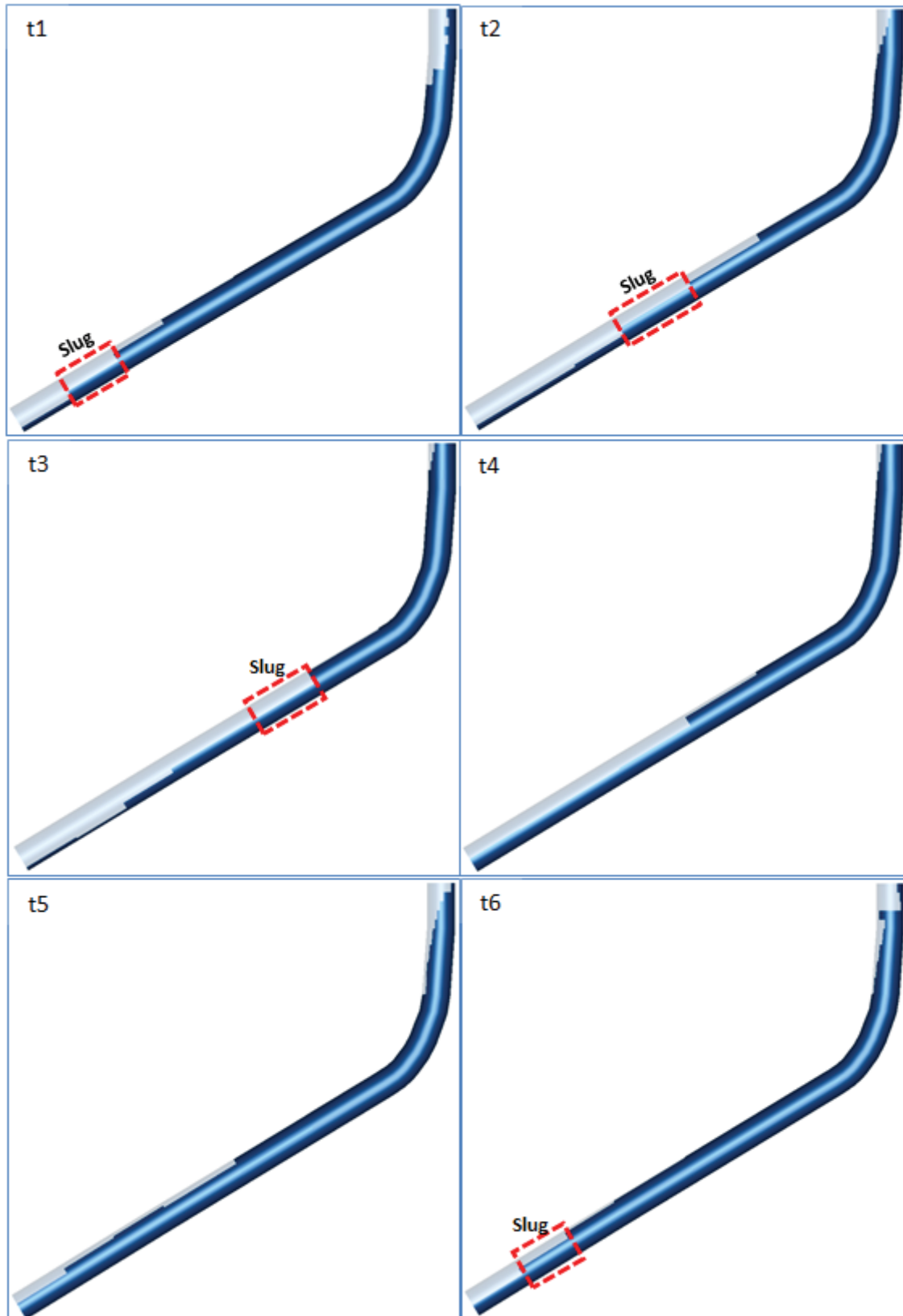


Figure 4-5 Dynamic Unloading Sequence Shown as Liquid Holdup (a)

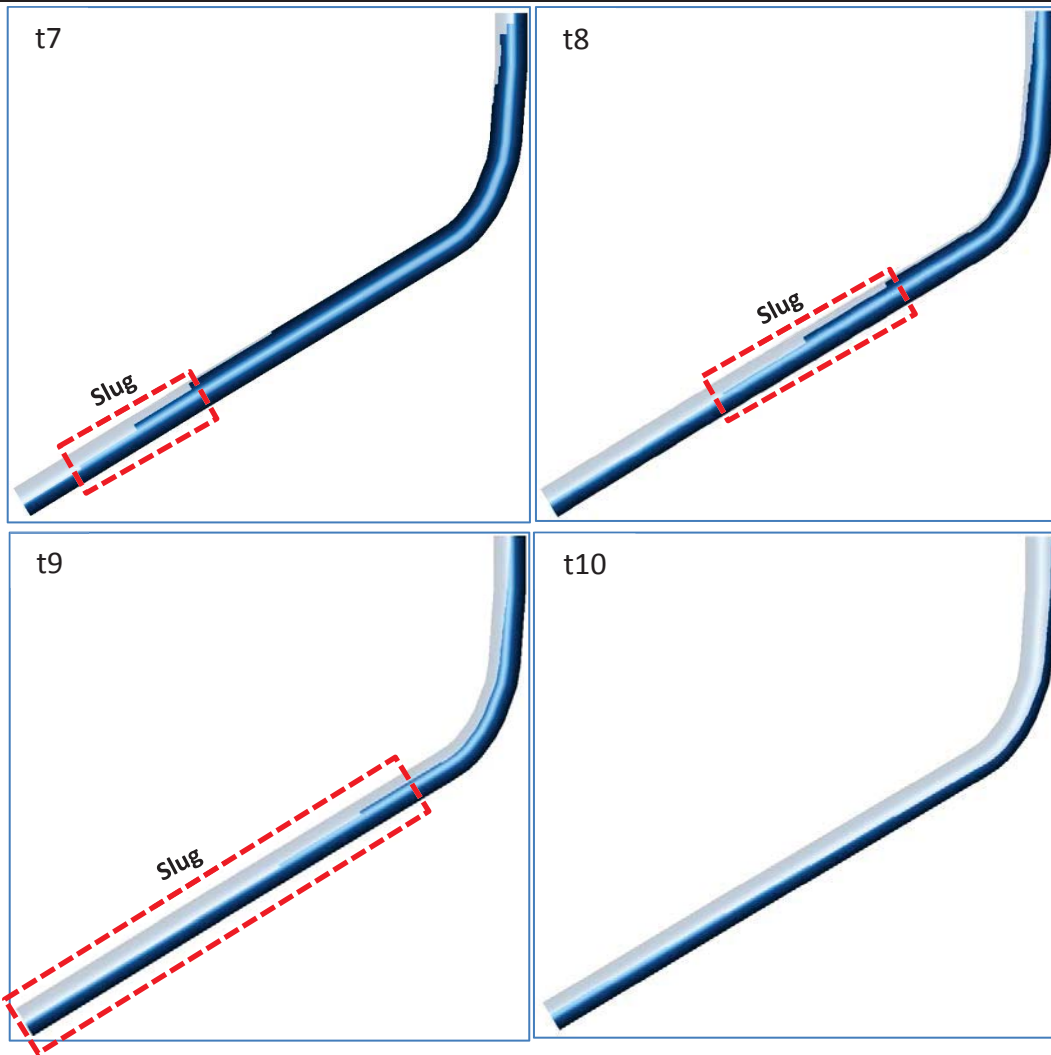


Figure 4-6 Dynamic Unloading Sequence Shown as Liquid Holdup (b)

Table 4-1 Result of Base Case

Case combination	Liquid Production at WH	Oil Rate (STB/D)	Gas Rate (MMSCFD)	Time to produce since injection (hours)	Time to stable since production (hours)	GOR (m^3/m^3)	Note
Base Case	Yes	6043.7	6.97	0.41	13	205	-

The rates at stable flow period, as shown in Figure 4-1, are 6.97 MMSCF/d for gas and 6043.7 STB/d for oil. The system needs 0.41 hours from injection time until it produces and 13 hours from production time until it stabilizes. The complete result of base case can be seen in Table 4-1. At stable flow period, the regime for J-shaped gas-lift well is bubble flow.

The flow regime map for vertical flow is presented in Figure 4-7. Although one can use vertical flow models for deviated well by simply applying an inclination angle correction to the gravity component of pressure gradient equation, it is reported that the result should be used with caution (Kaya, Sarica, & Brill, 2001). Nevertheless, the physical mechanism remains the same. From Figure 4-7, it can be seen that the gas is dispersed into the liquid for

bubble flow. The gas-lift gas disperses into the liquid coming from reservoir, lowers the mixture density hence the hydrostatic pressure, gives the fluid mixture kinetic energy, and lifts the liquid to the wellhead.

Figure 4-8 shows that the pressure gradient increases in the deeper section which starts from below injection point down to the heel and up to the toe. This is because the fluids in those sections have lower superficial velocities than the section above injection point as shown in Figure 4-10. Figure 4-10 also presents that the superficial velocity of oil and gas at section between toe and injection point are almost constant as a result of inflow from reservoir. The values of these superficial velocities are 0.75 m/s (2.46 ft/s) for oil and 0.31 m/s (1.02 ft/s) for gas. These superficial velocities can be used to predict the flow regime by plotting them to flow regime map.

Flow regime map in Figure 2-5 can be used to identify the flow regime for toe to heel section because this section has low inclination toward horizontal. From the figure, it can be seen that the regime is elongated bubble. However the flow regime as shown by Figure 4-11 is stratified from toe to heel. It is understandable because in OLGA elongated bubble is categorized in stratified. Thus the result from OLGA and the prediction by flow regime map are not contradicting.

Flow regime map in Figure 4-7 can be used to identify the flow regime for heel to injection point section because this section has high inclination and is almost vertical. With the same oil and gas superficial velocities as mentioned before, from the figure, it can be seen that the regime is slug. It is in agreement with the flow regime predicted from OLGA model as shown by Figure 4-11.

As can be seen from Figure 4-10, the fluid above injection point has higher velocity due to gas-lift injection and the flow becomes dispersed bubble as shown by Figure 4-11. As previously discussed, dispersed bubble flow regime reduces the pressure gradient. Therefore, the flow above injection point has lower pressure gradient compare to the flow below injection point as depicted in Figure 4-8. Figure 4-9 also shows that the temperature changes significantly in the wellbore, hence it is important to consider the effect of temperature on the fluid as its composition and properties also change with the temperature.

According to previous discussion, the pressure and the temperature change along the wellbore. Investigation has shown that composition of the fluid may vary point by point in the wellbore as function of pressure, temperature, and slip between phases (Pourafshary, Varavei, Sepehmoori, & Podio, 2008). The oil phase and gas phase that enter the wellbore from reservoir have different composition from produced fluid. This composition can be also completely different from the oil or gas composition at standard condition.

Figure 4-12 and Figure 4-13 the composition of the components mole fraction of the liquid and gas, respectively at the toe, injection point, wellhead, and standard conditions. Both figures show the percentage of each component from the total mixture at Y-axis. The composition of the liquid and the gas phase at toe, injection point, and wellhead are calculated both at flowing condition from OLGA model and recombined equilibrium condition from PVTsim. Reservoir fluid and gas-lift gas were recombined at different conditions at their corresponding location as presented in Table 4-2. The GOR at those points remains constant from toe to wellhead as it reaches stable flow period. Furthermore, reservoir fluid and gas-lift gas recombination at standard condition is also done by PVTsim. This recombined fluid composition is shown in Table 4-3. It is based on reservoir composition shown in Table 3-4, gas-lift gas injection composition shown in Table 3-5, and production GOR shown in Table 4-1. It uses SRK as EOS, as explained in section 3.2.

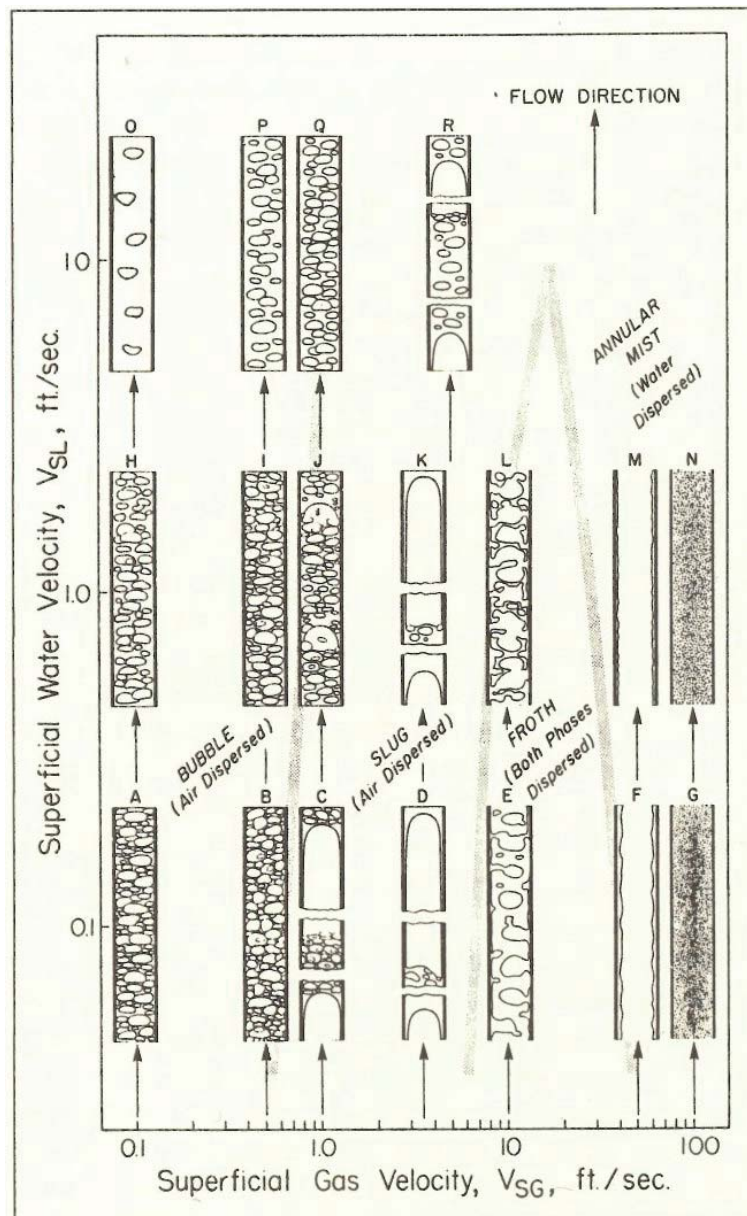


Figure 4-7 Two-phase Vertical Flow Regime Map(Beggs, 1991)

Figure 4-12 and Figure 4-13 show that at lower pressure and temperature (30.8 bara and 58.9°C at wellhead and 1.01 bara and 15.56°C at standard conditions), the content of the heavier components in the liquid phase, as expected is higher than lighter components. Moreover at higher pressure, light components dissolve in the liquid phase. The same behavior can be observed for the gas phase. At higher pressure in the gas phase, only very light components such as C1, C2, and C3 remain in high concentration. And at standard condition, there is small decrease of C1 content, while the heavier components increase in concentration.

It is necessary to compare the composition of flowing condition from OLGA model against in the recombined equilibrium condition. . In flowing conditions gas phase and liquid phase in hydrocarbon fluid mixture move at different velocities, i.e. there is insufficient time to reach equilibrium (Pourafshary, Varavei, Sepehmoori, & Podio, 2008). The calculation of composition in equilibrium is done in PVTsim by using SRK as EOS.

To consider the effect of slip velocities in the J-shaped gas-lift well model, it is assumed that at each block in the wellbore, the gas phase is in equilibrium with only a portion of the liquid phase. So the liquid phase is divided into two parts, one part that is in equilibrium with the gas phase and the other one which appears because of slip velocity and is not in equilibrium with the gas phase. This total liquid phase is a function of liquid holdup, gas compressibility factor, and liquid compressibility factor.

Then both the part that is in equilibrium with the gas phase and the other part that isn't are assumed to have the same composition and same compressibility factor. This assumption can lead to an error in predicting the fluid composition. Composition calculation in equilibrium condition on the other hand, calculates the fluid composition when pressure, temperature, and composition of the system remain constant.

From Figure 4-12, for gas phase at high pressure at injection point, the heavy components appear at a very low concentration. However at standard condition, C1 fraction decreases by 0.05 while the heavier components increase in concentration. The increase of heavier component is because as the pressure declines in the wellbore the lighter component in gas phase stops expanding.

It is also seen from the figure that the compositions in gas phase from the model and in equilibrium (PVTsim) are in a good agreement. Compositions of C1 and C2, respectively at dynamic state (by the model) and in equilibrium are the same at toe and wellhead locations. On the other hand C1 composition at injection point is 0.86 in equilibrium which is smaller compared to 0.87 in the model. This difference is very small.

The small compositions difference is also relevant for liquid phase. Figure 4-13 shows that the majority components in liquid phase are C1 and heavier components (C10+). Compositions of C1 and C10+, respectively at dynamic state (by the model) and in

equilibrium (PVTsim) are the same at toe and wellhead locations. C1 compositions at injection point is 0.3 in equilibrium which is higher compared to 0.27 in the model, and C10+ compositions at the same point is 0.36 in equilibrium which is smaller compared to 0.38 in the model.

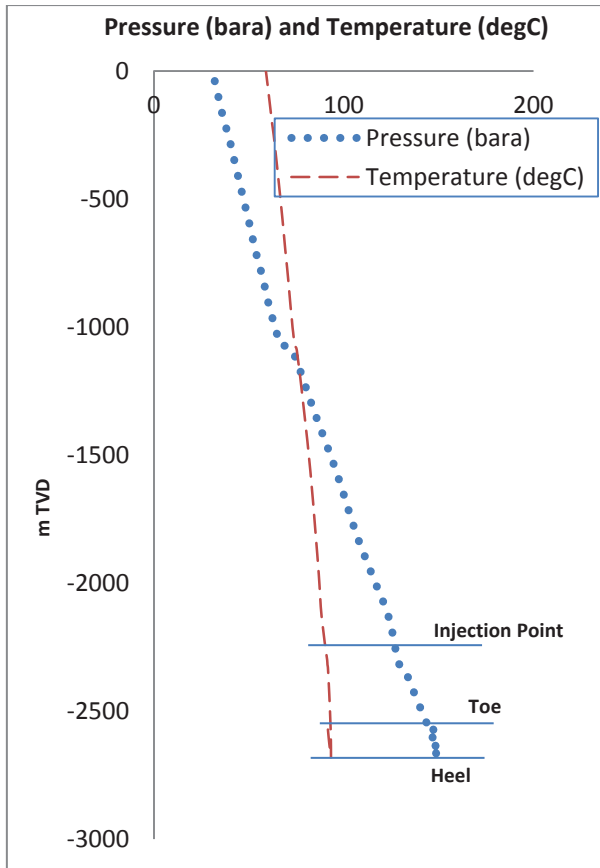


Figure 4-8 Pressure and Temperature Profile at Stable Flow Period

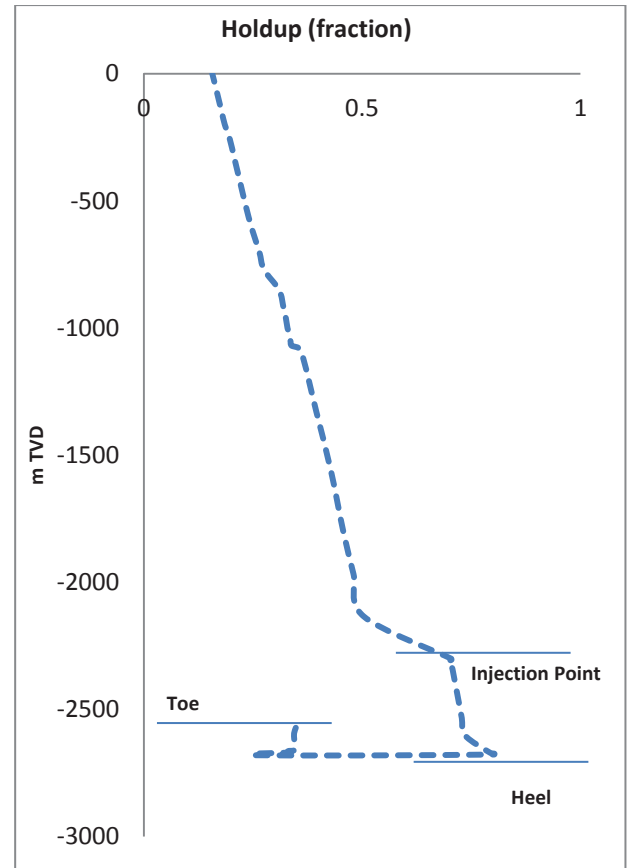


Figure 4-9 Liquid Holdup Profile at Stable Flow Period

Table 4-2 Pressure and Temperature at Different Point in the Wellbore

Description	Toe	Injection Point	Wellhead	Standard Condition
Pressure (bara)	147.2	123.7	30.8	1.01
Temperature (°C)	91.7	88.4	58.9	15.56
GOR (m ³ /m ³)	205	205	205	205

Table 4-3 Recombined Fluid Composition

Component	Mol %	Mol weight (g/mol)	Liquid Density (g/cm ³)
N ₂	0.267	28.014	
CO ₂	0.324	44.01	
C1	69.82	16.043	
C2	6.981	30.07	
C3	3.749	44.097	
iC4	0.753	58.124	
nC4	2.004	58.124	
iC5	0.817	72.151	
nC5	0.954	72.151	
C6	1.356	86.178	0.664
C7	0.892	96	0.7672
C8	0.845	107	0.7762
C9	0.802	121	0.7841
C10-C19	4.013	195.264	0.8166
C20-C27	2.495	322.745	0.8487
C28-C34	1.571	428.459	0.8674
C40+	2.359	519.876	0.8803

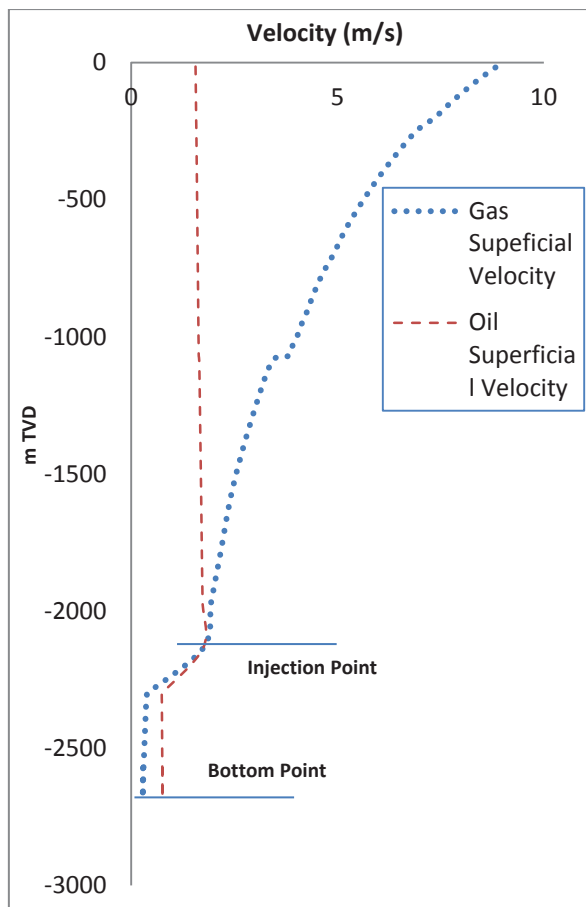


Figure 4-10 Velocity Profile

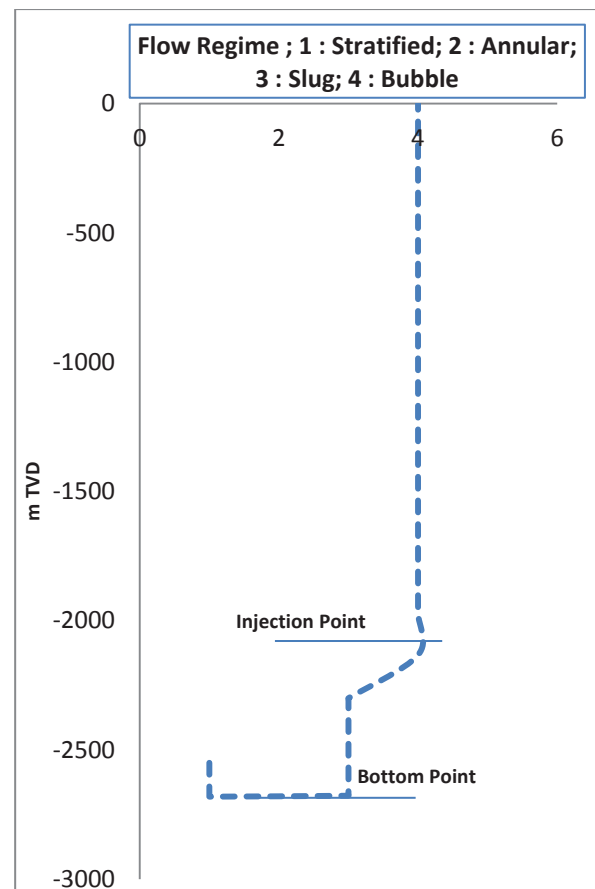


Figure 4-11 Flow Regime



Figure 4-12 Gas Composition

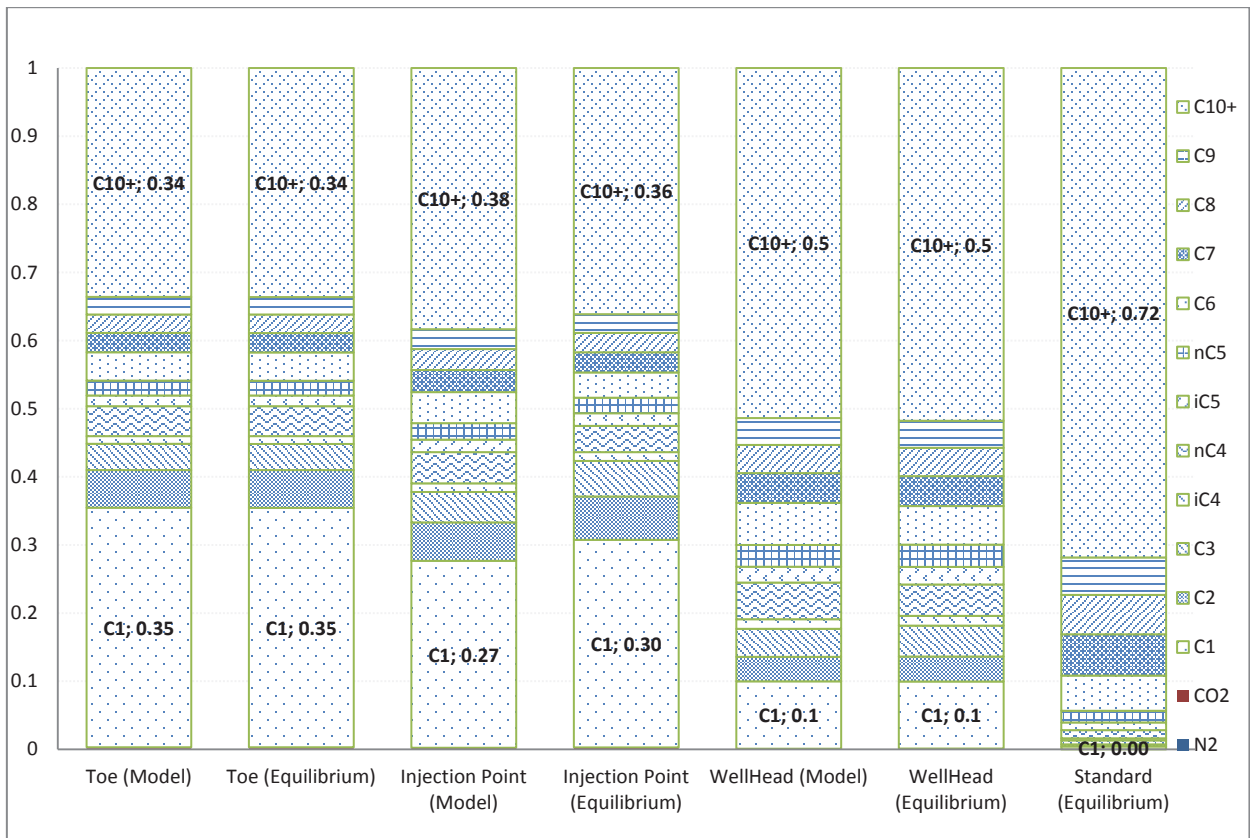


Figure 4-13 Oil Composition

4.2 Pure Component

Gas-lift gas with pure component combinations is used to replace the gas-lift gas composition used in the base case to do pure component sensitivity studies. The cases combinations have been described in section 3.2. The base case shows that unable to produce J-shaped well can be initiated and produce with the aid of gas-lift. However, it is essential as well to see what effect pure component gas-lift has to the unloading process and production performance.

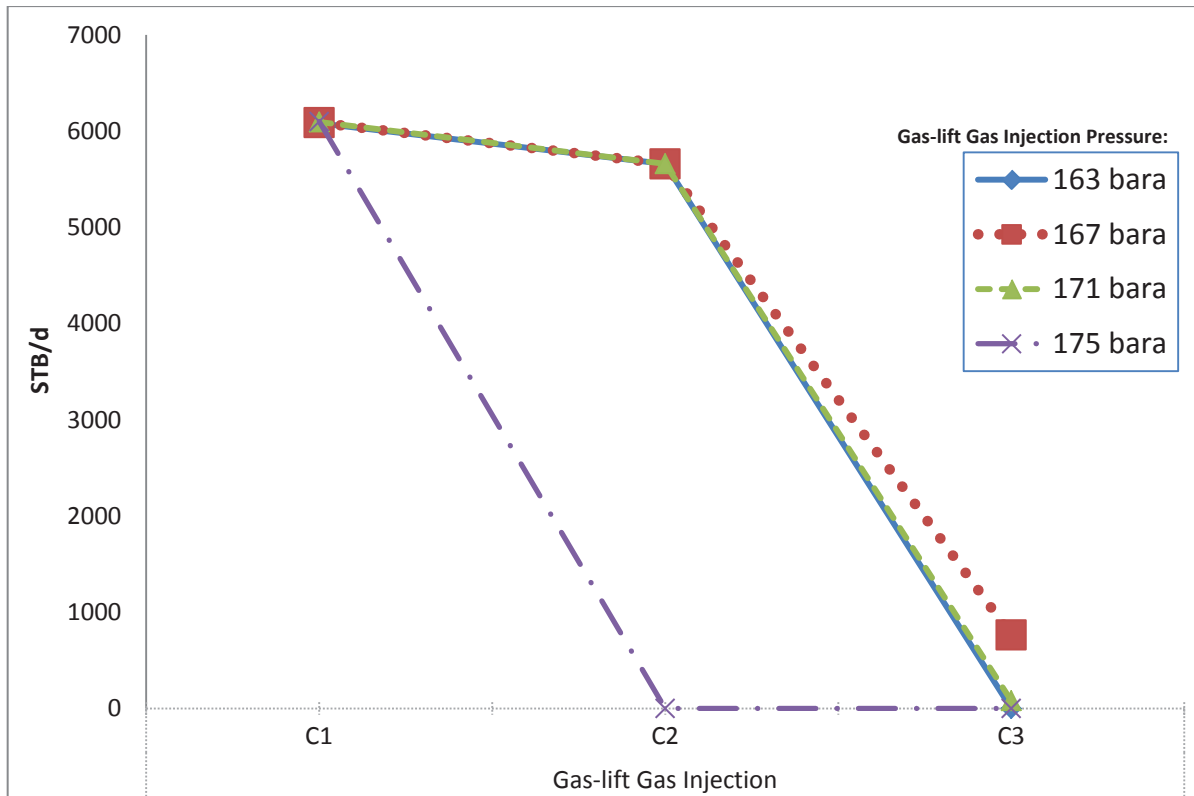


Figure 4-14 Oil Production Sensitivities of Pure Gas-lift Gas Injection (5°C T_{INJ})

Table 4-4 P_{WF} of Pure Components Case at P_{INJ} 163 bara

Gas-lift Gas	P _{WF} (bara)
C1	146.895
C2	149.594
C3	181.869

Figure 4-14 shows that the well can only produce with gas-lift gas consisted of only C1, C2, or C3. Those rates are at stable flow period, post the transient period that occurs immediately after the gas injection. The oil rates decrease with heavier component and practically have no effect of injection pressure. The well cannot produce with iC4, nC4, iC5, & nC5 gas-lift gas. These components are not recognized as gas by the simulator in the same pressure and temperature condition as the base case at the source of gas-lift gas injection (163 bara and 5°C).

As can be seen from Figure 4-15, at P_{INJ} 163 bara, C3 has the highest pressure gradient compared to C2 and C1 while C1 has the lowest pressure gradient. It is understandable that C1 gas-lift gas injection gives the highest oil production compared with the case when C2 and C3 are used as gas-lift gas injection. With P_{RES} value of 185 bara and P_{WF} value as shown in Table 4-4, it can be seen that with C1 as gas-lift gas, the drawdown is at its highest. Meanwhile C3 as the gas-lift gas gives the lowest drawdown. From that, one can infer that C1 gives the highest and C3 gives the lowest oil production. These phenomena of heavier component of gas-lift gas gives higher pressure gradient are relevant as well for the other P_{INJ} cases which have the pressure value of 167 bara, 171 bara, and 175 bara.

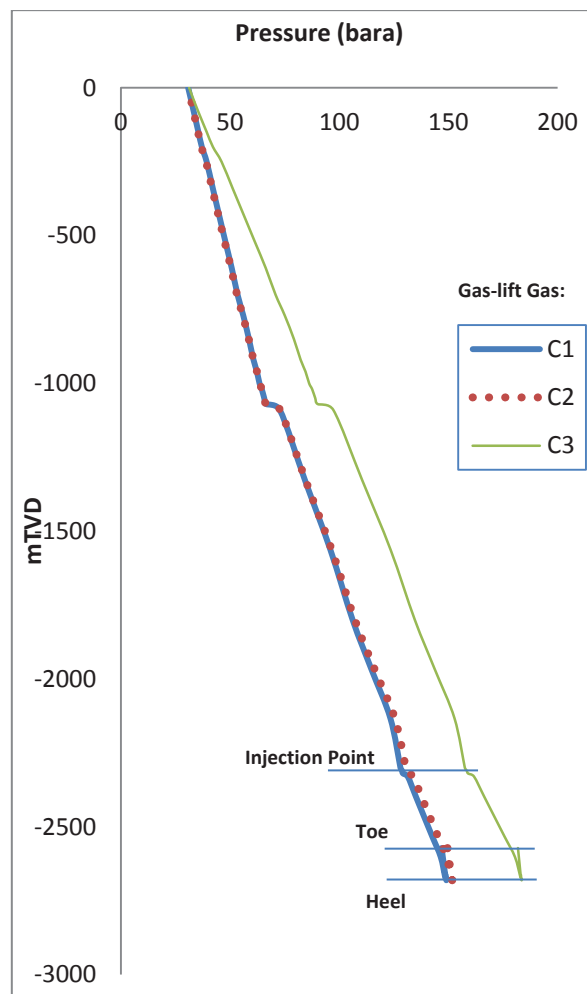


Figure 4-15 Pressure Profile of Pure Component Case with P_{INJ} 163 bara at Stable Flow Period

The difference in pressure gradient from different gas-lift gas component, as discussed before, is an indication of pressure drop difference. Pressure gradient is higher because the pressure drop is also higher. Gravitational pressure drop is more dominating most of the time compared to frictional pressure drop in J-shaped well even if the fluid is flowing. Furthermore frictional pressure drop is low if the fluid moves in relatively low velocity. On the other hand, the gravitational pressure drop is affected by density. By observing the density, the gravitational pressure drop can also be compared. Density is composition dependent as it is calculated using the selected equation of state.

Figure 4-16 shows density at different point in the wellbore from the model and in the equilibrium. Density calculation in the equilibrium is done in PVTsim with SRK as EOS. The density is in a good agreement at toe between model and in equilibrium as shown in Figure 4-16. This is because the reservoir fluid at this point has not mixed with gas-lift gas, thus the velocity and composition have not changed. At this point, slip may not have effect to the density because the oil and gas superficial velocity still has low value. On the other hand, density at injection point and wellhead show differences as shown in Figure 4-16. This may be explained by the slip that starts to have effect, so in the OLGA model the equilibrium is not achieved. Only a portion of liquid that is in equilibrium with gas phase which makes each point has different composition, thus it also gives different fluid properties.

The pressure and the temperature are also different at each point and different gas-lift gas injection as shown in Table 4-5. Even though there are differences in density between in the model and in the equilibrium, they show similar trend. Densities are increasing as the heavier the gas-lift gas components become and decreasing as it reaches the wellhead due to lower pressure and temperature. This may explain that C3 has the highest pressure gradient and C1 has the lowest pressure gradient.

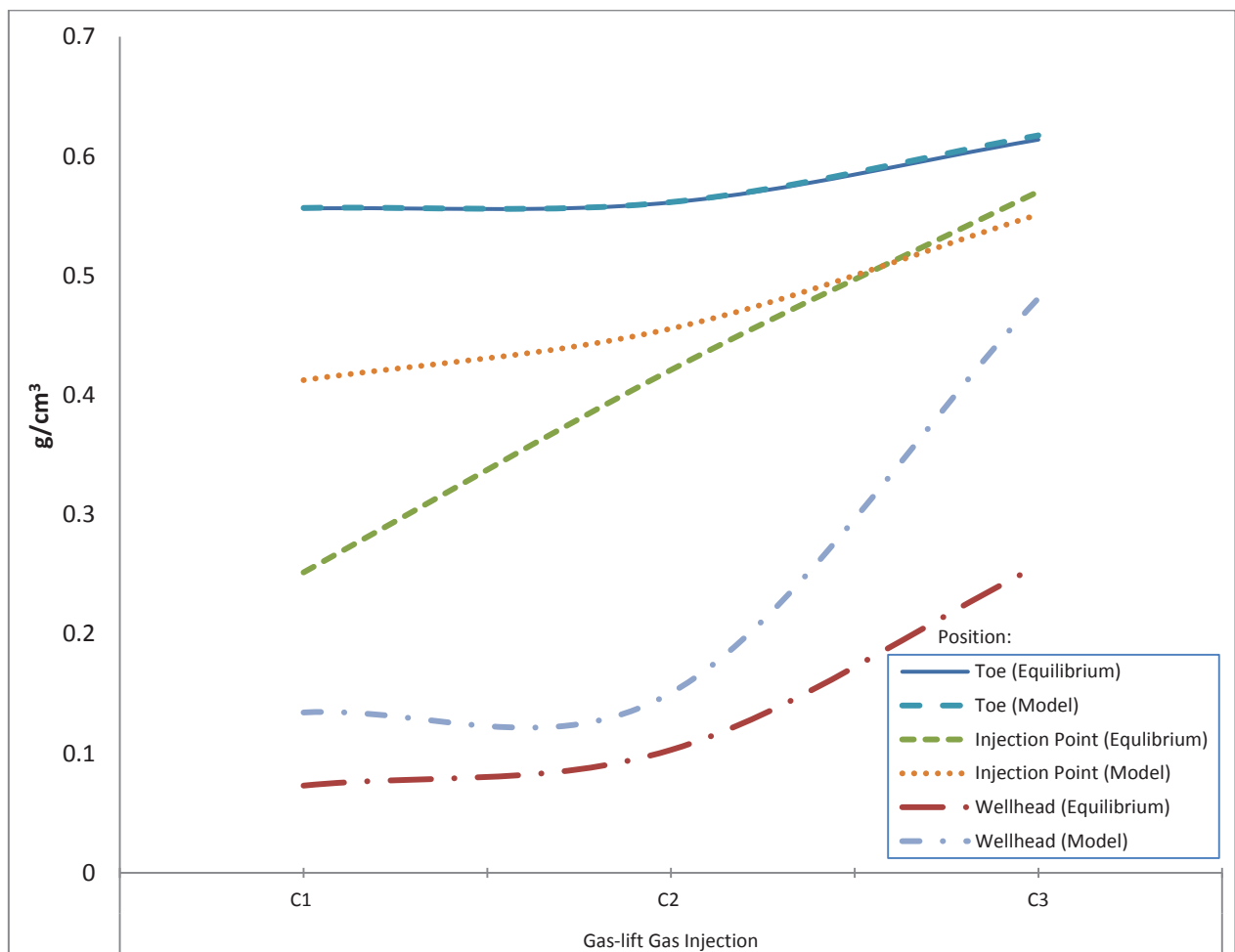


Figure 4-16 Density at different Points in The Well for Individual Pure Component Cases

Table 4-5 Pressure and Temperature at Wellbore for Pure Component Cases

Point	C1 Gas-lift Gas Injection		C2 Gas-lift Gas Injection		C3 Gas-lift Gas Injection	
	Pressure (bara)	Temperature (°C)	Pressure (bara)	Temperature (°C)	Pressure (bara)	Temperature (°C)
Toe	146.90	91.66	149.59	91.77	181.87	93.12
Injection Point	128.02	91.26	130.47	91.36	157.52	90.08
Wellhead	30.79	59.34	30.77	53.63	31.23	38.87

Injection pressure doesn't give effect to the oil production if pure component is used as gas-lift gas as shown by Figure 4-14. It is because injection pressure only affects the gas in annulus and injection line. Furthermore it doesn't give effect to the pressure gradient inside the tubing. Except when P_{INJ} 175 bara is used, It doesn't show production on wellhead if C2 and C3 are used as gas-lift gas injection as shown by Figure 4-14.

It seems that injection pressure is too high and increases the already higher pressure gradient inside the tubing when C2 and C3 are used as gas-lift gas injection. Figure 4-17 shows that the pressure gradients, when C2 is used as gas-lift gas with P_{INJ} 163 bara, 167 bara, and 171 bara, are overlying each other. When P_{INJ} 175 bara is used, the pressure gradient increases, yielding P_{WF} 204.5 bara while P_{RES} 185 bara. It is obvious that there will be no flow from reservoir with this condition.

To confirm that P_{INJ} 175 bara on C2 gas-lift gas injection imposes high pressure on the fluid inside the tubing, a close look of compressibility around injection point before and after injection is needed. As can be seen from Figure 4-18, before injection, the compressibility is almost constant from toe to section near heel which is around 0.00024 1/bar. Then it decreases until near injection point section. The compressibility at that section is 0.000157 1/bar.

After that point, the compressibility is almost constant again which is around 0.00015 1/bar. The section from toe to near heel has higher compressibility compared to the other section because, before injection, there is an amount of pressure trying to create an influx from reservoir. However it doesn't have enough energy to overcome the hydrostatic pressure as its effect decreases in the heel and finally loses around injection point.

As can be seen from Figure 4-18, at injection point for the most period after injection, the compressibility is very high that is 0.001416 1/bar. It increases the compressibility of surrounding region upward and downward with respect to the injection point. Downward, the compressibility is high until heel that is 0.000371 1/bar and still has some effect down to toe that is 0.000196 1/bar. Meaning that, the gas-lift injection imposes additional pressure to the liquid inside the tubing.

This is why the case when injecting C2 gas-lift gas injection with P_{INJ} 175 bara yields high P_{WF} . Upward, the compressibility imposed by the gas-lift gas injection is not sufficient to push the

liquid column. The compressibility decreases to 0.000133 1/bar at some distance from injection point. It cannot overcome the hydrostatic pressure caused by the liquid column. That's why the compressibility is high around injection point and quickly decreases as it goes upward.

Table 4-6 P_{WF} of C2 Gas-lift Gas Injection Case at Different P_{INJ}

P_{INJ} (bara)	P_{WF} (bara)
163	149.6
167	149.6
171	149.6
175	204.5

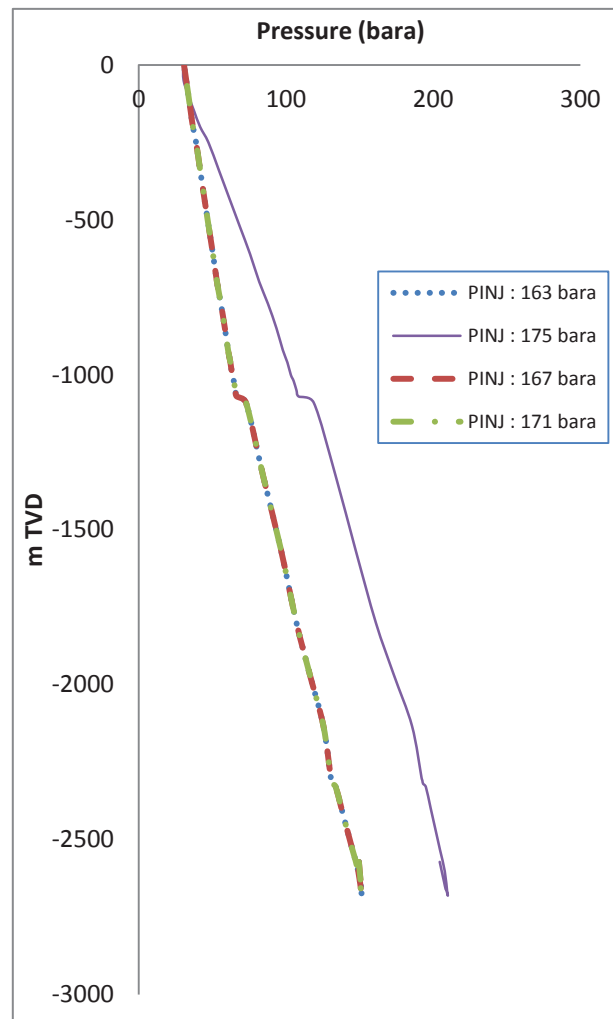


Figure 4-17 Pressure Profile of C2 Case with Different Casing Pressure at Stable Flow Period

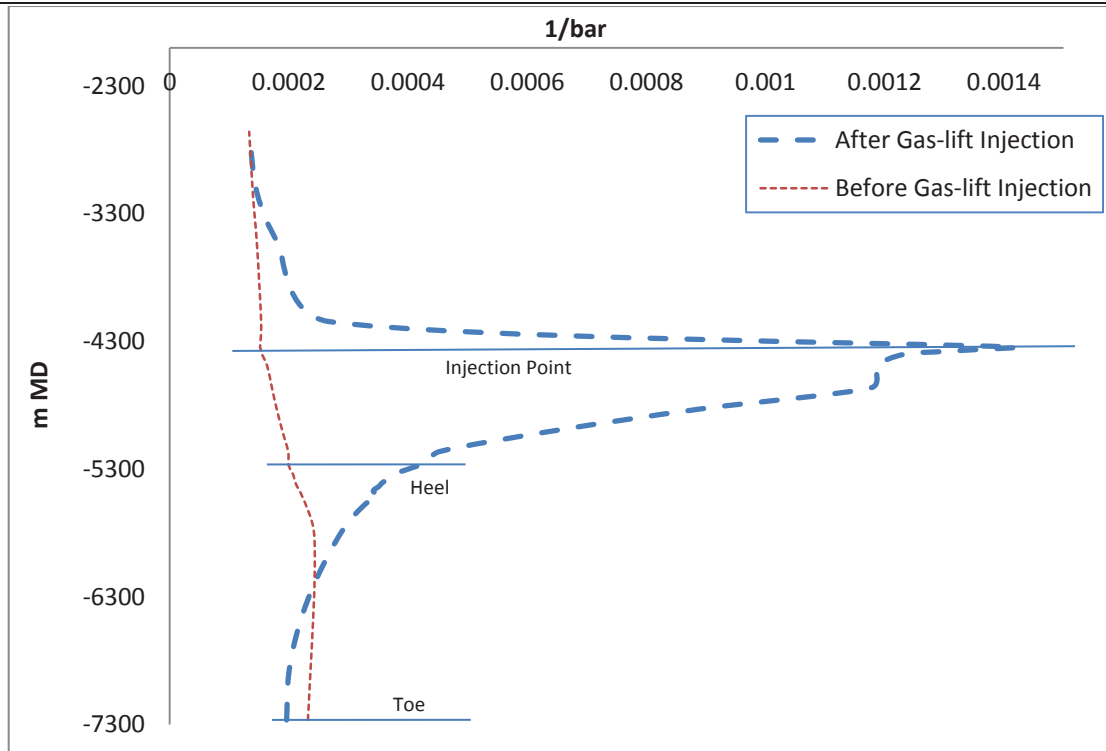


Figure 4-18 Compressibility of Fluid Around Injection Point (PINJ 175 bara, C2 Gas-lift Gas) Before and After Gas-lift Injection

4.3 Binary Component

The subsequent cases group to concentrate is when binary component is used as gas-lift gas injection. The used binary gas compositions are limited to what is considered as gas by the program at 163 bara and 5°C. In this work C1 is considered the main component and the composition is adjusted according to the addition of the component under investigation. The cases combinations have been described in section 3.2. The ones that give production on wellhead are the gas-lift gas that composed by 95C1-05Cx, 90C1-10Cx, 85C1-15Cx, 80C1-20Cx, 75C1-25C2, 75C1-25C3, 70C1-30C2, 70C1-30C3, 65C1-35C2, 65C1-35C3, 60C1-40C2, 60C1-40C3, 55C1-45C2, 55C1-45C3, 50C1-50C2, and 50C1-50C3.

The first four cases groups give result for all component combination composing the multicomponent mixture gas-lift gas, that are C1, C2, C3, iC4, nC4, iC5, and nC5. In Figure 4-19, these cases groups are presented in the curves with six data points. While for the rest of the cases groups, only combination of C1-C2 and C1-C3 give results. Those are presented in the curves with two points in Figure 4-19. The cases combinations that are not mentioned here don't give production on the wellhead as they are not recognized as gas by the simulator at the same pressure and temperature condition as the base case at the source of gas-lift gas injection (163 bara and 5°C). The complete oil rates result at stable flow period can be found in Figure 4-19.

It can be seen that C1 is the main and majority component in the binary gas-lift gas. C1 is combined with the additional components mentioned before. It can be seen from Figure

4-19, that the smaller portion of additional component gives little effect to the oil rate. If the portion of additional component is increased, it gives higher effect to oil rate particularly it decreases the rate.

It is interesting to observe that component iC4 gives the lowest oil rates, while nC5 gives the highest. The change of the content affects in oil rate as illustrated in Figure 4-19. From the figure, it shows that oil rates decrease as C3 and iC4 are used as the second component in the binary mixture. However, production increases as nC4, iC5, and nC5 are used.

iC4 gives the lowest production for all additional component portion combination. These trends of production can be related to the surface tension between the gas-lift gas injection and the liquid from reservoir. This association is based on the fact that surface tension can be related to gas solubility and the gas solubility can be related to how much the gas dissolves and remains in liquid phase, and how much the gas bubble is dispersed into liquid.

Recombination of different gas-lift gas combination with oil from reservoir at injection point results new fluid with new composition and properties in the well, one of the properties is surface tension. Surface tensions of the fluid recombination calculated for the OLGA model and in equilibrium are presented in Figure 4-20 and Figure 4-21. One is at wellhead and the other one is at injection point respectively. Surface tension calculation in equilibrium is done in PVTsim with SRK as EOS. It can be seen from the figures that the smaller portion of additional components has little effect to the surface tensions. As the portion of additional components increase, the surface tensions decrease.

It can be inferred from Figure 4-20 and Figure 4-21, both surface tensions from OLGA model and in the equilibrium show consistent trend. From the figures, OLGA model shows that surface tension decreases as C3 and iC4 are used as additional component to the gas-lift gas. However, surface tension increases as nC4, iC5, and nC5 are used. iC4 gives the lowest surface tension for all additional component portion combination. From the figures, surface tension in equilibrium decreases as C3 and iC4 are used as additional component.

However in equilibrium, there are dips when heavier components are used. nC4 increases the surface tension, then it decreases when using iC5 and increases again when using nC5. These dips are consistent with different portion of additional component and at different points in the well. However in general, Figure 4-20 and Figure 4-21 reveal that heavier additional components give higher effect to the surface tension which can decrease the surface tension.

Beecher and Parkhurst reported that dissolved gas in oil reduces the surface tension of crude oil (Beecher & Parkhurst, 1926). As the dissolved gas escapes from the oil, the surface tension increases. This is in accordance with the values shown in Figure 4-20 and Figure 4-21 which reveals that surface tension at wellhead is higher than at injection point. The result is make sense because at lower part of tubing, for example at injection point, as the gas-lift gas

is injected, more gas dissolves and remains in the oil in the liquid phase due to high pressure and low surface tension. As the fluid travels from lower part to the upper part of the tubing, the pressure reduces and more gas escapes from the oil thus increases the surface tension. This analysis suggests that the solubility of gas in oil changes in the surface tension between the gas and oil. As the solubility of gas in oil decreases, the surface tension also increases.

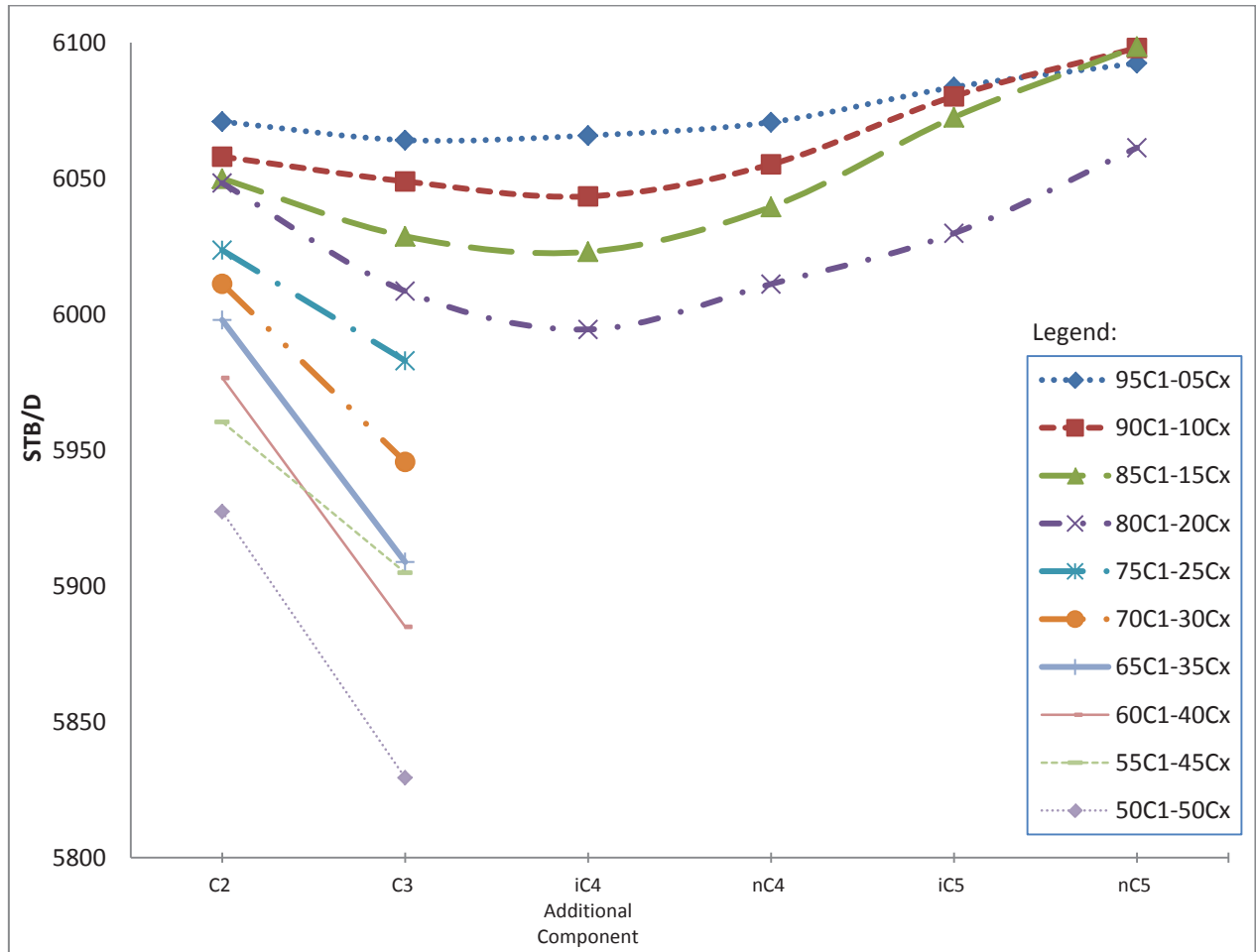


Figure 4-19 Oil Production on Wellhead for Binary Component Gas-lift Gas Injection Cases

Beecher and Parkhurst also reported that a natural gas consists mostly of methane is not as soluble as ethane (Beecher & Parkhurst, 1926). Hence, the surface tension of ethane is lower than methane. This study is in agreement with surface tension result shown in Figure 4-20 and Figure 4-21. However, this is not applicable for the heavier components. As mentioned before, C2, C3 and iC4 show decreasing surface tension while the heavier components show increasing surface tension with some dips for nC4 and iC5 for calculated surface tension in equilibrium.

So far it has been showed that solubility is affected by the surface tension. As more gas is soluble in the liquid, less gas remains in the gas phase. As previously discussed before, the gas bubble also disperses into the oil. When the flow reaches stable flow period, the flow shows no more slugs as it reaches bubble flow regime in which the gas bubble disperse into

the oil and lifts the liquid to the wellhead. That gives the understanding that the less gas remains in the gas phase, the less bubble disperses into the oil which makes the less oil is lifted to the wellhead. The less oil is lifted, the less the oil rate is.

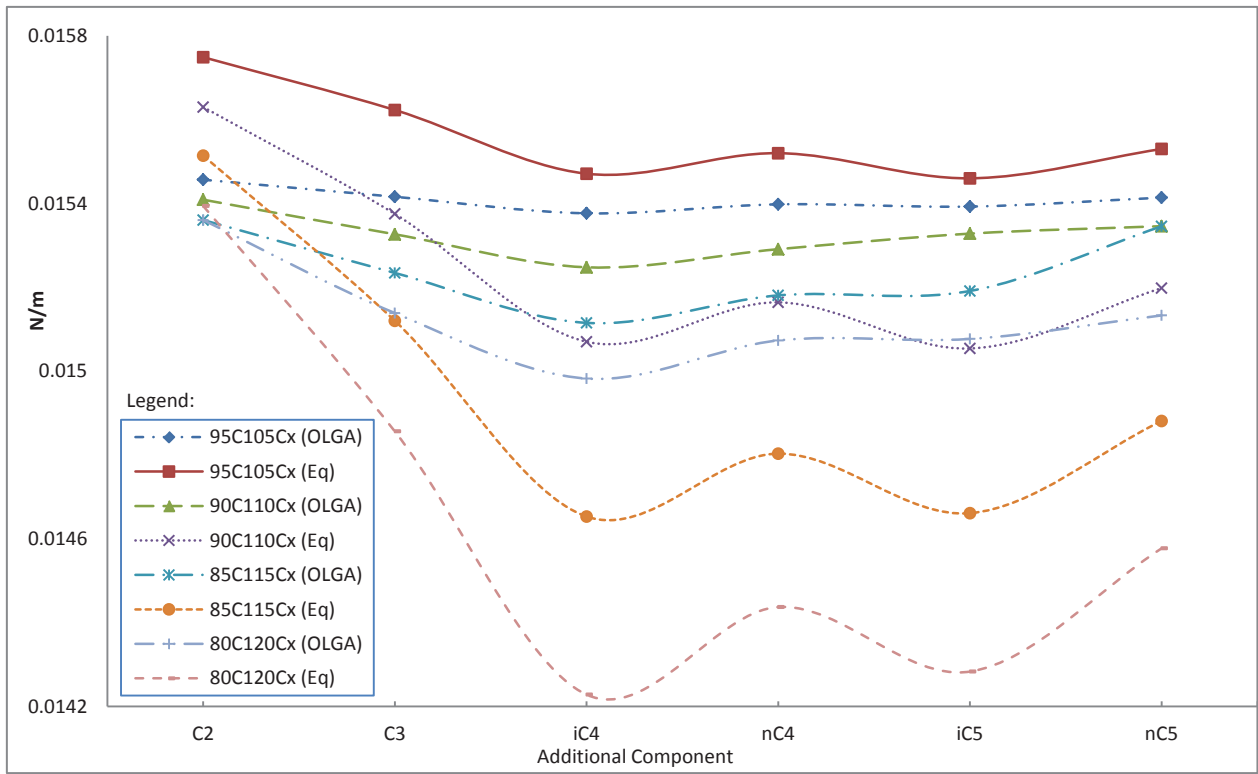


Figure 4-20 IFT at Wellhead at Stable Flow Period (Binary Component Cases)

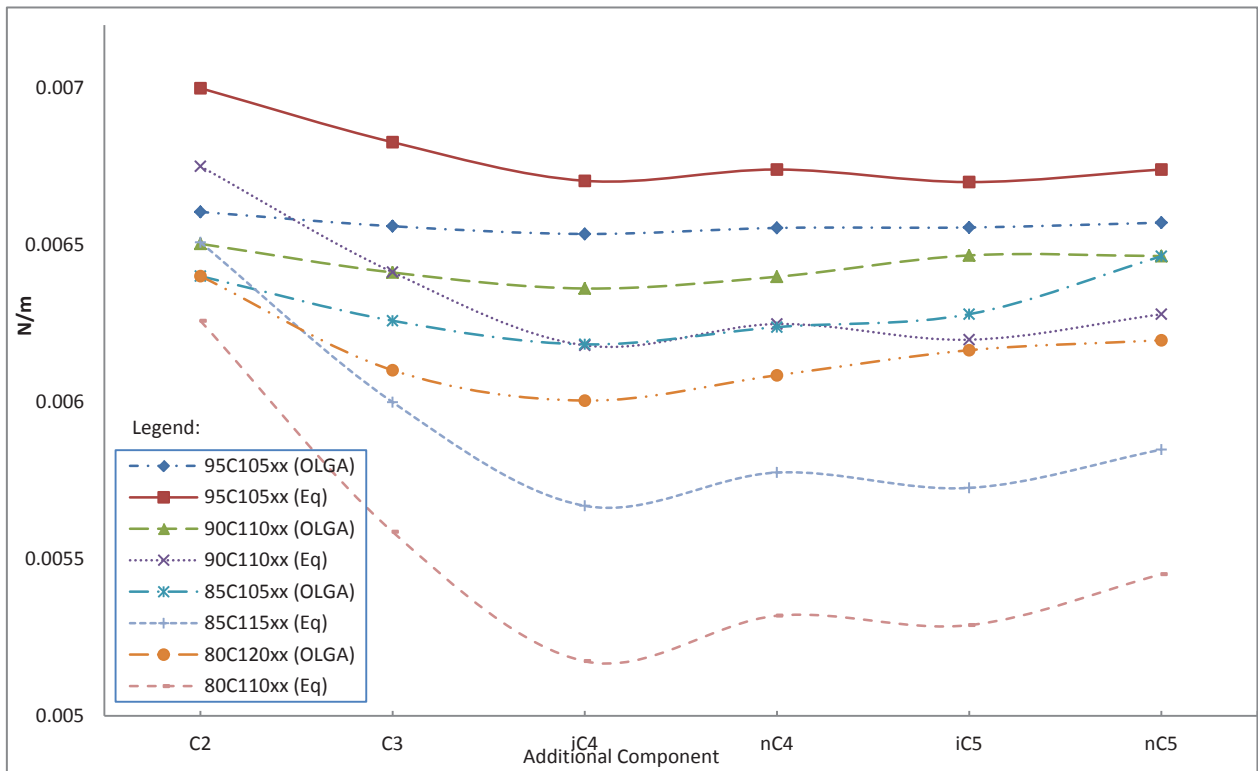


Figure 4-21 IFT at Injection Point at Stable Flow Period (Binary Component Case)

It is clear that there is relevance from oil production rates in Figure 4-19 with surface tension in Figure 4-20 and Figure 4-21. Taken together, these results suggest that the lower the surface tension is, the higher the gas solubility in oil will be thus less gas remains in the gas phase. Therefore less bubble disperses into the oil and less the oil production rate is. It can be concluded that the lower the surface tension value makes the oil production rate lower as well. However there are conditions that heavier additional gas gives significantly higher oil productions which are nC5 is used as additional component of gas-lift gas injection with 5%, 10%, and 15% of nC5 in total binary mixture.

4.4 Multicomponent Mixture

The last cases group to investigate is when multicomponent mixture is used as gas-lift gas injection. The cases combinations have been described in section 3.2 in Table 3-6, Table 3-7, Table 3-8, and Table 3-9. The oil production rate at stable flow period of these cases is shown in Figure 4-22. It can be seen from the figure that any increase in C1 portion in the mixture has little effect on the production rate. 1% increase to each component in the mixture has little effect as well. When the content of any component is increased by 5%, 8%, and 10%, it gives larger effect to oil rate which makes the rate decreases. With the same increased proportion, iC4 gives the lowest oil rates while nC5 gives the highest oil rates for the most cases.

The change of proportion to each component in the mixture also gives effect in oil rate as shown in Figure 4-22. From the figure, for 5%, 8%, and 10% increase, oil rates decrease as the proportion of C2, C3, and iC4 are increased in the gas-lift gas mixture while productions increase as the proportion nC4, iC5, and nC5 are increased in the mixture. The observed trend on the effect of the different components that was addressed in the previous section was held, where nC5 gave the highest oil rates in most cases. The increased proportion of iC4 gives the lowest production for most cases as well. Figure 4-22 illustrated that for an increase of 5%, 8%, and 10% for C2, C3 and iC4, oil rates decreased. However, production rate increased when the content of nC4, iC5, and nC5 in the gas mixture increased. The increased proportion of iC4 gives the lowest production for most cases. The lowest one is 5999.3 STB/d when iC4 was increased to 10%. For 1% increase to each component in the gas-lift gas mixture, the figure shows that oil rates decrease 2.7 STB/d and 1.4 STB/d as the proportion of C2 and C3 are increased, respectively. But the production increases 2.3 STB/d, 1.4 STB/d, 2.4 STB/d, and 1.6 STB/d as the proportion of iC4, nC4, iC5, and nC5 are increased, respectively. However, as mentioned before the oil rate changes are small.

As previously discussed in section 4.3, these trends of production can be related to the surface tension between the gas-lift gas injection and the liquid from reservoir. This principle is also applied to analyze the behavior of multicomponent mixture as the gas-lift gas injection.

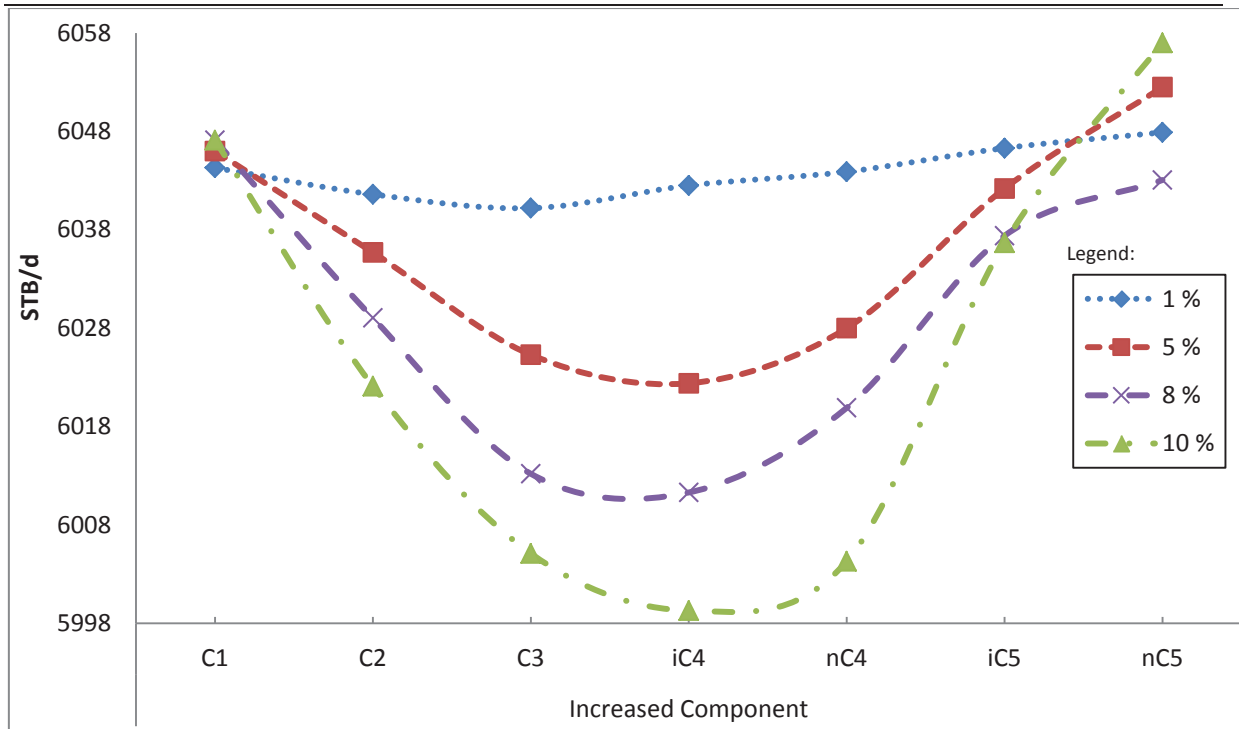


Figure 4-22 Oil Production on Wellhead for Multicomponent Mixture Gas-lift Gas Injection Cases

Surface tensions of the multicomponent gas-lift gas cases calculated for the OLGA model and in the equilibrium, which is done in PVTsim with SRK as EOS, are presented in Figure 4-23 and Figure 4-24. The one is at wellhead and the other one is at injection point respectively. It can be seen from the figures that small addition of components has inconsiderable effect to the surface tensions. As the content increased, the surface tensions decreased. There is no significant change in surface tension when each component is increased by 1%. For 1% increase to each component in the gas-lift gas mixture at injection point as calculated by OLGA, Figure 4-24, shows that surface tensions decrease 0.021 mN/m, 0.009 mN/m, 0.004 mN/m as the proportion of C2, C3, iC4 are increased, respectively. But they increase 0.004mN/m, 0.0002 mN/m, and 0.003 mN/m, as the proportion nC4, iC5, and nC5 are increased, respectively. As the components are increased by 5%, 8%, and 10%, the surface tension shows a decreasing trend. 10% component increase gives the highest decrease in surface tension. For example at injection point as calculated by OLGA, 10% increase to iC4 decreases the surface tension by 0.361 mN/m referred to 10% increase to C1.

It can be seen from Figure 4-23 and Figure 4-24, both surface tensions from OLGA model and in the equilibrium show consistent trend. From the figures, OLGA model shows that surface tension decreases as the proportion of C2, C3, and iC4 are increased in the gas-lift gas mixture while surface tension increases as the proportion nC4, iC5, and nC5 are increased in the mixture. The increased proportion of iC4 gives the lowest surface tension for all cases. From the figures, surface tension in equilibrium decreases as the proportion of C2, C3, and iC4 are increased in the mixture. However in the equilibrium, there are dips as heavier components are increased. Increased proportion of nC4 increases the surface

tension, then it decreases when the proportion of iC5 is increased and increases again when nC5 is increased. These dips are consistent with different proportion of increased component and at different points in the well. However in general, Figure 4-23 and Figure 4-24 reveal that heavier increased components give higher effect to the surface tension which is decreasing the surface tension.

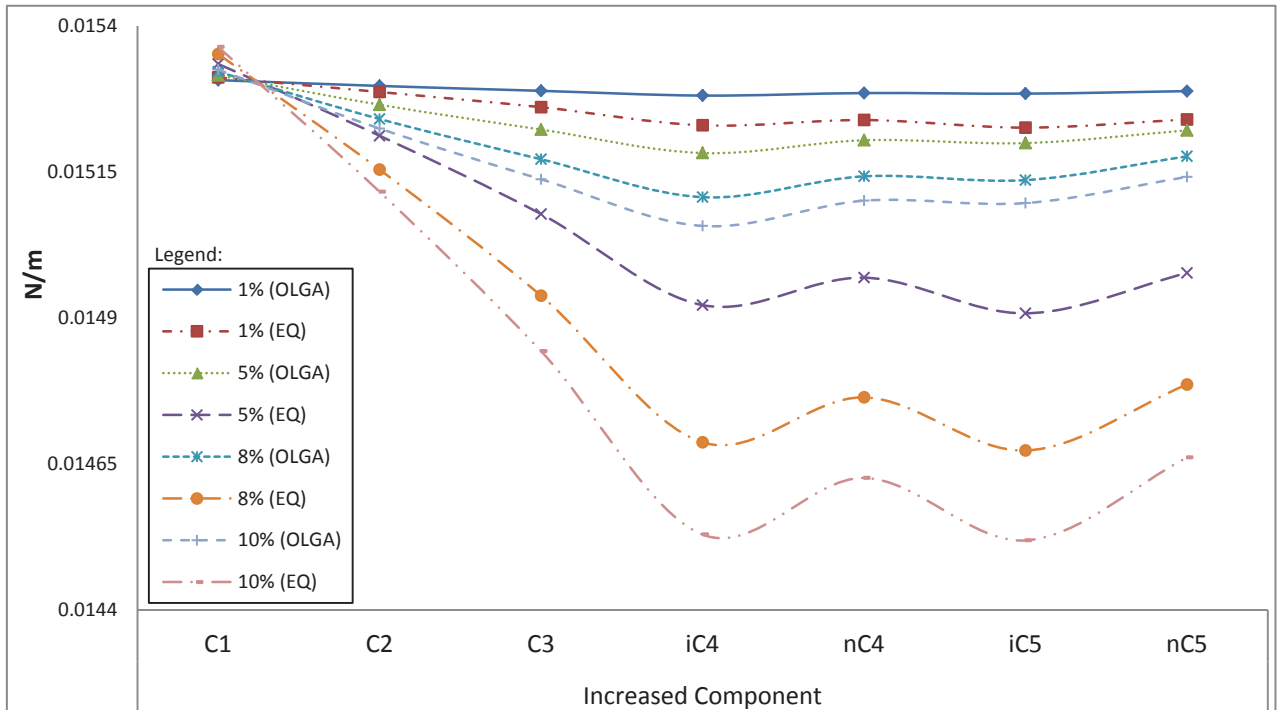


Figure 4-23 IFT at Wellhead at Stable Flow Period (Multicomponent Cases)

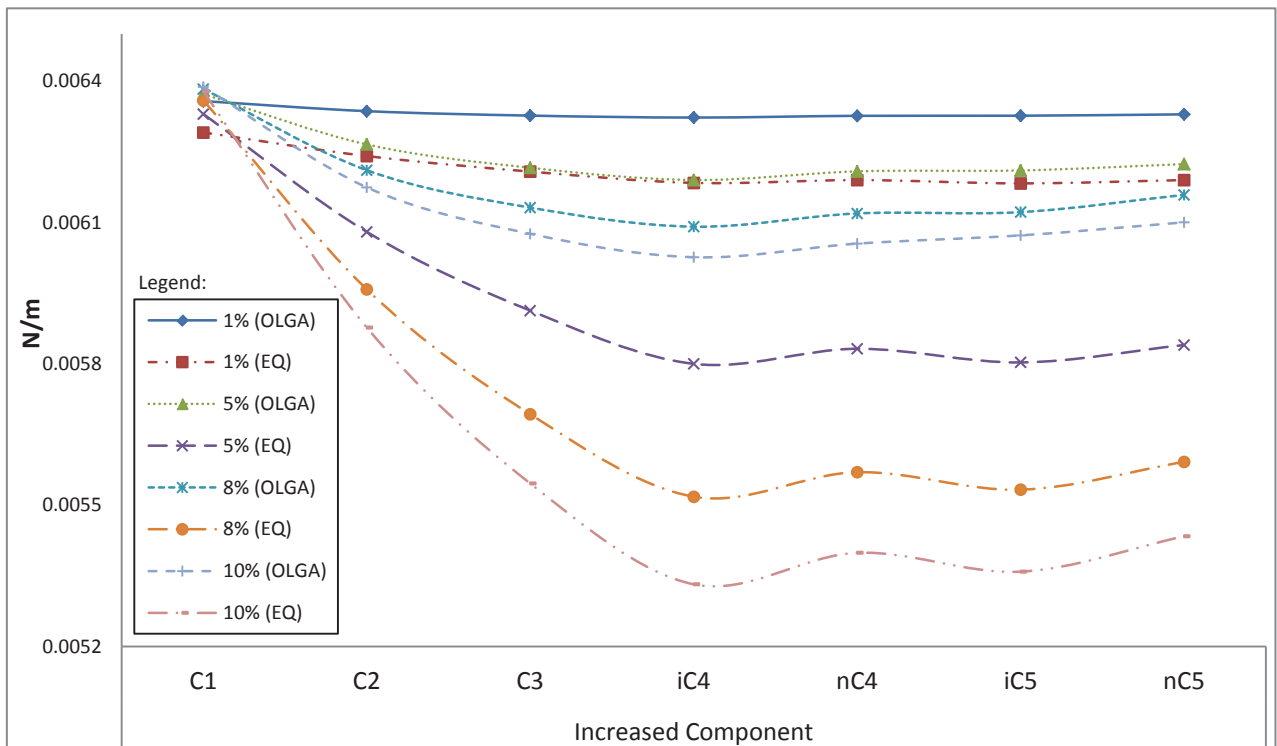


Figure 4-24 IFT at Injection Point at Stable Flow Period (Multicomponent Cases)

The study of multicomponent mixture becomes important to evaluate which system is better when it is compared to binary component gas-lift gas. Oil rates from binary component gas-lift gas cases in Figure 4-19 can be put together with oil rates from multicomponent gas-lift gas cases in Figure 4-22 to see which ones is better. As can be seen from Figure 4-25, most of binary component cases give higher oil rate compared to multicomponent mixture cases. Moreover, binary component gas-lift gases with any portions of additional nC5 give the highest oil rates. However, to use C1 as the major component in the binary or multicomponent gas-lift gas system consistently gives higher oil rates in the most cases. This oil rate result is consistent with the finding that lower surface tension makes lower oil production rate. It can be seen from Figure 4-20, Figure 4-21, Figure 4-23, and Figure 4-24 that most of binary component cases give higher surface tension compared to multicomponent mixture cases.

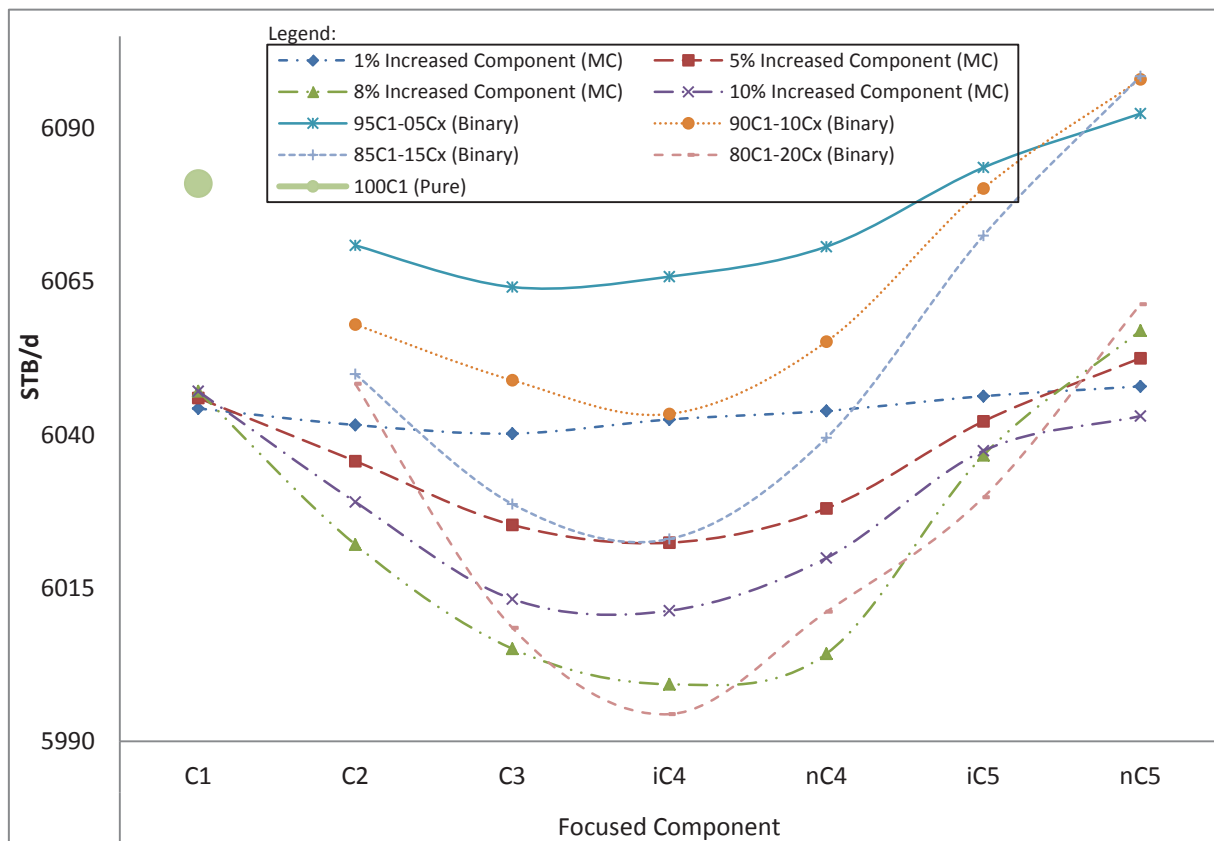


Figure 4-25 Oil Rate for Binary Cases and Multicomponent Cases

5. Conclusion

The present investigation has compared four case groups of gas-lift gas injection in J-shaped gas-lift well model. The case groups are using the base multicomponent mixture, pure component, binary component, and increased multicomponent mixture as gas-lift gas. The investigation was designed to explain the mechanism of the dynamic accumulation of the fluid and the development of pressure in the J-section and injection point of J-shaped gas-lift well, and determine the effect of composition to the production performance.

This study has shown that to unload the liquid column in J-shaped well with gas-lift gas, it has to go through some mechanism. In the beginning, the gas pushes the liquid which creates slug, then portion of gas bubble disperses into the liquid lowering the hydrostatic pressure of the liquid, and finally after the gas has developed sufficient energy, it pushes the remaining liquid column. As the result, the well can produce. Regarding the flow in the stable flow period, this study has explained that after the well is initiated, the gas-lift gas disperses into the liquid and reaches dispersed bubble flow regime to be able to stably lift the liquid.

The next result was regarding pure component to be the gas-lift gas injection, the heavier gas reduces the oil production. The heavier the gas, the higher the mixture density is. Therefore, the pressure drop is also higher. Moreover, injection pressure gives almost no effect to the oil production, up to certain point where the already high pressure drop in the well because of using the heavier component is added with the high gas-lift gas injection pressure. The gas-lift gas injection increases the compressibility of surrounding region upward and downward with respect to the injection point. Consequently, the pressure gradient is higher making the P_{WF} higher than P_{RES} causing no inflow from reservoir.

The next major finding was that the lower the surface tension, the lower the oil production rate is. It has been shown that the lower the surface tension is, the higher the gas solubility in oil. The higher the gas solubility in oil, the less gas remains in the gas phase. Therefore the less bubble disperses into the oil, and the less the oil production rate is. Regarding the surface tension, the lighter components decrease the surface tension while the heavier components increase the surface tension.

The next result was regarding the selection of component as gas-lift gas. It has been shown that using C1 as the major component in gas-lift gas system consistently gives higher oil rates. However, using nC5 in high proportion next to C1 would give highest oil rates. In the contrary, using iC4 in high proportion next to C1 would give lowest oil rates.

The last finding was that small proportion increase to each component in the multicomponent mixture doesn't give much effect to the production. When the proportion of increased component is increased, it decreases the production rate. Regarding the surface tension, generally multicomponent mixture for the gas-lift gas injection give lower surface

tension compared to binary component gas-lift gas system. Consequently, gas-lift gas with binary component gives higher oil rate compared to gas-lift gas with multicomponent mixture. Therefore, if there's a choice to use binary system as gas-lift gas, it's better to use the binary system.

The findings from this study make several contributions to the current literature. It demonstrates that there are effects of composition to the production performance. This study suggests which component selection is better to choose as gas-lift gas, if choices of different component of gas are given. However, these findings are limited by the use of OLGA as simulator, the given J-shaped well and only particular type of reservoir fluid. The study needs to be generalized to other type of wells, and reservoir fluids. And the use of OLGA as simulator has to be performed cautiously by always validating its physics.

6. Bibliography

- Ahmed, T. (2007). *Equation of State and PVT Analysis: Application for improved Reservoir Modelling*. Houston, Texas: Gulf Publishing Company.
- Alhanati, F., Schmidt, Z., Doty, D., & Lagerlef, D. (1993). *Continuous Gas-Lift Instability: Diagnosis, Criteria, and Solutions*. Houston: SPE-26554.
- Asheim, H. (1988). *Criteria for Gas-Lift Stability*. SPE-16468.
- Asheim, H. (1999). *Verification of Transient, Multi-Phase Flow Simulation for Gas Lift Applications*. Houston: SPE-56659.
- Avest, D. t., & Oudeman, P. (1995). *A Dynamic Simulator to Analyse and Remedy Gas Lift Problems*. Dallas: SPE-30639.
- Beecher, C. E., & Parkhurst, I. P. (1926). Effect of Dissolved Gas upon the Viscosity and Surface Tension of Crude Oil. *Society of Petroleum Engineers*, 51-69.
- Beggs, H. (1991). *Production Optimization: Using Nodal Analysis*. Tulsa: Oil & Gas Consultants International Inc.
- Bendiksen, K. H., Maines, D., Moe, R., & Nuland, S. (1991). The Dynamic Two-Fluid Model OLGA: Theory and Application. *Society of Petroleum Engineers* (p. 10). SPE-19451.
- Bendiksen, K. H., Maines, D., Moe, R., & Nuland, S. (1991). *The Dynamic Two-Fluid Model OLGA: Theory and Application*. SPE-19451.
- Danielson, T. J., Brown, L. D., & Bansal, K. M. (2000). Flow Management: Steady-State and Transient Multiphase Pipeline Simulation. *The 2000 Offshore Technology Conference* (p. 11). Houston, Texas: OTC-11965.
- Dharma, S. (2012). *Analyzing Vertical Lift Performance in ac Complex Gas Lift Well Geometry*. Stavanger: University of Stavanger.
- Guerrero-Sarabia, I., & Fairuzov, Y. (2013). Linear and non-linear analysis of flow instability in gas-lift wells. *Journal of Petroleum Science and Engineering*, 10.
- Guo, B., Lyons, W. C., & Ghalambor, A. (2007). *Petroleum Production Engineering: A computer-Assisted Approach*. Elsevier Inc.
- Hu, B. (2004). *Characterizing gas-lift instabilities*. Trondheim, Norway: Norwegian University of Science and Technology.
- Kaya, A. S., Sarica, C., & Brill, J. P. (2001). Mechanistic Modelling of Two-Phase Flow in Deviated Wells. *Society of Petroleum Engineers* (p. 10). Houston: SPE-72998.

- Mahmudi, M., & Sadeghi, M. T. (2013). The optimization of continuous gas lift process using an integrated compositional model. *Journal of Petroleum Science and Engineering*, 7.
- Maijoni, A., & Hamouda, A. (2011). *Effect of Gas Lift Gas Composition on Production Stability / Instability by Dynamic and Steady State Simulation for Continues Gas Lift Injection Mode*. Jakarta: SPE-147766-PP.
- O'bryan, P. L., Bourgoyne Jr, A. T., Monger, T. G., & Kopsco, D. P. (1988). An Experimental Study of Ga Solubility in Oil_based Drilling Fluids. *Society of Petroleum Engineers* (p. 10). New Orleans: SPE-15414.
- Poblano, E., Camacho, R., & Fairuzov, Y. (2005). *Stability Analysis of Continous-Flow Gas-Lift Wells*. San Antonio: SPE-77732-PA-P.
- Pourafshary, P., Varavei, A., Sepehmoori, K., & Podio, A. (2008). A Compositional Wellbore/Reservoir Simulator to Model Multiphase Flow and Temperature Distribution. *International Petroleum Technology Conference* (p. 14). Malaysia: IPTC-12115.
- Salman, Y., Wittfeld, C., Lee, A., Yick, C., & Derkinderen, W. (2009). *Use of Dynamic Simulation To Assist Commissioning and Operating a 65-km Subsea-Tieback GAs Lift System*. SPE-121187-PA-P.
- Thomas, D. C., Lea Jr., J. F., & Turek, E. A. (1984). Gas Solubility in Oil-Based Dilling Fluids: Effects on Kick Detection. *Society of Petroleum Engineers* (p. 10). New Orleans: SPE-11115.
- Xu, Z., & Golan, M. (1989). *Criteria for Operation Stability of Gas-Lift Wells*. Trondheim: SPE-019362.

Appendix

Appendix A1

General input in modelling J-shaped Gas-lift Well in PROSPER:

Fluid	: Oil and Water
Method	: Black Oil
Flow Type	: Tubing Flow
Well Type	: Producer
Method	: - None (for model without gas lift aid) - Gas Lift continuous (for model with gas-lift aid)
Correlation volume factor)	: - Standing (for bubble pressure, GOR, & formation - Beggs et al (for oil viscosity)
DownholeEq.	: - Tubing => 4168.54 m MD - Restriction - Casing => 7282.49 m MD
Overall Heat transfer coeff.	: 10 BTU/h/ft ² /F
Temperature at surface	: 5°C
Temperature at 7282.49 m MD	: 93°C

Appendix A2

Deviation survey used in PROSPER modelling

Point	Measured Depth (m)	True Vertical Depth (m)	Cumulative Displacement (m)	Angle (degrees)
1	0	0	0	0
2	250	250	0	0
3	611.65	610	34.5068	5.47521
4	703.84	700	54.4817	12.5136
5	782.11	770	89.4988	26.5762
6	957.57	920	180.527	31.2518
7	1070.71	1000	260.532	45.0015
8	1156.81	1050	330.626	54.4988
9	1246.25	1090	410.623	63.4341
10	2969.33	1800	1980.62	65.6661
11	4168.54	2300	3070.63	65.3584
12	4200.16	2310	3100.62	71.5633
13	4244.88	2330	3140.62	63.4341
14	5077.47	2670	3900.63	65.8979
15	5148.18	2680	3970.63	81.8698
16	5208.18	2680	4030.63	90
17	5278.89	2670	4100.62	98.1301
18	5429.22	2660	4250.62	93.8141
19	7282.49	2550	6100.62	93.4027

Appendix B1

General input in modelling J-shaped Gas-lift Well in OLGA:

Files

Feedfile : (input *.CTM feedfile generated by PVTsim from reservoir fluid composition taken from Table 3-4)

Integration

Endtime : 60 hours

Maxdt : 60 seconds

Starttime : 0 second

Options

Temperature : Ugiven

Steadystate : off(for dynamic simulation) ; on(for steady state simulation)

Compositional: on

Comoptions

Flashtype : default

Viscositycorr : Corrstate

Feed: Gas-lift gas injection

Component : (refer to Table 3-5)

Molefraction : (refer to Table 3-5)

Appendix B2

Annulus flowpath flow component input in modelling J-shaped Gas-lift Well in OLGA:

Heattransfer

Pipe : All
Interpolation : Vertical
Intambient : 5°C
Outambient : 85°C
Uvalue : 10 W/m²°C

Initialconditions

Interpolation : Vertical
Intemperature : 5°C
Outtemperature: 85°C
Inpressure : 163 bara
Outpressure : 173 bara
Pipe : All
Massflow : 0 kg/s
Voidfraction : 1
Watercut : 0
Feedname : Gas-lift gas injection
Feedmolefraction : 1

Source: Gas-lift Injection

Time : 8.01 hours
Sourcetype : Pressuredriven
Temperature : 5°C
Pressure : 163 bara
Valvemodel : hydrovalve

Pipe : Surface Line
Section : 1
Feedname : Gas-lift gas injection
Feedmolefraction : 1
Gasfraceq : 1
Oilfraceq : 0
Waterfraceq : 0
Sovaphase : Gas
Equilibriummodel : Frozen
CD : 0.84
Stroketime : 0 second
Thermalphaseeq : No

Checkvalve: GL check valve

Direction : Ppositive
Pipe : Lower inclined + GLM
Sectionboundary : 3

Valve: GLV

Valvetype : Gasliftvalve
Time : 8.01 hours
Pipe : Lower inclined + GLM
Sectionboundary : 3
Diameter : 12/64"
CD : 0.84

Appendix B3

Tubing flowpath flow component input in modelling J-shaped Gas-lift Well in OLGA:

Heattransfer

Pipe : All
 Interpolation : Vertical
 Intambient : 5°C
 Outambient : 85°C
 Uvalue : 10 W/m²°C

Initialconditions

Interpolation : Vertical
 Inpressure : 130 bara
 Outpressure : 30 bara
 Pipe : All
 Massflow : 0 kg/s
 Temperature : 82°C
 Voidfraction : 0
 Watercut : 0
 Feedname : (input *.CTM feedfile
 generated by PVTsim
 from reservoir fluid
 composition taken from
 Table 3-4)
 Feedmolefraction : 1

Valve: Surface Choke

Label : Surface Choke
 Model : Hydrovalve
 Equilibriummodel : Frozen
 Time : 0 hours
 Opening : 1
 Stroketime : 10 seconds
 Pipe : Upper vertical
 Sectionboundary : 5
 Diameter : 0.100533 m
 CD : 0.84

Appendix B4

Well/J-section flowpath flow component input in modelling J-shaped Gas-lift Well in OLGA:

Heattransfer

Pipe : All
 Interpolation : Vertical
 Intambient : 93°C
 Outambient : 85°C
 Uvalue : 10 W/m²°C

Initialconditions

Interpolation : Vertical
 Intemperature : 93°C
 Outtemperature: 85°C
 Inpressure : 175 bara
 Outpressure : 130 bara
 Pipe : All
 Massflow : 0 kg/s
 Voidfraction : 0
 Watercut : 0
 Feedname : (input *.CTM feedfile
 generated by PVTsim
 from reservoir fluid
 composition taken from
 Table 3-4)
 Feedmolefraction : 1

Well:Perforation

Label : Perforation
 Prodoption : Linear
 Injoption : Linear
 Respressure : 185 bara
 Restemperature : 93°C
 Time : 0 hours
 Location : Bottom
 Isothermal : Yes
 Feedname : (input *.CTM feedfile
 generated by PVTsim
 from reservoir fluid
 composition taken from
 Table 3-4)
 Feedmolefraction : 1
 Watercut : -1
 Gorst : -1
 Pipe : Toe
 Section : 1
 Injectivity : 8 sm³/d/bar
 Phase : Oil
 Prodi : 11 STB/d/psi

Appendix B5

Output component input in modelling J-shaped Gas-lift Well in OLGA:

Profiledata

Variable : AL, ALEXP, DPZA, DPZF, DPZG, EVRRHOMIX, GA, GAEXP, HOL, ID, LSBEXP, PT, QGST, QOST, REGIMETYPE, ROG, ROHL, ROL, SIG, TM, USG, USLT, USLTHL, USLTWT, VISHL, VISL, XG, XH

Context : Flowpath: Annulus; Flowpath: Tubing; Flowpath: Well

Trenddata

Variable : AL, ALEXP, DPZA, DPZF, DPZG, EVRRHOMIX, GA, GAEXP, HOL, ID, LSBEXP, PT, QGST, QOST, REGIMETYPE, ROG, ROHL, ROL, SIG, TM, USG, USLT, USLTHL, USLTWT, VISHL, VISL, XG, XH, VALVOP

Context : Flowpath: Annulus; Flowpath: Tubing; Flowpath: Well; J-shaped gas-lift well

Animate

Dtplot : 1 minute

Output

Column : 4

Dtout : 1 hour

Time : 0 second

Writefile : On

Profile

Dtplot : 20 minutes

Dttime : 0 second

Writefile : On

Trend

Dtplot : 0.5 minutes

Dttime : 0 second

Writefile : On

Trenddata

Variable : Valvop

Appendix B6

Nodes component input in modelling J-shaped Gas-lift Well in OLGA:

Node: Bottomhole

Label : Bottomhole

Type : Closed

Node: GL Injection Point

Label : GL injection point

Type : Closed

Node: Point of Injection

Label : Point of Injection

Type : Internal

Node: Wellhead

Label : Wellhead

Type : Pressure

Feedname : (input *.CTM feedfile
generated by PVTsim
from reservoir fluid
composition taken from
table 3-4)

Feedmolefraction : 1

Temperature : 5°C

Pressure : 30 bara

Time : 0 second

Appendix C1

Result of pure component cases at
stable flow period and 5 °C injection
temperature

Component	Gas-lift Gas Injection Pressure								Note
	163 bara		167 bara		171 bara		175 bara		
	Oil Rate (STB/d)	Gas Rate (MMSCF/d)	Oil Rate (STB/d)	Gas Rate (MMSCF/d)	Oil Rate (STB/d)	Gas Rate (MMSCF/d)	Oil Rate (STB/d)	Gas Rate (MMSCF/d)	
C1	6081.26	6.97	6086.54	7.05	6093.33	7.14	6098.82	7.22	
C2	5657.76	6.97	5658.25	6.99	5659.76	7.05	0	0	
C3	0	0	764.05	2.3	79.9	0.05	0	0	Several slugging period
iC4	n/a	n/a	n/a	n/a	n/a	n/a	n/a	n/a	Not recognized as gas by OLGA
nC4	n/a	n/a	n/a	n/a	n/a	n/a	n/a	n/a	Not recognized as gas by OLGA
iC5	n/a	n/a	n/a	n/a	n/a	n/a	n/a	n/a	Not recognized as gas by OLGA
nC5	n/a	n/a	n/a	n/a	n/a	n/a	n/a	n/a	Not recognized as gas by OLGA